CENTRAL RESEARCH LIBRARY
DOCUMENT COLLECTION

OAK RIDGE NATIONAL LABORATORY
operated by
UNION CARBIDE CORPORATION
for the
U.S. ATOMIC ENERGY COMMISSION

ORNL-NSIC-61
UC-80 — Reactor Technology

Cy. 1

HIGHWAY VEHICLE IMPACT STUDIES: TESTS AND MATHEMATICAL ANALYSES OF VEHICLE, PACKAGE, AND TIEDOWN SYSTEMS CAPABLE OF CARRYING RADIOACTIVE MATERIAL

O. A. Kelly
W. C. Stoddart

OAK RIDGE NATIONAL LABORATORY
CENTRAL RESEARCH LIBRARY
DOCUMENT COLLECTION
LIBRARY LOAN COPY
DO NOT TRANSFER TO ANOTHER PERSON
If you wish someone else to see this
document, send in name with document
and the library will arrange a loan.

NUCLEAR SAFETY INFORMATION CENTER

NSIC

Printed in the United States of America. Available from Clearinghouse for Federal Scientific and Technical Information, National Bureau of Standards, U.S. Department of Commerce, Springfield, Virginia 22151
Price: Printed Copy $3.00; Microfiche $0.65

LEGAL NOTICE

This report was prepared as an account of Government sponsored work. Neither the United States, nor the Commission, nor any person acting on behalf of the Commission:

A. Makes any warranty or representation, expressed or implied, with respect to the accuracy, completeness, or usefulness of the information contained in this report, or that the use of any information, apparatus, method, or process disclosed in this report may not infringe privately owned rights; or

B. Assumes any liabilities with respect to the use of, or for damages resulting from the use of any information, apparatus, method, or process disclosed in this report.

As used in the above, "person acting on behalf of the Commission" includes any employee or contractor of the Commission, or employee of such contractor, to the extent that such employee or contractor of the Commission, or employee of such contractor prepares, disseminates, or provides access to, any information pursuant to his employment or contract with the Commission, or his employment with such contractor.

ORNL NSIC-61

Contract No. W 7405-eng-26

Nuclear Safety Information Center

HIGHWAY VEHICLE IMPACT STUDIES: TESTS AND MATHEMATICAL ANALYSES OF VEHICLE, PACKAGE, AND TIEDOWN SYSTEMS CAPABLE OF CARRYING RADIOACTIVE MATERIAL

O. A. Kelly
W. C. Stoddart

General Engineering Division

FEBRUARY 1970

OAK RIDGE NATIONAL LABORATORY
Oak Ridge, Tennessee
operated by
UNION CARBIDE CORPORATION
for the
U.S. ATOMIC ENERGY COMMISSION

FOREWORD

Full-scale destructive vehicle tests, completely instrumented, are extremely costly, and yet in many instances they provide the only method of investigating the dynamic response of the structural members of a tractor-trailer load system. Because of its importance when the transport of irradiated materials is considered, a cooperative program to develop such information was undertaken between the U. S. Atomic Energy Commission and the Department of the Army.

Four vehicle impact tests were conducted at Aberdeen Proving Grounds, Maryland, during 1966, and the results were published in the Department of the Army Report DPS-2582 entitled "Final Report on Engineering Test of Transportation of Nuclear or Fissile Materials". Since the report received very limited distribution and was not suitable for additional reproduction in its present form, the Atomic Energy Commission requested that Oak Ridge National Laboratory revise the report, principally editing and clarifying it where needed. This report fulfills that request.

The primary effort in this report has been directed toward a more uniform organization of the information while attempting to emphasize those results and implications which to us seem important and reflect the purpose behind the tests. Not all of the hoped-for data were obtained; nevertheless, the tests were important and provide a firm benchmark for vehicular damage analyses under extreme accident conditions.

L. B. Shappert

L. B. Shappert, Coordinator
Fuel Transport Safety Studies

PREFACE

The Nuclear Safety Information Center was established in March 1963 at the Oak Ridge National Laboratory under the sponsorship of the U. S. Atomic Energy Commission to serve as a focal point for the collection, storage, evaluation, and dissemination of nuclear safety information. A system of keywords is used to index the information cataloged by the Center. The title, author, installation, abstract, and keywords for each document reviewed is recorded on magnetic tape at the central computer facility in Oak Ridge. The references are cataloged according to the following categories.

1. General Safety Criteria
2. Siting of Nuclear Facilities
3. Transportation and Handling of Radioactive Materials
4. Aerospace Safety
5. Accident Analysis
6. Reactor Transients, Kinetics, and Stability
7. Fission Product Release, Transport, and Removal
8. Sources of Energy Release Under Accident Conditions
9. Nuclear Instrumentation, Control, and Safety Systems
10. Electrical Power Systems
11. Containment of Nuclear Facilities
12. Plant Safety Features
13. Radiochemical Plant Safety
14. Radionuclide Release and Movement in the Environment
15. Environmental Surveys, Monitoring, and Radiation Exposure of Man
16. Meteorological Considerations
17. Operational Safety and Experience
18. Safety Analysis and Design Reports
19. Radiation Dose to Man from Radioactivity Release to the Environment
20. Effects of Thermal Modifications of Ecological Systems
21. Effects of Radionuclides and Ionizing Radiation on Ecological Systems

Computer programs have been developed that enable NSIC to (1) produce a quarterly indexed bibliography of its accessions (issued with ORNL-NSIC report numbers), (2) operate a routine program of Selective Dissemination of Information (SDI) to individuals according to their particular profile of interest, and to (3) make retrospective searches of the references on the tapes.

Other services of the Center include principally (1) the preparation of state-of-the-art reports (issued with ORNL-NSIC report numbers); (2) cooperation in the preparation of the bimonthly technical progress review, Nuclear Safety; (3) answering technical inquiries as time is available; and (4) providing counsel and guidance on nuclear safety problems.

Services of the NSIC are available without charge to government agencies, research and educational institutions, and the nuclear industry. Under no circumstances do these services include furnishing copies of any documents (except NSIC reports), although all documents may be examined at the Center by qualified personnel. Inquiries concerning the capabilities and operation of the Center may be addressed to

J. R. Buchanan, Assistant Director
Nuclear Safety Information Center
Oak Ridge National Laboratory
Post Office Box Y
Oak Ridge, Tennessee 37830

Phone: 615-483-8611, Ext. 3-7253
FTS 615-483-7253

ACKNOWLEDGMENTS

The assistance of H. T. Cline and D. A. J. Misiora of the Aberdeen Proving Ground, R. A. Meldrum of the Department of the Army, W. P. Gammill of the AEC-DRDT, and of L. B. Shappert of Oak Ridge National Laboratory in the preparation of this report has been greatly appreciated.

CONTENTS

Abstract 1
1. INTRODUCTION 1
2. SUMMARY 4
3. TEST FACILITIES AND TECHNIQUES 8
3.1 Test Site 8
3.2 Test Procedures 9
3.3 Instrumentation 14
4. TEST NUMBER ONE 19
4.1 Test Vehicle 19
4.2 Instrumentation 20
4.3 Results of First Test 21
5. TEST NUMBER TWO 27
5.1 Test Vehicle 27
5.2 Vehicle Cargo 27
5.3 Instrumentation 36
5.4 Results of Second Test 36
5.4.1 Results Recorded By High-Speed Photography 37
5.4.2 Measurements Recorded By Instruments 42
5.4.3 Measurements Taken From Photographs 42
5.4.4 Effects of Impact on Cargo 48
6. TEST NUMBER THREE 72
6.1 Test Vehicle 72
6.2 Vehicle Cargo 76
6.3 Instrumentation 79
6.4 Results of Third Test 84
7. TEST NUMBER FOUR 103
7.1 Test Vehicle 103
7.2 Instrumentation 107
7.3 Determination of Impact Speed for Fourth Test 110
7.4 Results of Fourth Test 113
7.4.1 Instrument Measurements 117
7.4.2 Photographic Measurements 117

8. MATHEMATICAL ANALYSIS OF TESTS 123
8.1 Definition of Problem 123
8.2 Approach to Solution Formulation 125
8.3 Mathematical Model 126
8.4 Limitations of Mathematical Model 129
9. APPRAISAL OF RESULTS, CONCLUSIONS, AND RECOMMENDATIONS 131
9.1 Appraisal of Results 131
9.1.1 First Test 131
9.1.2 Second Test 131
9.1.3 Third Test 132
9.1.4 Fourth Test 133
9.1.5 Comparison of Test Results 134
9.1.6 Mathematical Analysis 135
9.2 General Conclusions 136
9.3 Recommendations 137

LIST OF FIGURES

Figure Number	Title	Page Number
3.1	Barrier at End of Test Road	8
3.2	Remote-Control Mechanism for Emergency Braking	9
3.3	Remote-Control Mechanism for Steering the Vehicle	10
3.4	Remote-Control Mechanism for Adjusting the Throttle Setting	11
3.5	Instrumentation Van	12
3.6	Remote Control and Recording Equipment Mounted Inside the Instrumentation Van	12
3.7	Vehicle Control and Test Setup for High-Speed Collision Tests	14
3.8	Block Diagram of Data Acquisition System for Collision Tests	15
3.9	Load Cells on Front of Cab-Over-Motor Tractor	17
3.10	Locations of Cameras for Different Collision Tests	18
4.1	Vehicle Used in First Collision Test	19
4.2	Location of Transducers on Vehicle for First Test	20
4.3	Impact Force at 4.5 mph Velocity Measured by Load Cells	22
4.4	Axial Force Measurements on the Tractor and Trailer Frames Resulting From 4.5-mph Impact	23
4.5	Bending Moment Measurements on Tractor and Trailer Frames Resulting From 4.5-mph Impact	24
4.6	Axial Acceleration Measurements (Filter 5 to 240 Hz Bandpass) on Tractor and Trailer Frames Resulting From 4.5-mph Impact	25
5.1	Los Alamos Scientific Laboratory B of E Permit 1736 Combination Shipping Container ICC-2R and ICC-6J	28
5.2	Union Carbide Corporation, Nuclear Division, B of E Permit 1685 for 20-in. Birdcage in Banded Plywood Box for Enriched Uranium Metal or Dry Uranium Compounds	29
5.3	USAEC Design KKD-1 (or LLD-1) Rocky Flats Birdcage for Enriched Uranium and Plutonium Metal (B of E Permit 1757)	30
5.4	Eight-Inch Schedule-40 Pipe Inside 55-Gallon Drum Container	31

Figure Number	Title	Page Number
5.5	Union Carbide Corporation, Nuclear Division, B of E Permit 1561 for Y-12 Foamglas Shipping Container for Uranium Metal and Dry Uranium Compounds	32
5.6	Three-Liter Class-II Container	33
5.7	Cargo Loading Arrangement in Semitrailer for the Second Test	34
5.8	Cargo Weights in Semitrailer for Second Test	35
5.9	Cab-Behind-Motor Tractor Fifth Wheel Plate Attachment	37
5.10	Still Pictures Showing Impact of Test Vehicle Against Barrier at a Velocity of 41 mph in the Second Test	38
5.11	Overhead View of Tractor-Trailer Combination Following the 41-mph Impact With the Barrier in the Second Test	41
5.12	Force Measurements (filtered above 25 KHz) of Front Load Cells Resulting From 41-mph Impact	43
5.13	Axial Acceleration Measurements (filtered 5 to 240 Hz Bandpass) on Tractor and Trailer Frames Resulting From 41-mph Impact	44
5.14	Acceleration as a Function of Displacement of Point Over Fifth Wheel Resulting from the 41-mph Impact	46
5.15	Displacement, Velocity, and Acceleration of Fixed Point Over Fifth Wheel as a Function of Time Resulting from the 41-mph Impact	47
5.16	Interior of Trailer Following Second Impact Test	49
5.17	Los Alamos B of E Permit 1736 Containers (A-5 and A-6) in Damaged Array Before Removal From the Trailer After the 41-mph Impact	50
5.18	Damaged KKD-1 Containers and Union Carbide Corporation 20-in. Birdcage Containers Before Removal From Trailer After the 41-mph Impact	51
5.19	Damaged Containers Made of 8-in. Schedule-40 Pipe in 55-Gallon Drums Before Removal From Trailer After 41-mph Impact	52
5.20	Los Alamos Containers A-4 and A-5 Locked Together After 41-mph Impact	61
5.21	View of Inside of Los Alamos Container A-4 After 41-mph Impact	61
5.22	View of Inside of Los Alamos Container A-5 After 41-mph Impact	61

Figure Number	Title	Page Number
5.23	Outside of Los Alamos Container H-4 After Being Thrown From Trailer as a Result of the 41-mph Impact	62
5.24	View of the Inside of Los Alamos Container H-4 After the 41-mph Impact	63
5.25	Union Carbide Corporation 20-in. Birdcage B-4 With Outer Plywood Box Removed After 41-mph Impact	64
5.26	Union Carbide Corporation 20-in. Birdcage B-5 With a Portion of the Outer Plywood Box Removed After 41-mph Impact	64
5.27	USAEC Design KKD-1 Containers After Removal From the Trailer Following 41-mph Impact	66
5.28	Outside View of Container Comprised of 8-in. Pipe in 55-Gallon Drum in Position D-3 After 41-mph Impact	67
5.29	View of Inside of Container D-3 After the 41-mph Impact	67
5.30	Outside of Union Carbide Corporation Y-12 Foamglas Container E-3 Thrown From Trailer as a Result of the 41-mph Impact	68
5.31	View of Inside of Union Carbide Corporation Y-12 Foamglas Container E-3 With Containment Vessel Removed After 41-mph Impact	69
5.32	Outside of 3-Liter Class-II Container H-3 After It Was Thrown From the Trailer as a Result of the 41-mph Impact	70
5.33	View of the Inside of the 3-Liter Class-II Container H-3 After It Was Thrown From the Trailer as a Result of the 41-mph Impact	71
6.1	Tractor and Trailer Used in Third Test	72
6.2	Details of the Framing of the Tractor Used in the Third Impact Test	74
6.3	Details of the Framing of the Trailer Used in the Third Impact Test	75
6.4	Fifteen-Ton Cask Mounted on Flatbed Semitrailer for the Third Impact Test	77
6.5	Design of 15-Ton Cask Tie-Down to Trailer	78
6.6	Location of Accelerometers on the Cask and Transport Vehicle for the Third Impact Test	80
6.7	Location of Load Cells and Strain Gages on the Cask and Transport Vehicle for the Third Impact Test	81
6.8	Buckled Frame of Tractor Resulting From the 4-mph Impact	85

Figure Number	Title	Page Number
6.9	Damage Done to Tractor Frame Immediately Ahead of I-Beam Spacers for Fifth Wheel as a Result of the 4-mph Impact	85
6.10	Force Measurements as a Function of Time for the 4-mph Impact	87
6.11	Force Measurements of Cask Tie Rods and Horizontal Load Cells as a Function of Time for the 4-mph Impact	88
6.12	Force Measurements of Cask Vertical Load Cells as a Function of Time for the 4-mph Impact	89
6.13	Force and Moment Measurements on Tractor Frame as a Function of Time for the 4-mph Impact	90
6.14	Force and Moment Measurements on Trailer Frames as a Function of Time for the 4-mph Impact	91
6.15	Total Force Measured on Front Suspension of Tractor as a Function of Time for the 4-mph Impact	92
6.16	Total Force Measured on Rear Suspension of Tractor as a Function of Time for the 4-mph Impact	93
6.17	Total Force Measured on Trailer Suspension as a Function of Time for the 4-mph Impact	94
6.18	Total Force Measured on Rear Main Frames and Outside Frame of Trailer as a Function of Time for the 4-mph Impact	95
6.19	Total Moment Measured on Rear Main Frames and Outside Frame of Trailer as a Function of Time for the 4-mph Impact	96
6.20	Vertical and Longitudinal Acceleration Measured on Trailer Frame as a Function of Time for the 4-mph Impact	97
6.21	Longitudinal Acceleration Measured on Front and Rear Axles of Tractor as a Function of Time for the 4-mph Impact	98
6.22	Vertical Acceleration Measured on Front of Trailer Frame as a Function of Time for the 4-mph Impact	99
6.23	Longitudinal Acceleration Measured on Front of Trailer Frame as a Function of Time for the 4-mph Impact	100
6.24	Vertical and Longitudinal Acceleration Measured on Rear of Trailer Frame and Longitudinal Acceleration Measured on Trailer Axle as a Function of Time for the 4-mph Impact	101

Figure Number	Title	Page Number
6.25	Vertical and Longitudinal Acceleration Measured Near the Cask Center of Gravity on Left Side and Vertical Acceleration Measured on Trailer Frame Under Cask as a Function of Time for the 4-mph Impact	102
7.1	Tractor and Flatbed Semitrailer Used in Fourth Test	103
7.2	Dimensions and Physical Properties of the 2.5-Ton M275 Military Tractor Used in the Fourth Impact Test	106
7.3	Location of Accelerometers on Cask and Transport Vehicle for the Fourth Impact Test	108
7.4	Location of Load Cells and Strain Gages on the Cask and Transport Vehicle for the Fourth Test	109
7.5	Arrangement of Markers on Test Vehicle and Cask for Photographic Measurement of the Fourth Impact Test	111
7.6	Plot Resulting From Empirical Analysis to Determine Whether the Force at a Given Impact Velocity Can Be Predicted	112
7.7	Still Pictures Showing Impact of Cask Transport Vehicle Against the Barrier at a Velocity of 28.5 mph in the Fourth Test	114
7.8	Lateral Shift of Tractor-Trailer Combination About the Fifth-Wheel Area During the 28.5-mph Impact	116
7.9	Force Measurements on Cask and Cask Tie Rods as a Function of Time for the 28.5-mph Impact	118
7.10	Sixth-Degree Fit for Deceleration Versus Displacement of Point on Semitrailer Over Fifth Wheel for the 28.5-mph Impact	120
7.11	Sixth-Degree Fit for Point Displacement, Velocity, and Acceleration as a Function of Time for the 28.5-mph Impact	121

LIST OF TABLES

Table Number	Title	Page Number
5.1	Average Container Dimensions After 41-mph Impact	53
5.2	Measured Positions of Containers in Trailer Before and After 41-mph Impact	54
5.3	Measurements of Individual Containers After the 41-mph Impact	56
6.1	Physical Properties of Materials of the Tractor and Trailer Used in the Third Impact Test	73
6.2	Weight Distribution on Modified Tractor-Trailer Rig When Empty and When Loaded for the Third Test	77
7.1	Physical Features of Tractor Used in the Fourth Test Compared With Those of Tractor Used in the Third Test	104
7.2	Weight Distribution on Loaded Cask Transport Vehicle Used in the Fourth Impact Test	107

HIGHWAY VEHICLE IMPACT STUDIES: TESTS AND MATHEMATICAL ANALYSES OF VEHICLE, PACKAGE, AND TIEDOWN SYSTEMS CAPABLE OF CARRYING RADIOACTIVE MATERIAL

Abstract

Four vehicle impact tests were conducted in February through November of 1966 at the Aberdeen Proving Ground as part of an initial study to develop test and instrumentation techniques and to acquire quantitative data on nuclear material transport systems that might be used to describe the dynamics of transportation accidents. The impact tests were performed with three different combinations of truck tractors and semitrailers and two types of cargo. A 350-ton barrier was constructed at the end of a paved road and the remotely operated test vehicles were impacted against it at various velocities. The tests were executed successfully, but the instruments installed on the tractors for quantitative measurements were damaged prior to conclusion of the impact phenomena because of the inherent weakness of the tractors. Photographic measurements provided the most meaningful description of the dynamic behavior of the transport systems during the impact tests. The mathematical model developed in conjunction with these tests did not accurately describe the actual behavior of the vehicles during impact. Even though all the desired quantitative data were not obtained, sufficient structural and transportability data were gained to assure a positive approach for evaluating the dynamics involved in future impact tests.

1. INTRODUCTION

Advances in modern technology are resulting in the production and distribution of certain materials and commodities for which a continuous review of transportation safety practices and standards is necessary. Radioactive and fissile materials are in this category, and adequate safety is a prime consideration in the transportation of such materials. However, technical criteria on the various types of transportation accidents are not described informatively or are not known. Therefore, the United States Atomic Energy Commission (USAEC) and the Department of the Army (DA) agreed to undertake a study to scientifically determine the

effects of a serious transportation accident on the total transport system comprised of the vehicle, cargo, and restraints. The objective of the study was "to provide a realistic understanding of the dynamics of transportation accidents as a basis for establishing or modifying movement standards, container designs, and transportation procedures that will assure maximum practical safety at minimum cost in the transport of radioactive materials".

The objective envisioned was that the study would encompass all modes of transportation. To determine whether such studies are feasible and whether the dynamic phenomena could be described, an initial study simulating a highway accident was undertaken. Mathematical and experimental analyses using automatic electronic methods to record the phenomena were to be developed. Following the experimental tests, the practicability of the recording system and whether the experimental values obtained could be correlated with the analytical values were to be determined. It was recognized that while considerable work relative to passenger carrying vehicles had been done by various investigators, very little work involving cargo carrying vehicles had been pursued, and that procedures for conducting investigations involving cargo carrying vehicles could not be similar to those used for passenger vehicles.

Prior to initiation of the initial study, research was conducted on the designs of shipping containers for radioactive materials, types of transport vehicles (rail and highway) used, and the accident statistics. This research indicated that overturn and collision with fixed objects had the higher density in highway transportation. Consequently, a head-on collision of the highway transport vehicle with a fixed object was selected as the accident condition for the initial study. Other factors in this selection were that this condition was more suitable for mathematical analysis, required fewer vehicles, and was easier controlled than other conditions considered, and it also afforded minimum cost for execution.

Discussions were held to review the expected behavior of the vehicles during collision, the analysis of the anticipated dynamic motions, the types and location of sensors to obtain value correlation with the mathematical analysis, the degree of restraint for the cargo, and the

measurement of strain during inelastic deformation of structural members. Excerpts of these discussions are contained in the minutes of the meetings of the Technical Working Group and are given in Appendix IV of the Department of the Army Report DPS-2582, "Final Report on Engineering Test of Transportation of Nuclear and Fissile Materials," November 1967.

The Franklin Institute Research Laboratories had done prior work and published a report on the development of a mathematical model as an approach to the vehicle collision problem (The Franklin Institute Report No. I-A2412-4, December 1964), and it was agreed that this reported pilot study would be used to determine the validity of the model and to further advance such work. Therefore, consideration was given to the input data required for the model in the selection of sensors and their location on the transport system. The Franklin Institute Research Laboratories performed the mathematical analysis work done in conjunction with the initial study, and this is reported by K. D. Doshi in Final Report F-B2397 entitled "Analysis for the Longitudinal Vehicle Collision Test of Joint AEC-DA Pilot Study," August 1967.

All of the field work, including the development of the test site, facilities, techniques, and procedures, was performed by the Development and Proof Services of the Aberdeen Proving Ground in Maryland.

2. SUMMARY

The test site selected had a level paved road 40 ft wide with sufficient straightaway to accommodate the proposed tests. A 350-ton barrier was constructed at the end of the road to provide, for all practical purposes, the immovable object against which the test vehicles would impact. Test procedures and instrumentation plans were developed. These involved remote control of each test vehicle's own propulsion system from an instrumentation van in which the test data from sensors located on the vehicle were recorded. Photographic coverage of each test was also provided for both documentary and photomeasurement purposes.

After construction of the barrier and related test facilities, four separate vehicle impact tests were conducted. The first test collision at a velocity of 4.5 mph without cargo in the van type of semitrailer was conducted to familiarize personnel with the test facilities and techniques and to record limited quantitative force and accelerometer measurements as a basis for predicting the optimum transducer gain levels for subsequent impacts at higher speeds. No physical damage to the tractor or the trailer resulted from this test.

The second collision test at a velocity of 41 mph was conducted with the same tractor-semitrailer combination used in the first test but with a loosely stowed cargo of 33 birdcage packages, representing 6 types of nuclear material containers, between cargo containers filled or partially filled with crushed stone. This 27,000-lb cargo was stowed in two levels in the van type of semitrailer. The objectives of this test were to determine photographically the dynamic behavior of the transport system and its cargo during a head-on collision with a fixed object and to obtain quantitative measurements of force for use in the mathematical study. The cab of the tractor was completely demolished as a result of the 41-mph impact, the fifth wheel also separated from the tractor and allowed the semitrailer to strike the barricade, and a portion of the cargo was thrown from the trailer.

The third collision test at 4 mph was a nondestructive test conducted with a cab-over-motor tractor and a flatbed semitrailer with a rigidly

attached 15-ton cask. This test was conducted to obtain quantitative measurements for the mathematical model and to evaluate the effectiveness of the instrumentation. However, the frame of the tractor buckled at a point in front of the fifth wheel as a result of the impact, and the tractor was damaged beyond economical repair. There was no observable damage done to the semitrailer or the cask.

The fourth and final collision test in the series was conducted with the same semitrailer and cask used in the third test, but a 2.5-ton military tractor was used to propel the vehicle into the barrier at a velocity of 28.5 mph. This test was conducted to investigate the behavior of the cask transport system during a destructive high-speed collision and to quantify the behavior to the extent possible. The tractor and trailer did not separate during the impact, but the tractor frame buckled ahead of the fifth wheel attachment and the tractor was crushed to the extent that the trailer essentially came into contact with the barrier through the fully compressed material of the tractor. The frame of the trailer showed permanent deformation, but the cask tie-down to the trailer remained intact.

As a result of these tests, it was concluded that the test site, barrier, remote-control capability, and the operating procedures and techniques used in this investigation were entirely satisfactory. These tests did illustrate that the ability to remotely direct the test vehicle so that the impact would occur normal to the barrier requires considerable skill on the part of the operator of the remote-control system. Although representative of the severity of the impact, a diagonal force input affects the transmission and magnitude of the forces and accelerations occurring in the various components of the transport system during impact. However, the technical experience gained during the tests has assured that the dynamic phenomena occurring during the impact of tractor-semitrailer combinations against an unyielding surface can be electronically measured and recorded.

Diverse behavior patterns were demonstrated during the investigation. In the high speed test conducted with the birdcage containers, the cargo was loaded with a minimum tie-down; while in the high-speed test conducted with the 15-ton cask, the cargo was rigidly attached to the bed of the

semitrailer. When the fully loaded tractor-trailer rigs collided with the barrier, the weight of the cargo was sufficient to cause complete destruction of the tractor through either failure of the fifth wheel or buckling of the tractor frame. In the test with the cargo of birdcage containers, only a minimum of energy was absorbed by the tractor because of the fifth wheel separation. Near maximum energy was absorbed by the more complete crushing of the tractor during the high-speed test with the cask. Complete quantitative measurements were not obtained because of the early failure of the tractor frames, which did not behave according to the pretest theory. Photographic measurements provided the most meaningful description of the dynamic behavior of the transport systems during these impacts.

Meaningful, although limited, structural and transportability data were obtained for use in developing the approach to solution formulation in the mathematical analysis of these tests. The mathematical model developed in the analysis does not describe accurately the actual behavior of the test vehicles during the impact tests, but when simplified to correspond with the dynamic behavior of the vehicles, the model should provide more compatible results. A model using the Runge-Kutta integration method for numerical solution requires high computation time. It would appear that when appropriate stiffness parameters are established for the principal elements, analog or hybrid simulation could provide a more flexible and versatile prediction of the actual response or dynamic behavior of the transport system under longitudinal head-on impact conditions.

It is recommended that the inherent weakness of the tractor-trailer combination and the physical limitations involved in measuring the transmission of force through the tractor be considered in any future development of a mathematical model. If future tests are conducted, it is recommended that the instrumentation plan be revised and that the impact force be measured on the barrier if correlation of values with a mathematical model is required. The tractor should be treated as a nonlinear spring with little or no instrumentation, and its behavior should be measured by high-speed photography. The quantitative electronic measurements should be made primarily on the trailer and cargo, and unbonded

strain-gage accelerometers with direct-current response should be used at the trailer and cargo load. Consideration should also be given to individual tension and compression forces in each member of the trailer.

Until such time that additional experimental data are made available, transportation criteria for the movement of high-density casks, such as the 15-ton cask used in this study, should ensure that the cask tie-down be designed to eliminate separation of the cask from the trailer. This can be accomplished by providing an adequate baseplate for the cask with tie rod connections attached. The force magnitudes experienced in the actual tests provide guidelines for designing the cask tie-down. For highway transport of nuclear or fissile materials, the fifth wheel of the vehicle and the fifth-wheel connections should be adequate to assure that the tractor and trailer will not separate as a result of a collision.

3. TEST FACILITIES AND TECHNIQUES

Four collision tests were performed with three different combinations of truck tractors and semitrailers. These vehicles were reported as surplus by the Army and Navy and were obtained at no cost except for processing and shipping expenses. The test site, test procedures, and the instrumentation used to record test data are described in this chapter.

3.1 Test Site

The site selected for the tests had a level 40-ft-wide road with a paved surface and sufficient straightaway to accommodate the tests. A barrier was placed at the south end of the road. This barrier, shown in Fig. 3.1, was constructed of armor plate braced with worn gun tubes. The materials, which weighed approximately 350 tons, were embedded in the road in a manner designed to provide for all practical purposes an immovable

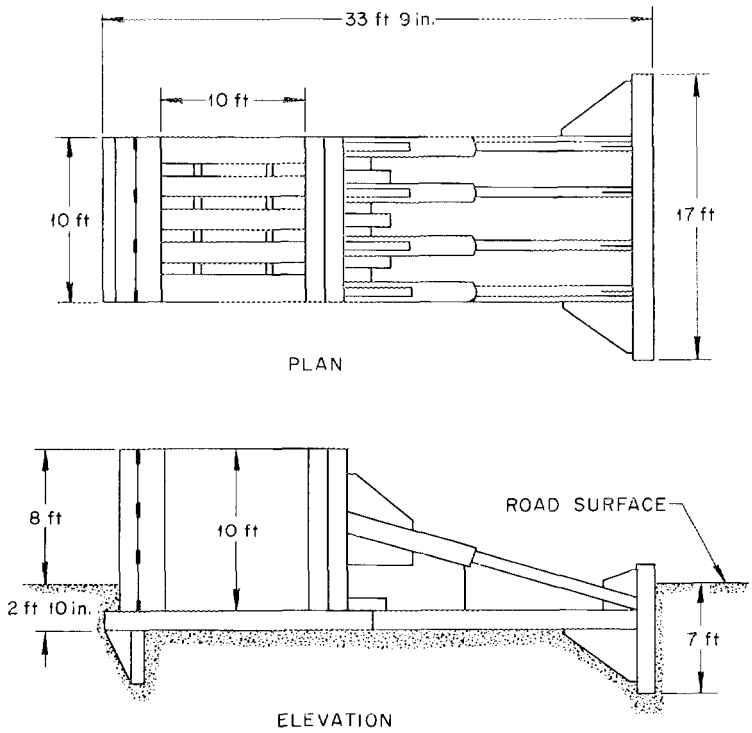

Fig. 3.1. Barrier at End of Test Road.

barricade. Initially, guide rails were provided near the barrier as a safety measure in the event that control of the test vehicle should be lost during a high-speed crash, but these rails were removed after the first test.

3.2 Test Procedures

Various methods were considered for propelling test vehicles into the barrier, but the method selected involved the use of each vehicle's own propulsion system. This required that each vehicle be fitted with devices for remote control of braking, steering, and throttle position. The remote-control mechanism for emergency braking is shown in Fig. 3.2,

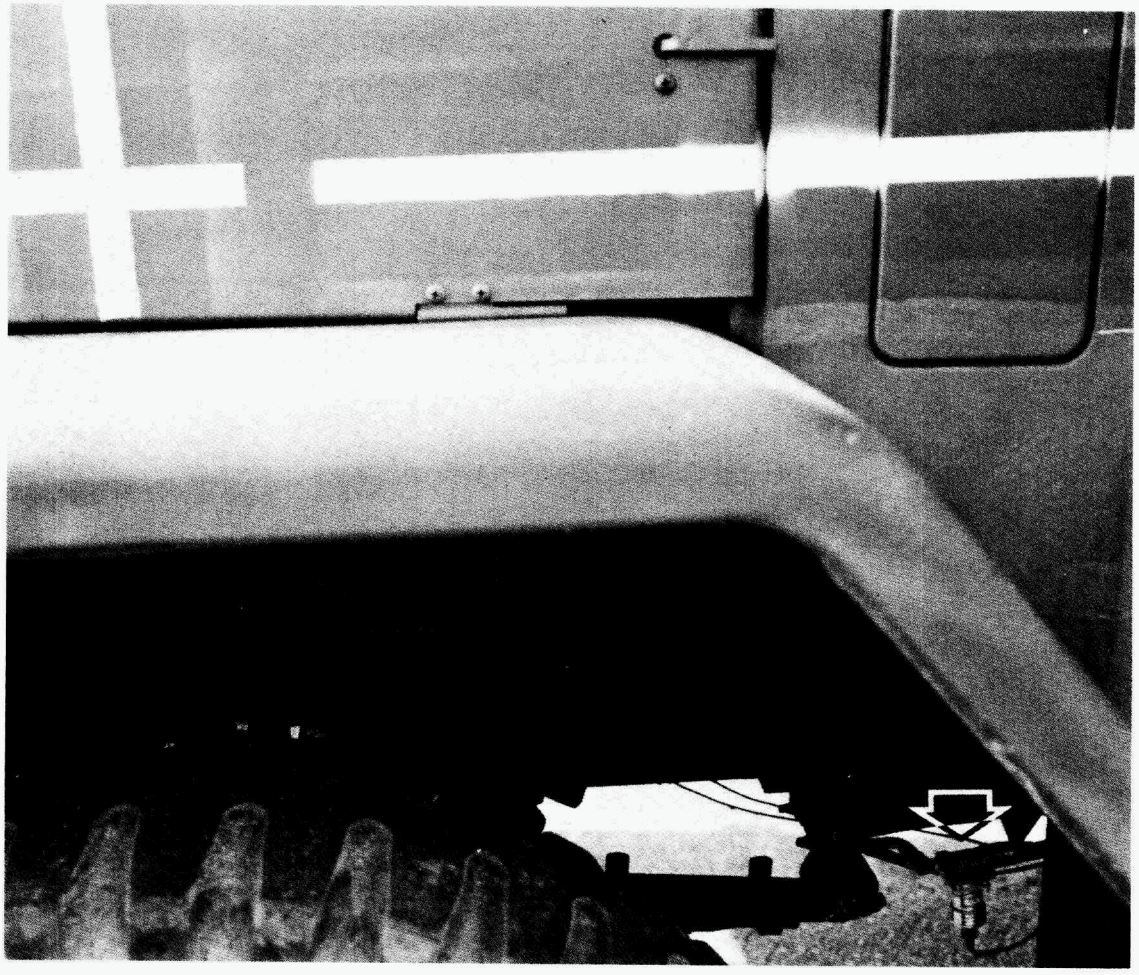

Fig. 3.2. Remote-Control Mechanism for Emergency Braking.

the remote-control mechanism for steering the vehicle is shown in Fig. 3.3, and the remote-control mechanism for adjusting the throttle setting is illustrated in Fig. 3.4.

Fig. 3.3. Remote-Control Mechanism for Steering the Vehicle.

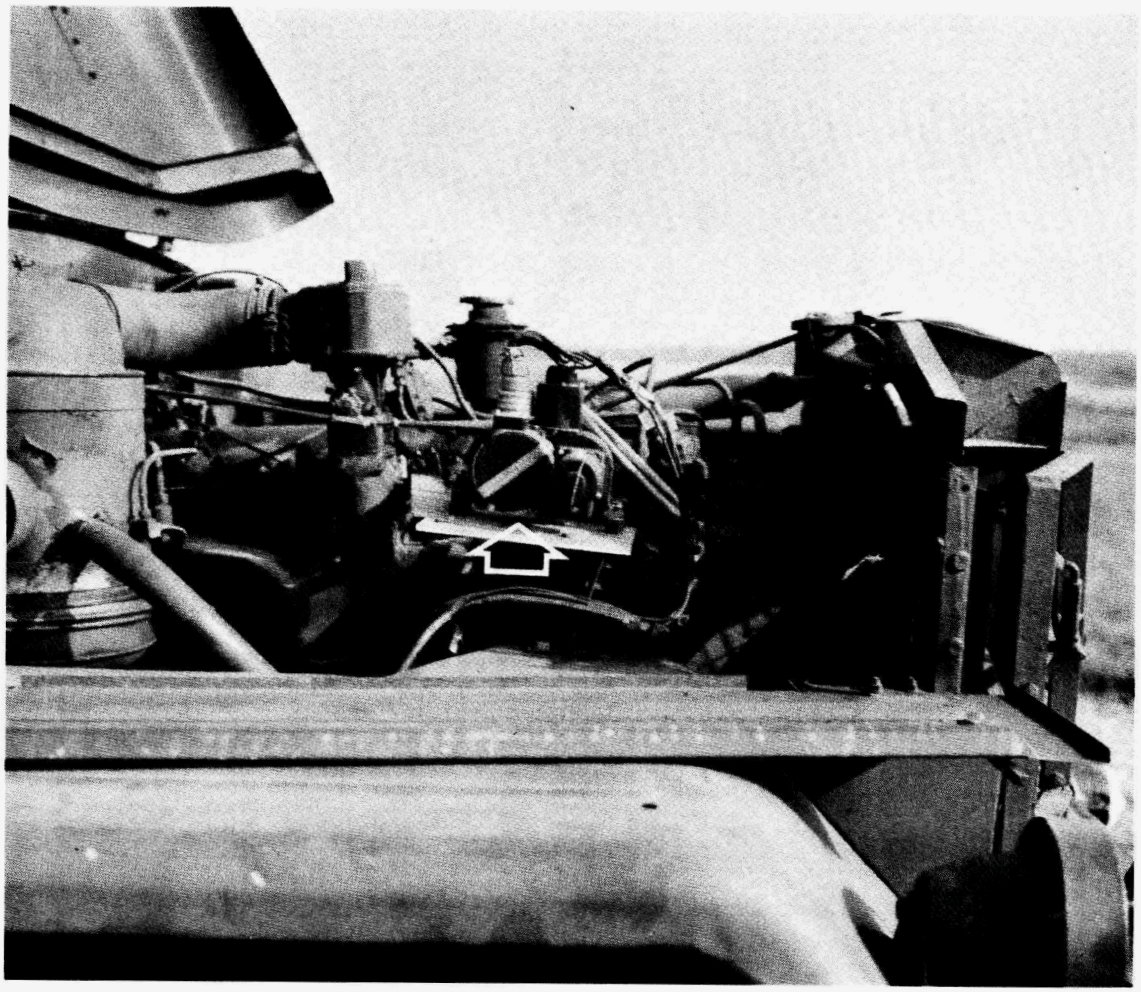

Fig. 3.4. Remote-Control Mechanism for Adjusting the Throttle Setting.

During all tests, the test vehicle was followed closely by an instrumentation van, shown in Fig. 3.5, from which remote control was provided and in which all transducer output was recorded. Umbilical cables 200 ft long encased in a vinyl sheath for protection against abrasion were used to interconnect the remote-control panel, shown in Fig. 3.6, with the control mechanisms in the test vehicle. These cables were also used for telemetering data by interconnecting transducers with the signal-conditioning and recording equipment.

The remote-control system was fabricated mostly from salvaged World-War-II aircraft components, and it had the capability for

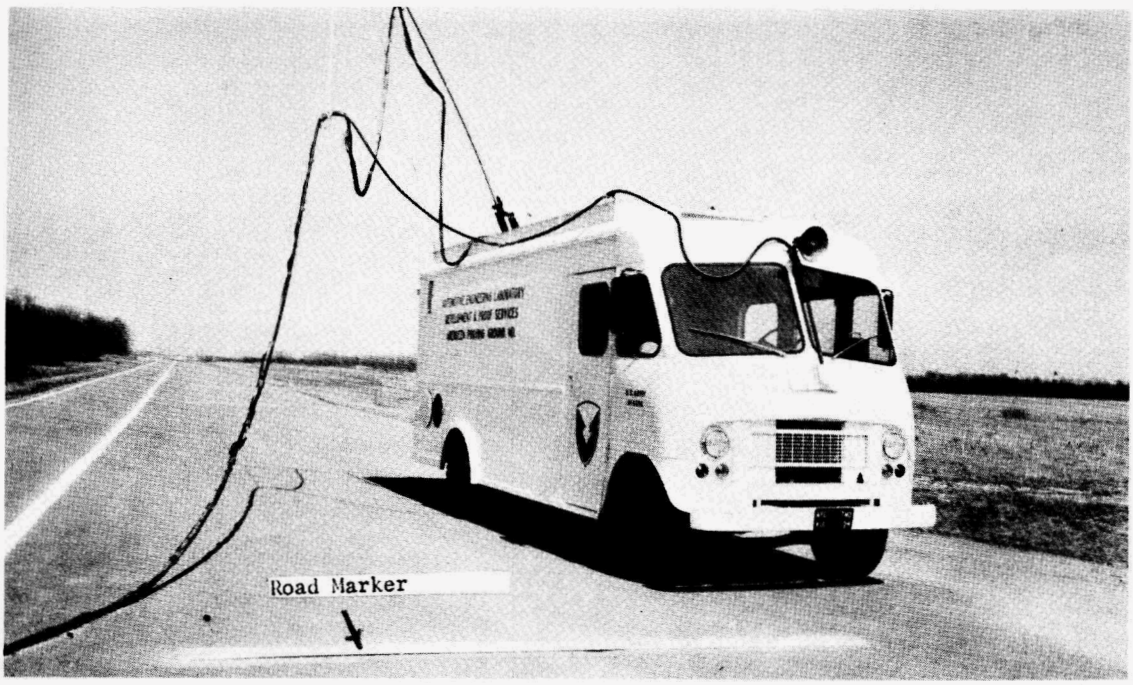

Fig. 3.5. Instrumentation Van.

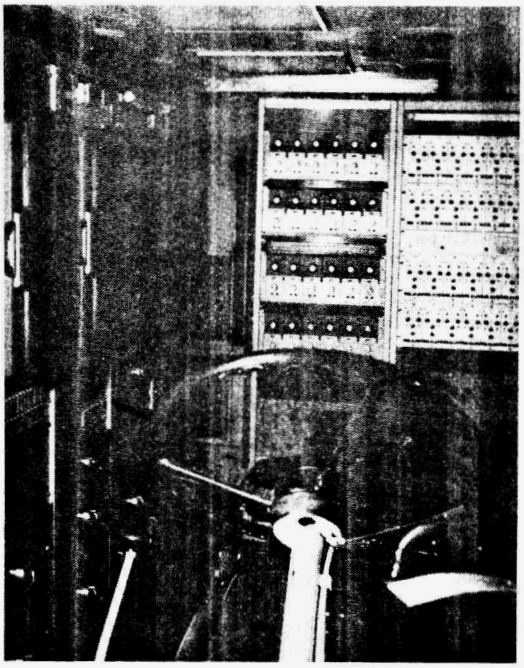

Fig. 3.6. Remote Control and Recording Equipment Mounted Inside the Instrumentation Van.

1. right and left steering,
2. adjusting the throttle setting,
3. controlled emergency braking to abort the test at any point up to the point of total commitment, and
4. fail-safe emergency braking should the umbilical cables be severed during the time the test vehicle was obtaining target speed.

The safety of personnel was of primary concern in conducting the high-speed collision tests. A preliminary study was made to determine the reaction time of drivers and the suitability of the remote steering and controls at high-speed operation. The stopping distance of the instrument van within the allowable separation distance of two vehicles for the limited cable length was also determined. Road markers were placed to indicate where the driver of the instrument van was to reduce speed, apply brakes, and stop the vehicle. These markers were made of 1- by 6-in. wood strips about 12 ft long that were nailed on the bituminous concrete road, as shown in Fig. 3.5. These wood strips were visible during approach, and they also were felt by the driver as the wheels of the vehicle passed over them.

At the beginning of each test run, the instrumentation van was positioned within about 30 ft of the test vehicle. The umbilical cable was pulled toward the test vehicle until it was suspended in the desired configuration and then attached to the test vehicle with a breakaway binding. The breakaway link was simple jute twine stranded to give a breaking strength of about 120 lb. The surplus cable was coiled on the rear deck of the test trailer so it would pay out smoothly as required. Strips of rubber with a breaking strength of about 50 lb that were cut from an unserviceable truck-tire innertube were used to tie each loop of the coiled cable to the trailer as a precaution against cable fouling. This cable suspension and tie-down arrangement permitted the instrument van to break away from the test vehicle at a predetermined point and come to a stop at a safe distance from the point of impact of the test vehicle, as illustrated schematically in Fig. 3.7.

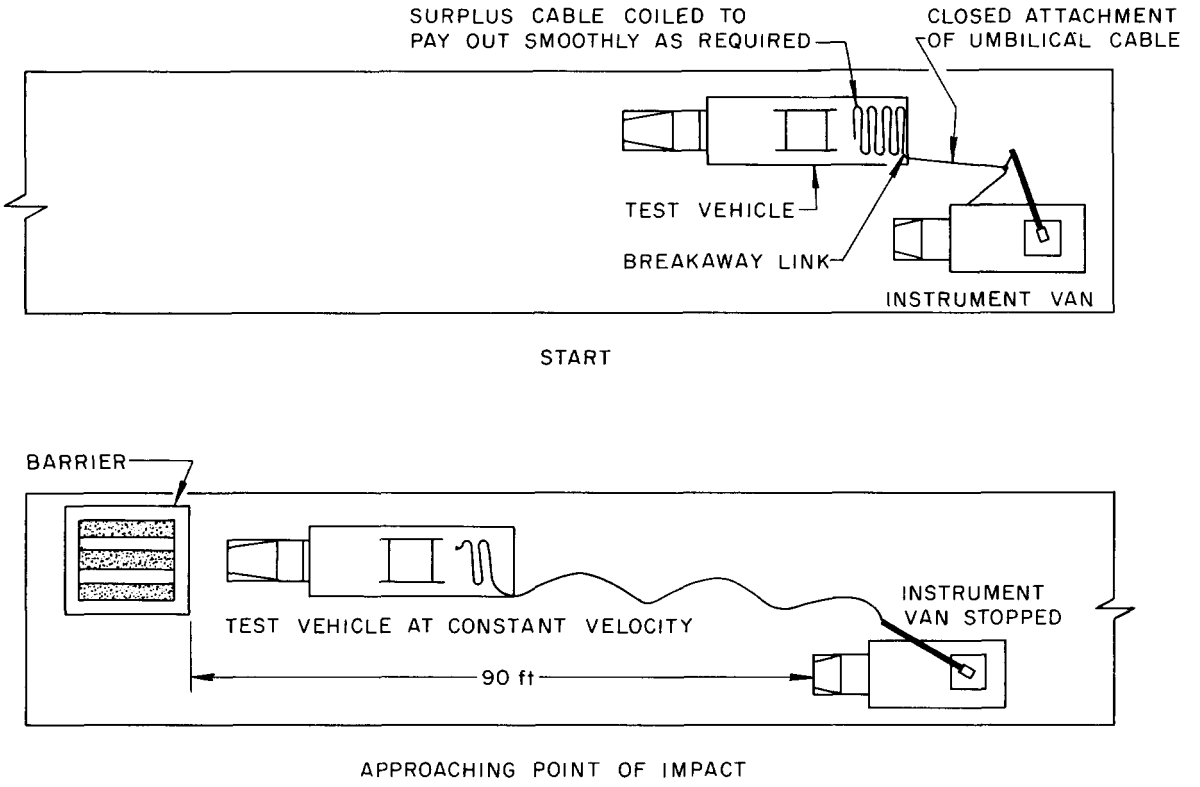

Fig. 3.7. Vehicle Control and Test Setup for High-Speed Collision Tests.

Initially, the test vehicle was started in low gear by a driver. When a speed of about 5 mph was attained, the driver shifted the tractor into the highest gear range practicable to achieve the required impact velocity, and he then abandoned the tractor. At this point, complete control of the test vehicle emanated from within the instrumentation van. The test vehicle was remotely brought up to impact speed and guided into the barrier.

3.3 Instrumentation

The recording systems used in the acquisition of force and acceleration data are illustrated in the block diagram shown in Fig. 3.8. This

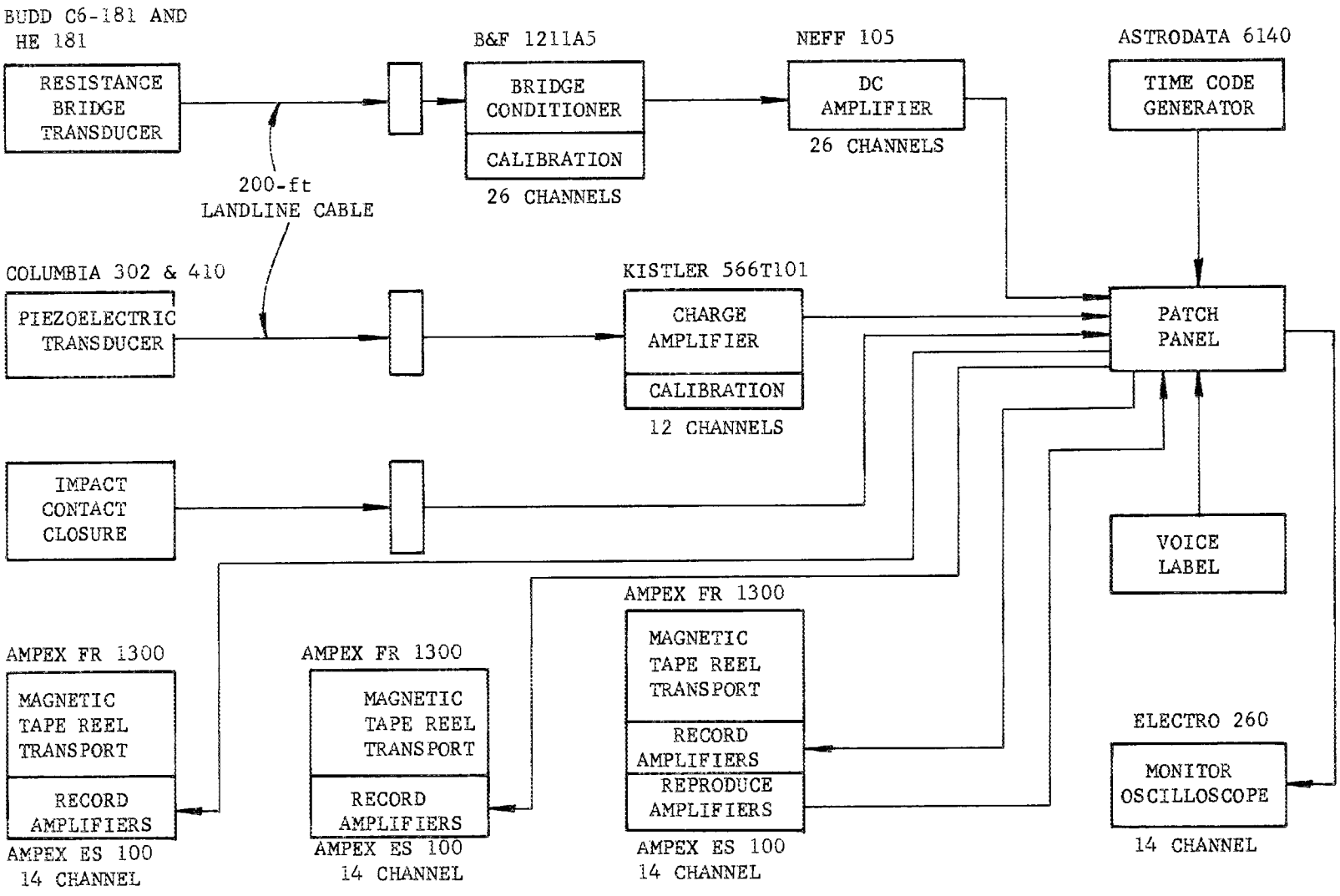

Fig. 3.8. Block Diagram of Data Acquisition System for Collision Tests.

basic system was used in each of the four tests described although the number of channels recorded ranged from 15 to 38 in the tests. Because each test vehicle was instrumented differently, the instrumentation plan for each test is described in the appropriate chapter. However, in all four tests, the recording system was operated to give 10 Hz to 18 kHz response and three types of transducers were used.

1. Force measurements were made with Budd Company metal-film strain gages, types HE-181B and C6-181. The resistance of these gages was 120 $\pm$ 0.2 ohms, and the gage factors were 2.05 $\pm$ 0.5% and 2.08 $\pm$ 0.5%, respectively.

2. The acceleration transducers were Columbia Research Laboratories, Inc., Models 300 and 302 piezoelectric accelerometers. Their range was 40,000 "g" and the frequency response was flat within $\pm$ 4% over the range 10 Hz to 6kHz.

3. Load cells for measuring the force of impact, as shown in Fig. 3.9, included two hollow cylindrical steel columns with a yield point of 75,000 psi. The steel columns were strain gaged and calibrated in a standard testing machine. Then one column was attached to each of the two frame members of the tractor. The strain gages were wired to measure the total force of impact and the force in one of the frame members [$F \epsilon (F/2)$]. The load cells had the capability to measure a force of impact of 1.88×10^6 lb and still behave elastically.

The actual speed of the test vehicle immediately prior to impact was measured by using a simple chronograph. The chronograph itself was an electronic counter triggered at a rate of 100,000 pulses per second. It was activated "on" by the front wheels and "off" by the rear wheels of the truck tractor passing over a tape switch stretched across the road about 20 ft in front of the barrier. The distance traveled during the indicated time was then the wheelbase or the distance between the vertical center lines of the front axle and the rear axle of the tractor.

Fig. 3.9. Load Cells on Front of Cab-Over-Motor Tractor.

The types and locations of sensors were selected to provide input data required to determine the validity of the mathematical model previously developed by The Franklin Institute Research Laboratories (Report I-A2412-4, December 1964). Photographic coverage was provided for both documentary purposes and for photomeasurement. Extreme coverage, as shown in Fig. 3.10, was provided for the high-speed impacts, but only documentary coverage was provided for the low-speed exploratory tests.

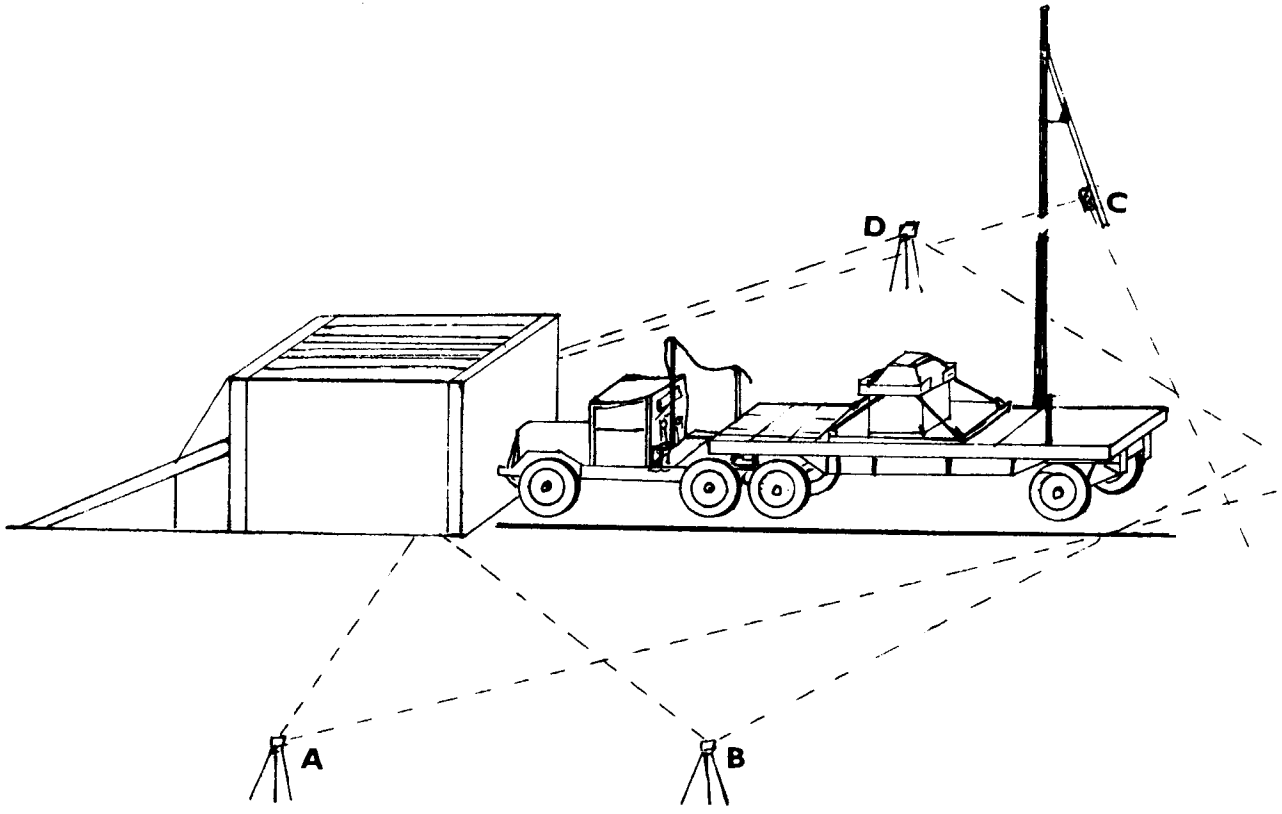

Locations:

A	B	C	D
1 - 2000 f/s (16-mm Fastax)	1 - 30 f/s (70-mm Hulcher)	1 - 30 (70-mm Hulcher)	1 - 100 (35-mm Mitchell)
1 - 1000 f/s (16-mm Fastax)	2 - 1000 f/s (16-mm Photo Sonics)	1 - 100 (35-mm Mitchell)	
1 - 100 f/s (35-mm Mitchell)	1 - 2000 f/s (16-mm Fastax)		
1 - 1000 f/s (16-mm Photo Sonics)	1 - 100 f/s (35-mm Mitchell)		
1 - 200 f/s (16-mm Benson Lehner Color)	1 - 200 f/s (16-mm Benson Lehner Color)		

Fig. 3.10. Locations of Camera for Different Collision Tests.

4. TEST NUMBER ONE

The first test was an exploratory nondestructive test with a low speed impact against the barrier and no cargo in the semitrailer. A velocity of 4 mph was selected as the nominal or target velocity for this exploratory impact test, but the actual speed immediately prior to impact was measured as 4.5 mph. This test was conducted to

1. familiarize testing personnel with the facilities, equipment, and techniques;
2. test the operation of the remote-control equipment; and
3. record limited quantitative force and accelerometer measurements as a basis for predicting the optimum transducer gain levels for subsequent impacts at higher speeds.

4.1 Test Vehicle

The first test was conducted with a 4 by 2 cab-behind-motor commercial type of tractor and an empty van type of semitrailer, as shown in Fig. 4.1. The gross weight of the tractor-trailer combination for this test was 17,915 lb.

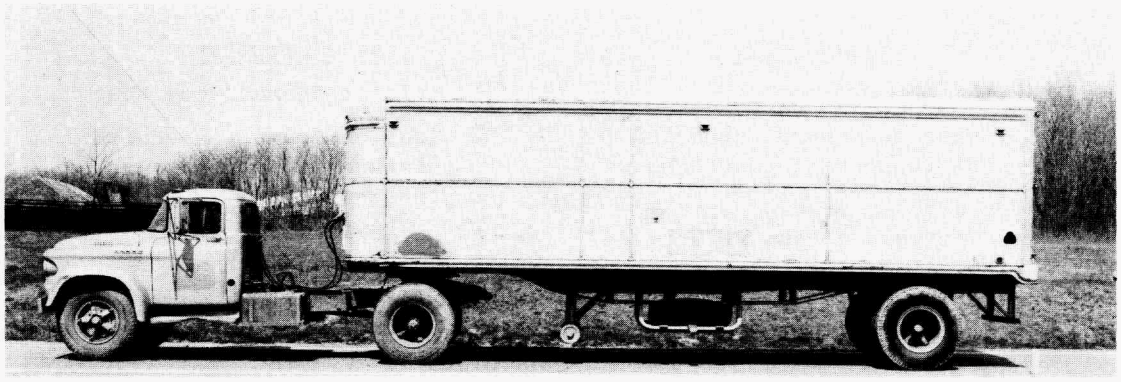

Fig. 4.1. Vehicle Used in First Collision Test.

4.2 Instrumentation

The front bumper of the test tractor was modified by adding two load cells. A typical arrangement for measuring the total impact force was illustrated in Fig. 3.9. Three strain gage bridges were allotted for measuring the right, left, and total load-cell force. Six additional strain-gage bridges were applied to the tractor frame and one other bridge was applied on the tractor suspension. Only two strain-gage bridges were applied to the frame of the semitrailer. Five piezoelectric accelerometers were installed on the tractor-trailer combination. A diagram of this instrumentation is shown in Fig. 4.2.

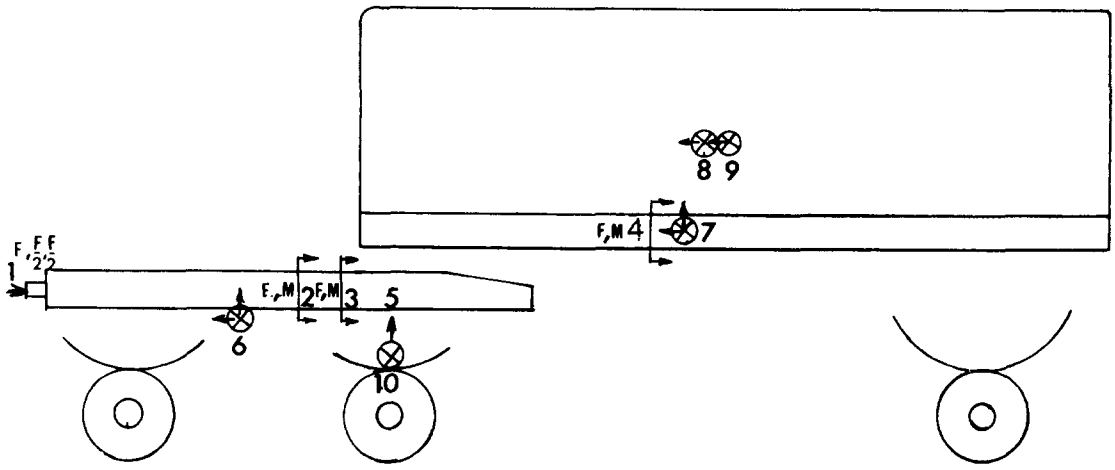

Strain Gage		Accelerometer	
1	Front Dynamometers	6	Tractor frame, under cab
2	Tractor frame, front of forward spring attachment	7	Trailer frame, one-third distance from front end of trailer
3	Tractor frame, rear of forward spring attachment	8*	Birdcage package
4	Trailer frame, one-third distance from front end of trailer	9*	Birdcage package
5	Tractor, rear spring	10	Tractor, top of differential housing

*Not included in first test

Fig. 4.2. Location of Transducers on Vehicle for First Test.

Limited photographic coverage of the test provided high-speed movie film of the left side of the vehicle at 1000 fps (16 mm) and of the right side at 1000 fps (16 mm) and at 100 fps (35 mm). Exclusive of photographic coverage, all other operating and recording techniques and procedures described in Chapter 3 that were applicable to this low-speed impact were followed.

4.3 Results of First Test

As previously mentioned, the actual speed of the test vehicle immediately prior to impact was 4.5 mph. Time histories of forces and accelerations were recorded during the impact, and the total force measured by the load cells reached a peak value of about 62,000 lb, as is shown in Fig. 4.3. However, the load cells mounted on the front of the vehicle did not strike the barricade squarely. The left load cell struck first as a result of the left front wheel of the tractor striking the guard rail during the approach. The tractor was deflected to the right immediately prior to contact with the barrier.

The guard rails appeared to influence the remote-control operator's perspective during the approach of the test vehicle to the barrier even at the slow speed of 4.5 mph. As the vehicle entered the most restrictive part of the guard funnel, the operator was prone to overcontrol the tractor-trailer rig. Based on the demonstrated precision of the remote control system and the subjective evaluation of the operating personnel, it was decided that the guard rails were more hindrance than help. The rails were therefore removed for all the subsequent tests, and reliance was placed on the ability of the remote-control operator to steer the test vehicle into the barrier by using a painted road stripe as an aiming reference.

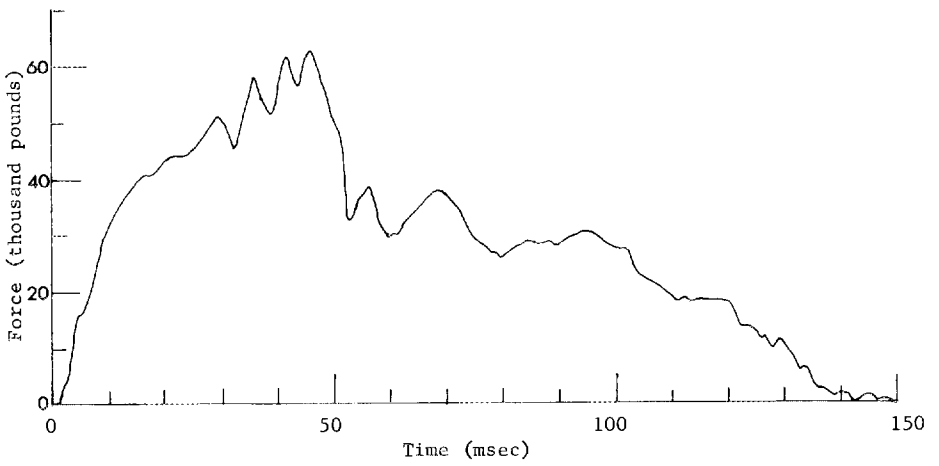

(a) Total Impact Force on Front Load Cells

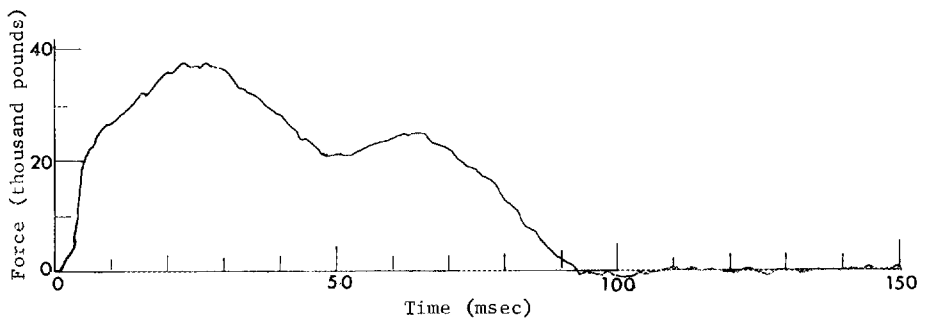

(b) Impact Force on Left Load Cell Only

Fig. 4.3. Impact Force at 4.5 mph Velocity Measured By Load Cells.

The axial force measurements that were recorded are shown in Fig. 4.4, the bending moment measurements recorded for the tractor frame and trailer frame are shown in Fig. 4.5, and the axial acceleration measurements for the tractor and trailer frames are shown in Fig. 4.6.

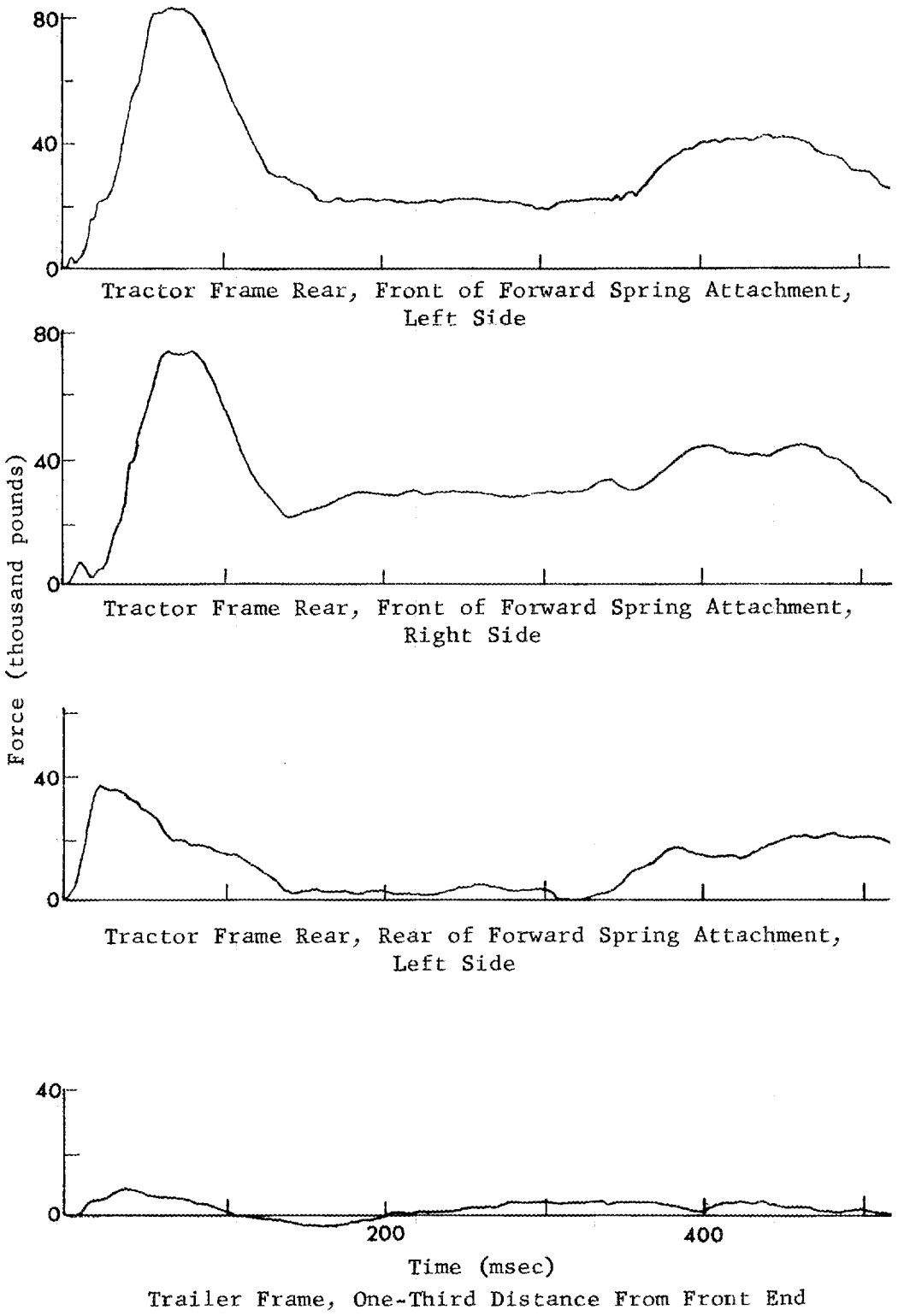

Fig. 4.4. Axial Force Measurements on the Tractor and Trailer Frames Resulting From 4.5-mph Impact.

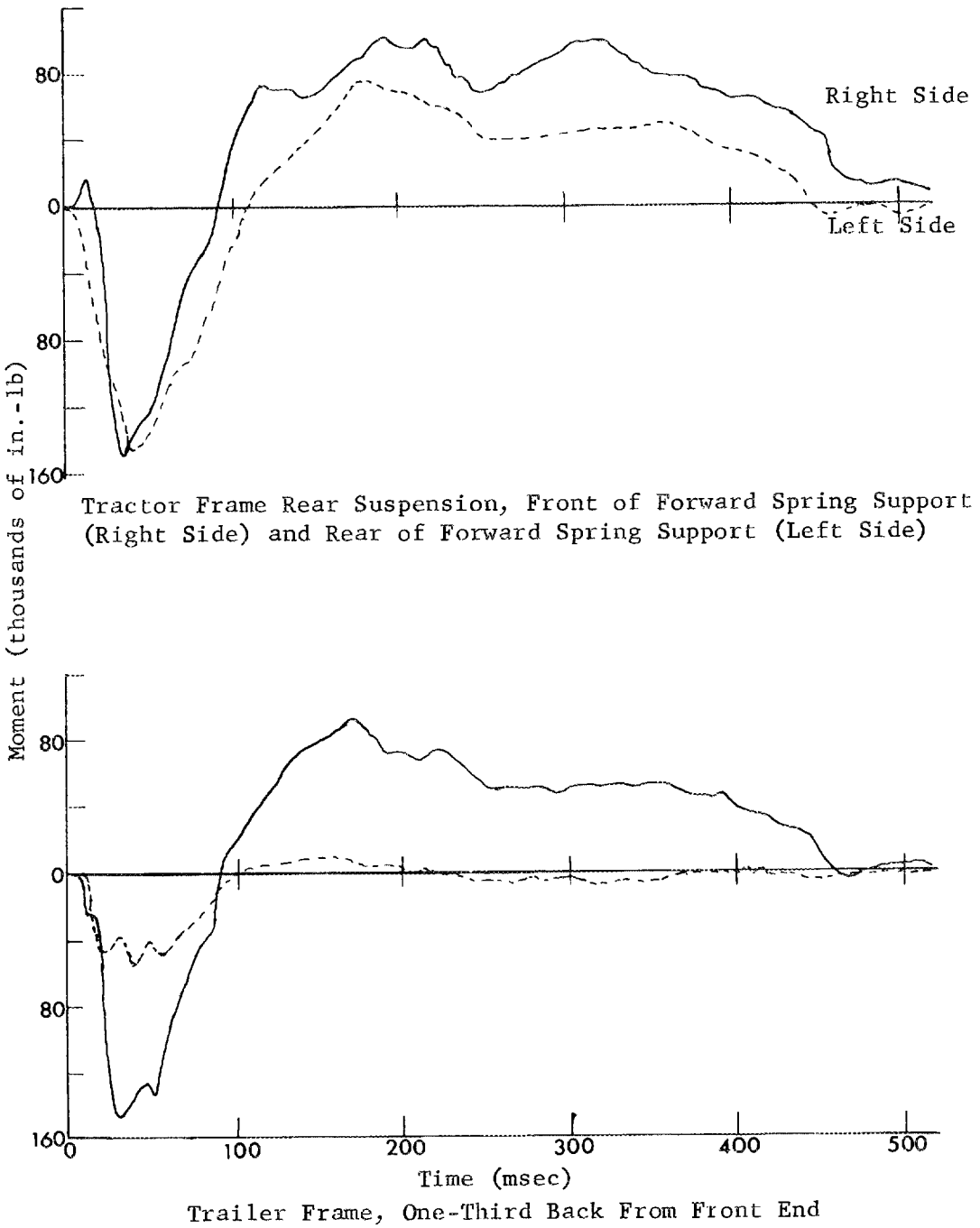

Fig. 4.5. Bending Moment Measurements on Tractor and Trailer Frames Resulting From 4.5-mph Impact.

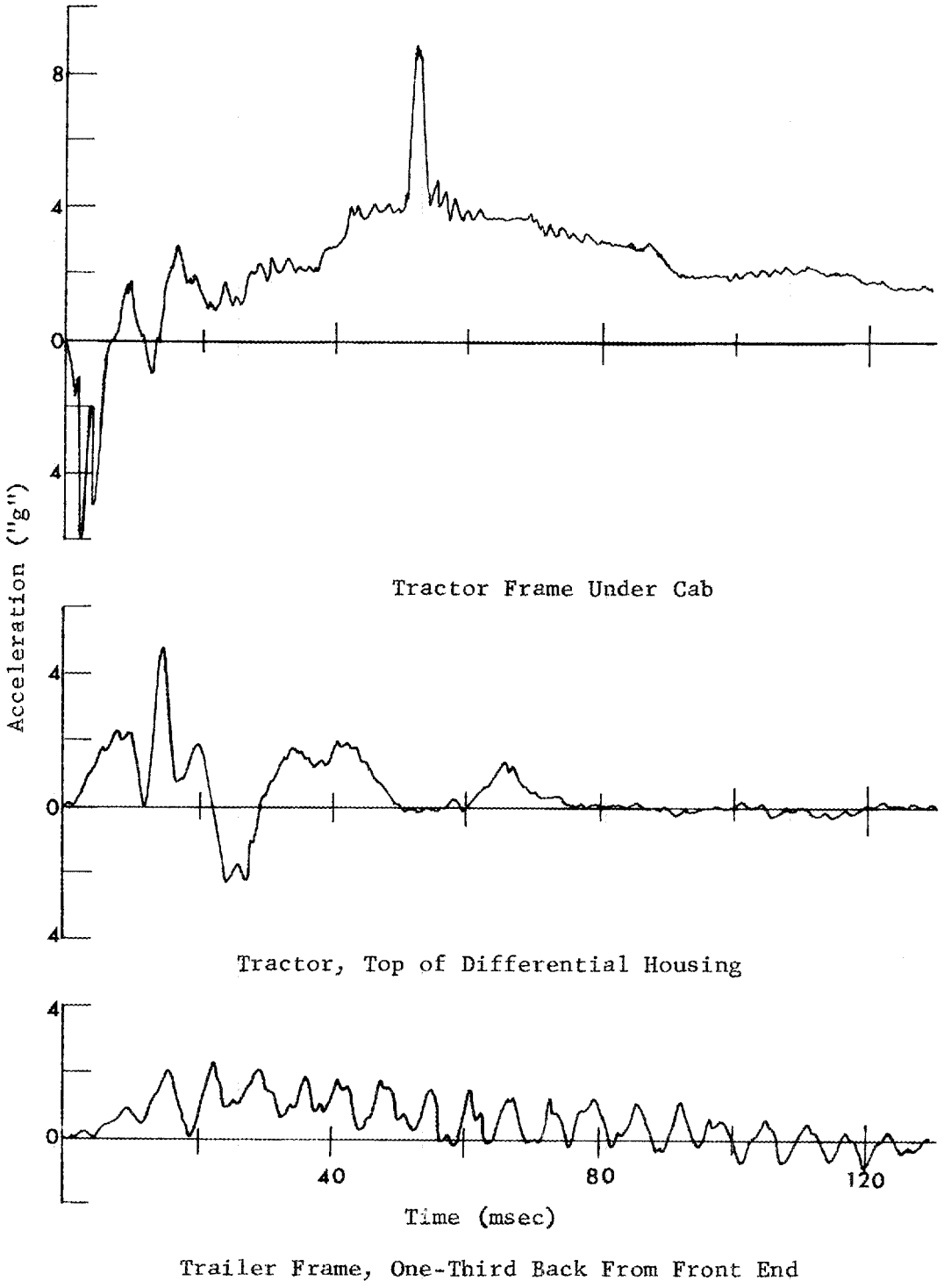

Fig. 4.6. Axial Acceleration Measurements (Filter 5 to 240 Hz Bandpass) on Tractor and Trailer Frames Resulting From 4.5-mph Impact.

It was stated in the report from the Aberdeen Proving Ground that there was no physical damage to the tractor or trailer as a result of this first test. The extent and scope of examination of the test vehicle for structural defects either before or after the exploratory collision test was not reported. However, this lack of detailed information may be more representative of actual transportation conditions than a detailed examination would have been.

5. TEST NUMBER TWO

A nominal velocity of 45 mph was selected as the vehicle speed upon impact with the barrier for the second test, which was conducted with cargo in the trailer. There were two broad objectives of the second test. The primary objective was to determine photographically the dynamic behavior of the transportation system and its loosely stowed cargo during a head-on collision. The resultant damage to the cargo would then be assessed. The secondary objective was to obtain quantitative measurements of force for subsequent use in the mathematical study.

5.1 Test Vehicle

The test vehicle used in the second test was the same 4 by 2 cab-behind-motor commercial type of tractor and van type of semitrailer that was used in the first test. However, the roof of the van semitrailer was removed to permit motion-picture coverage of the cargo with the overhead cameras. In addition, the rear doors of the trailer were removed to provide access to the rear deck where the surplus umbilical cable was coiled. The axle ends were painted white, and reference marks were painted on the left side of the van. The extreme front mark was aligned with the rear axle of the tractor, and the extreme rear mark was aligned with the rear axle of the trailer. The total weight of the test vehicle and cargo was approximately 45,000 lb.

5.2 Vehicle Cargo

For this preliminary high-speed collision test, it was decided by the Advisory Committee of the Joint AEC-DA Transportation Study that the semitrailer would be loaded with several types of so-called birdcage containers then in use for the shipment of nuclear material. Thirty-three birdcage packages representing six types of these containers were placed

in the trailer. These six types were the

1. Los Alamos Scientific Laboratory B of E Permit 1736 (now designated as DOT Specification ICC-6L) combination shipping container ICC-2R and ICC-6J, shown in Fig. 5.1;
2. Union Carbide Corporation, Nuclear Division (Oak Ridge, Tennessee), B of E Permit 1685 20-in. birdcage in banded plywood box, shown in Fig. 5.2;
3. USAEC Design KKD-1 (or LLD-1) container, shown in Fig. 5.3;
4. eight-inch Schedule-40 pipe inside 55-gallon drum container, shown in Fig. 5.4;
5. Union Carbide Corporation, Nuclear Division, B of E Permit 1561 Y-12 foamglas shipping container shown in Fig. 5.5; and
6. three-liter class II container shown in Fig. 5.6.

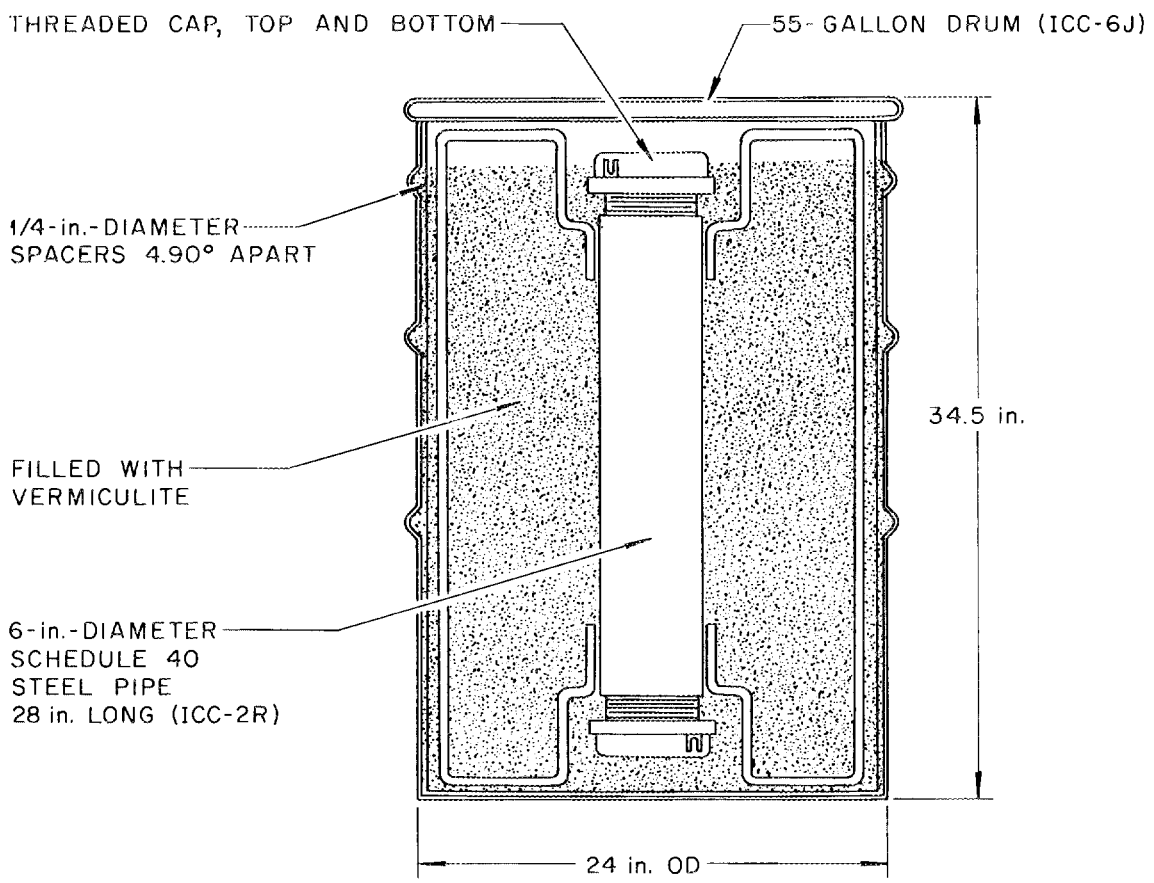

Fig. 5.1. Los Alamos Scientific Laboratory B of E Permit 1736 Combination Shipping Container ICC-2R and ICC-6J.

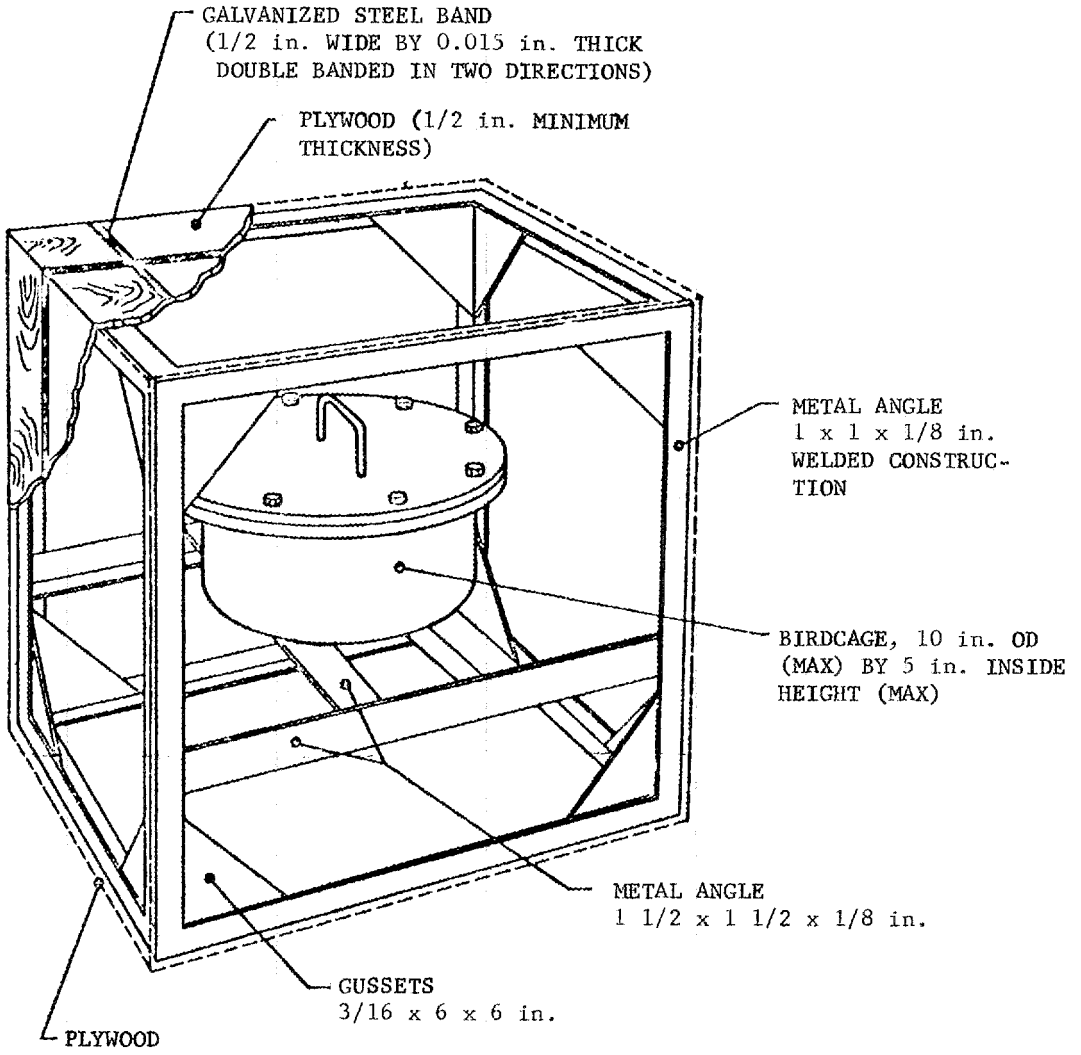

Fig. 5.2. Union Carbide Corporation, Nuclear Division, B of E Permit 1685 for 20-in. Birdcage in Banded Plywood Box for Enriched Uranium Metal or Dry Uranium Compounds.

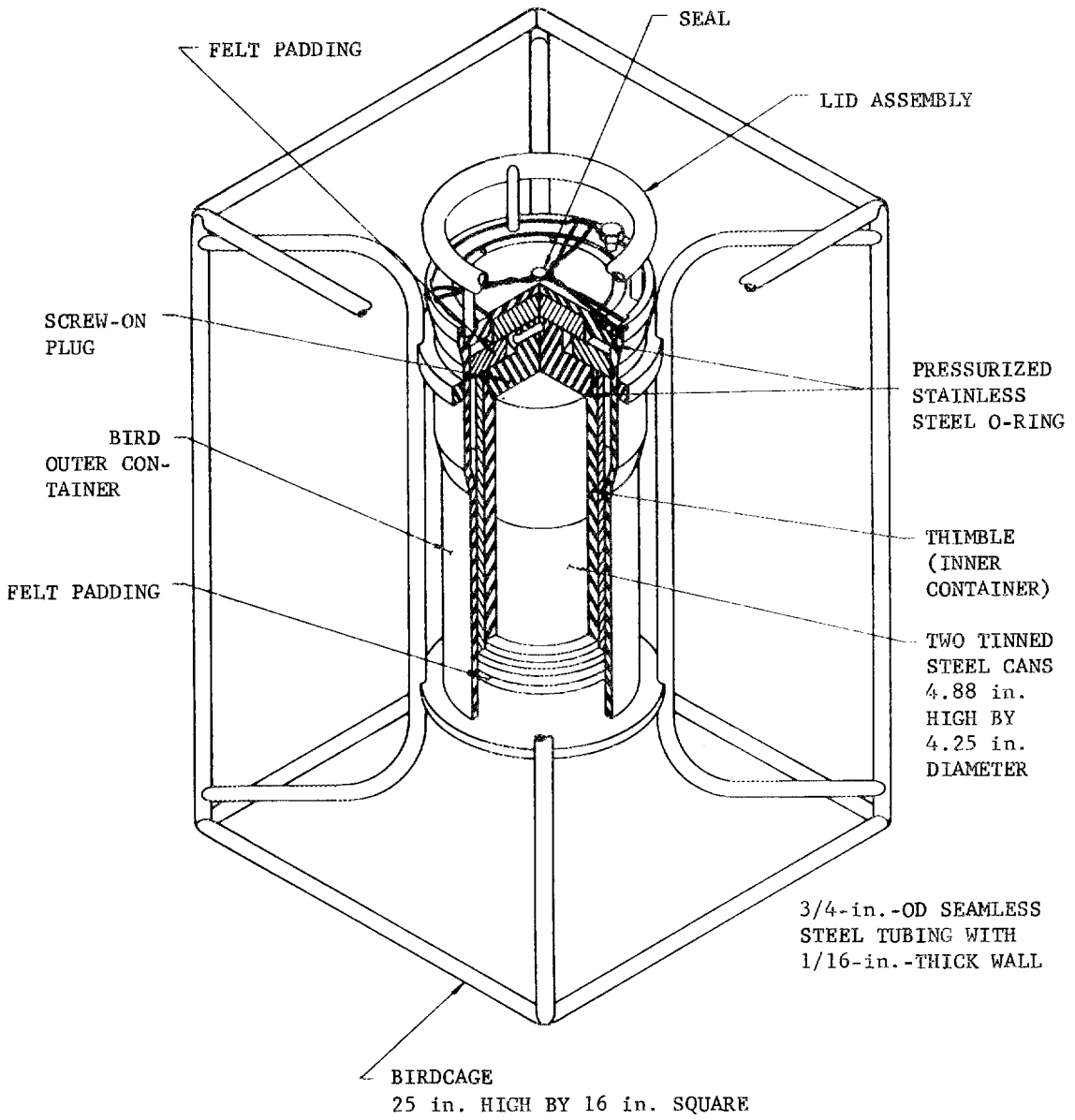

Fig. 5.3. USAEC Design KKD-1 (or LLD-1) Rocky Flats Birdcage for Enriched Uranium and Plutonium Metal (B of E Permit 1757).

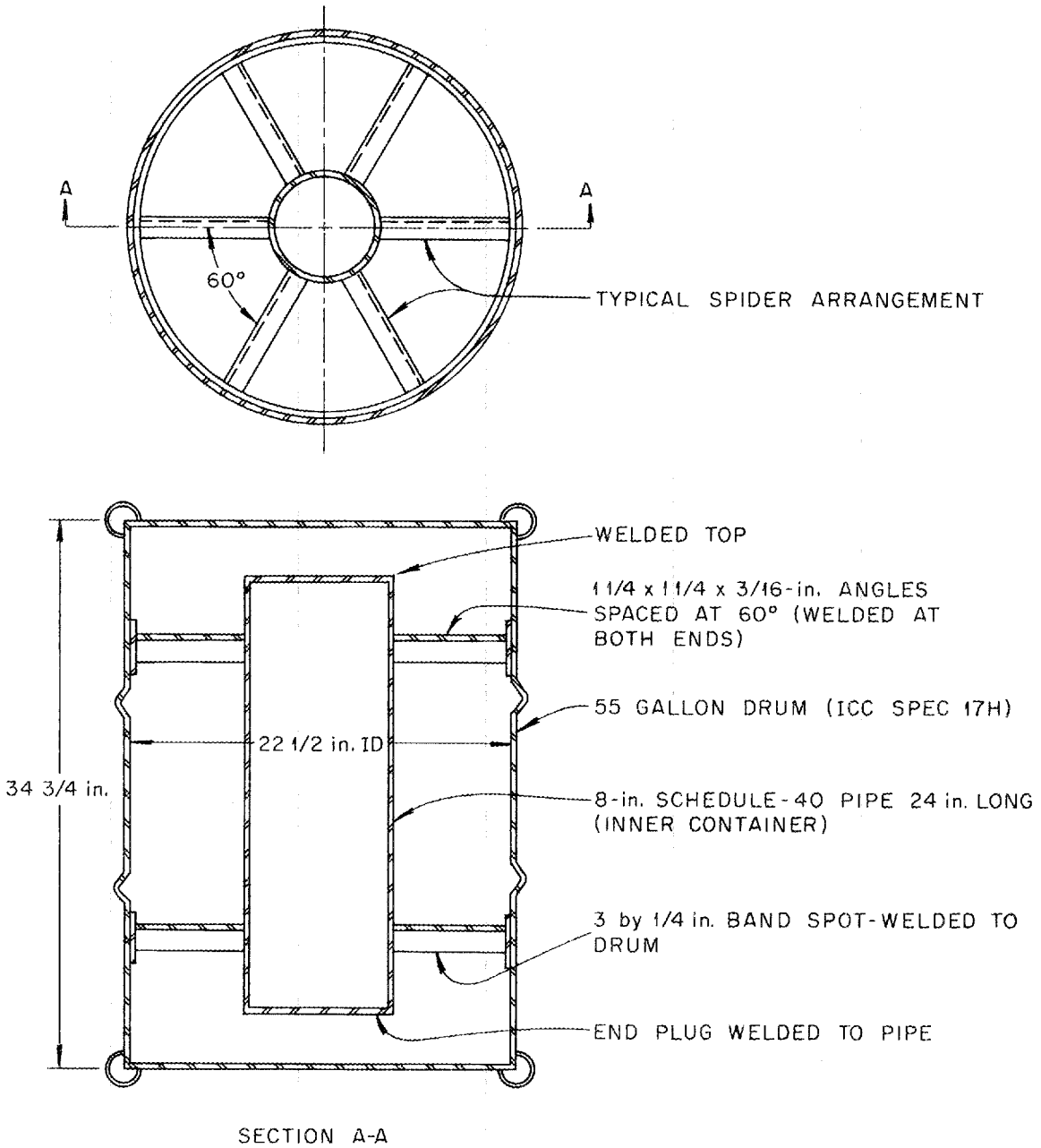

Fig. 5.4. Eight-Inch Schedule-40 Pipe Inside 55-Gallon Drum Container.

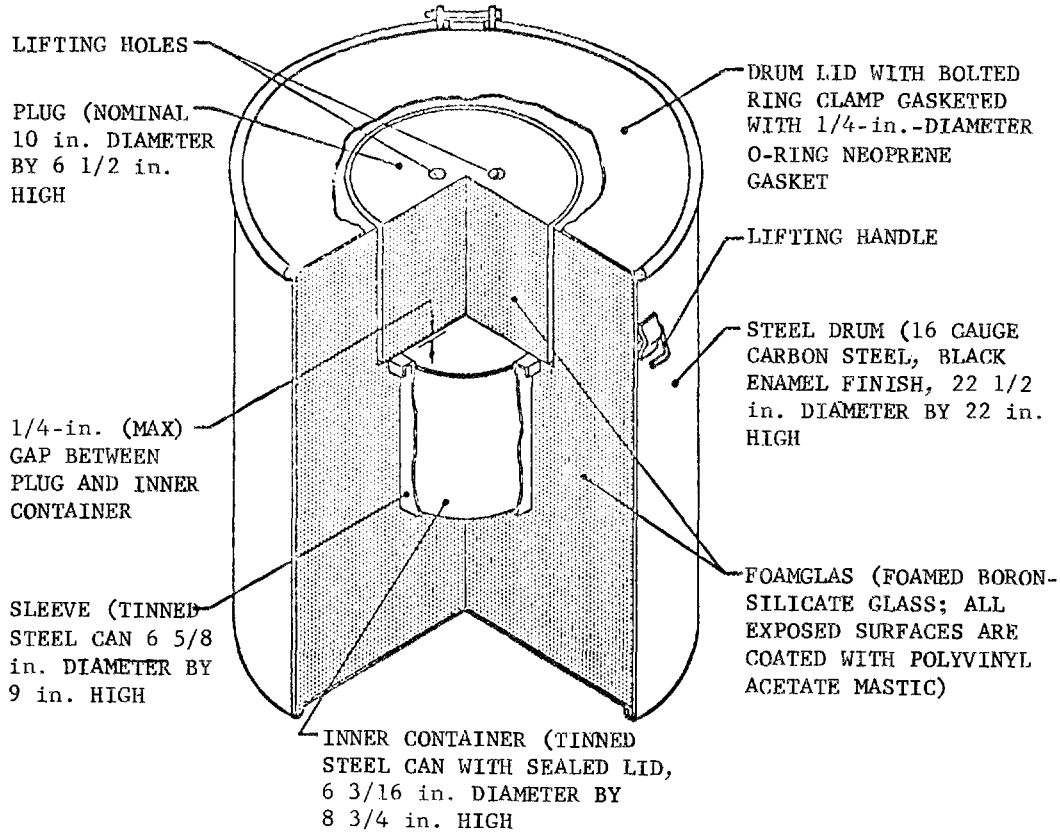

Fig. 5.5. Union Carbide Corporation, Nuclear Division, B of E Permit 1561 for Y-12 Foamglas Shipping Container for Uranium Metal and Dry Uranium Compounds (Ref. Documents Y-KB-22 and Y-KC-28).

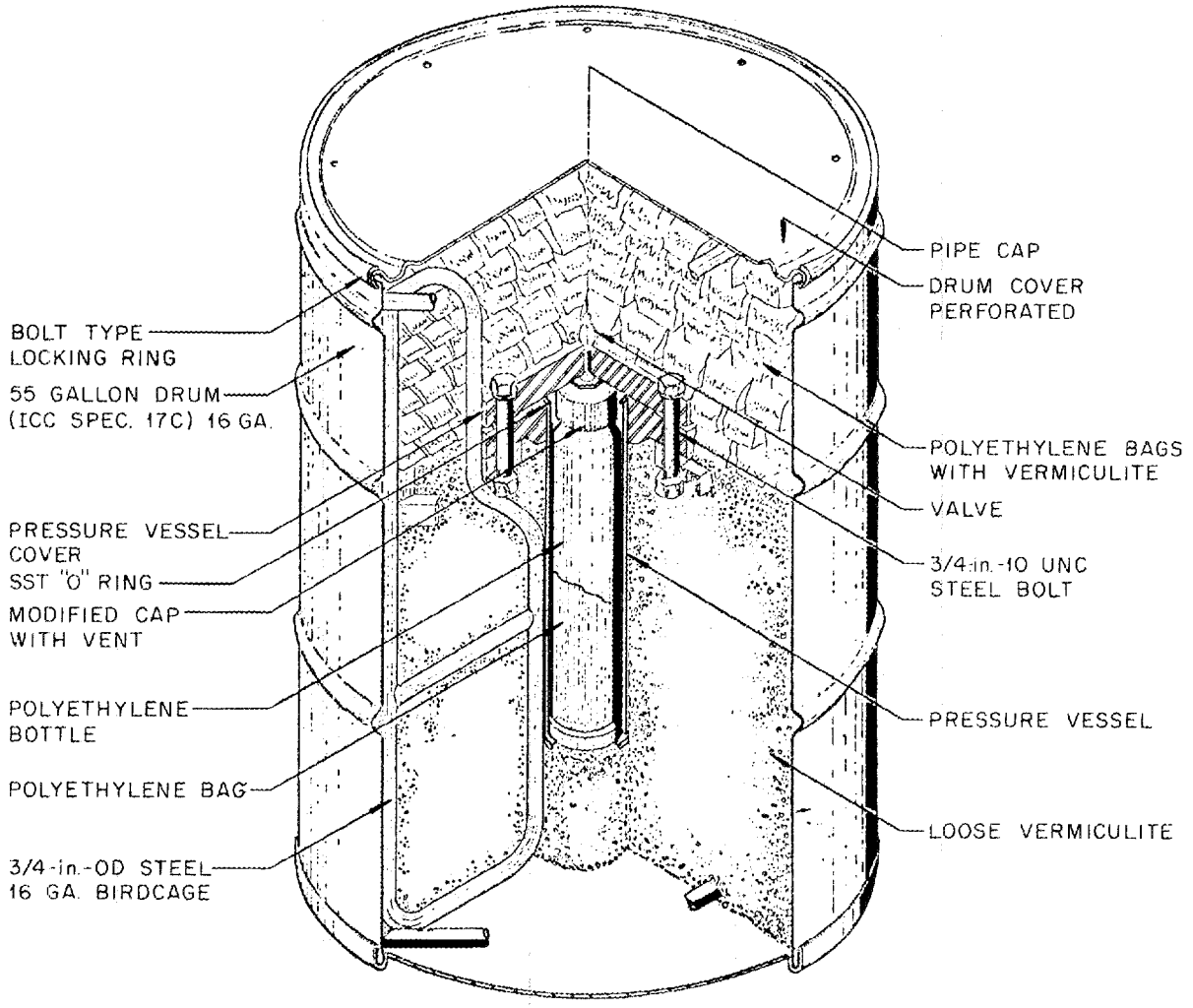

Fig. 5.6. Three-Liter Class II Container.

Since it was felt that special packages containing nuclear materials were sandwiched between heavy loads in a large portion of the shipments made by common carrier trucks, the loading plan for the trailer provided for the test packages to be loaded between cargo containers of crushed stone in 30- and 55-gallon steel drums, as shown in Fig. 5.7. There were two levels of loading in the trailer with four rows of test containers in the lower level (Rows A, B, C, and D) and four rows in the upper level (Rows E, F, G, and H). However, the two middle rows (F and G) were empty

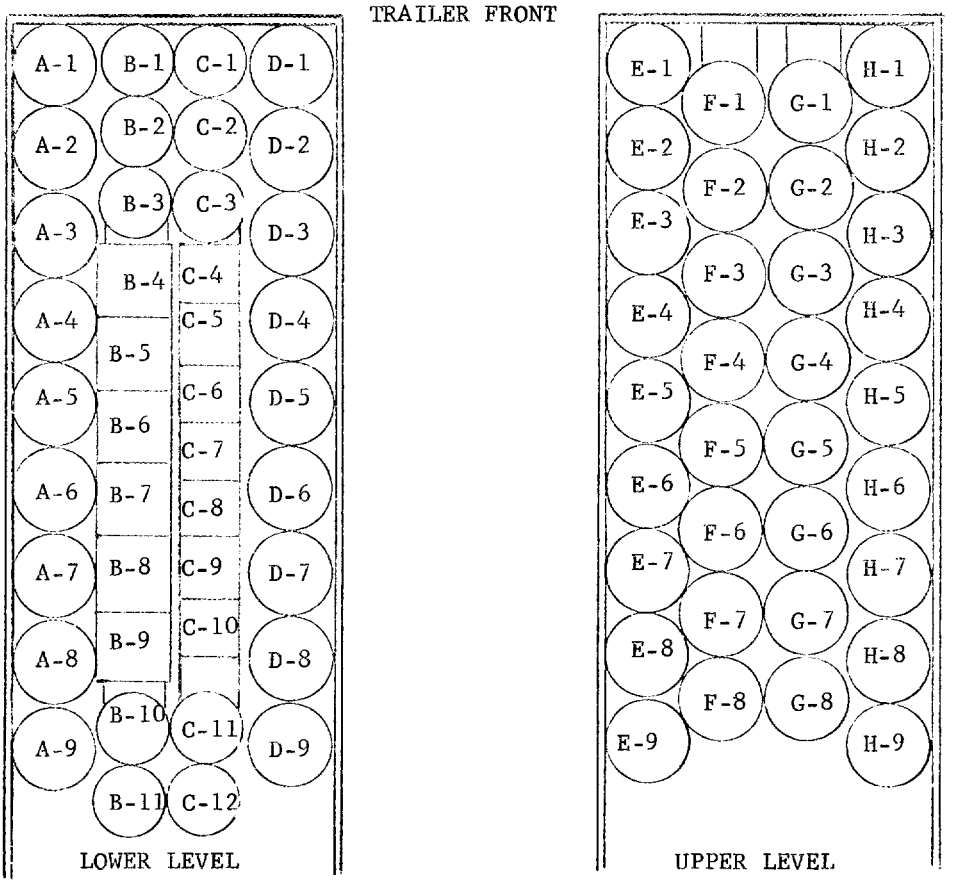

Birdcage Containers

Row A: L.A. Containers B of E Permit 1736, A-3 to A-7, inclusive
Row B: UCC 20-in. birdcage containers, B-4 to B-9, inclusive
Row C: KKD-1 Containers, C-4 to C-10, inclusive
Row D: 8-in. Schedule-40 pipe in 55-gallon drum, D-3 to D-7, inclusive
Row E: UCC Y-12 foamglas containers, E-3 to E-7, inclusive
Row H: 3-liter Class II containers, H-3, H-5, and H-7
L.A. Containers, B of E Permit 1736, H-4 and H-6

Cargo Drums

Row A: 55-gallon drums completely filled, A-1, A-2, A-8, and A-9
Row B: 30-gallon drums with 20-in.-load, B-1, 2, and 3, and B-10 and 11
Row C: 30-gallon drums with 25-in.-high load, C-1, 2, and 3, and C-11 and 12
Row D: 55-gallon drums completely filled, D-1, D-2, D-8, and D-9
Row E: 55-gallon drums with 22-in.-high load, E-1, E-2, E-8, and E-9
Row H: 55-gallon drums completely filled, H-1, H-2, H-8, and H-9

Empty (Fill-in) 55-Gallon Drums

Row F: F-1 to F-8, inclusive
Row G: G-1 to G-8, inclusive

Fig. 5.7. Cargo Loading Arrangement in Semitrailer for the Second Test.

fill-in drums. One type of test container was placed in each row except for Row H, which was made up of two types of test containers.

The cargo weight was arranged as shown in Fig. 5.8. The loading plan called for 10,500 lb of cargo containers located in front of the

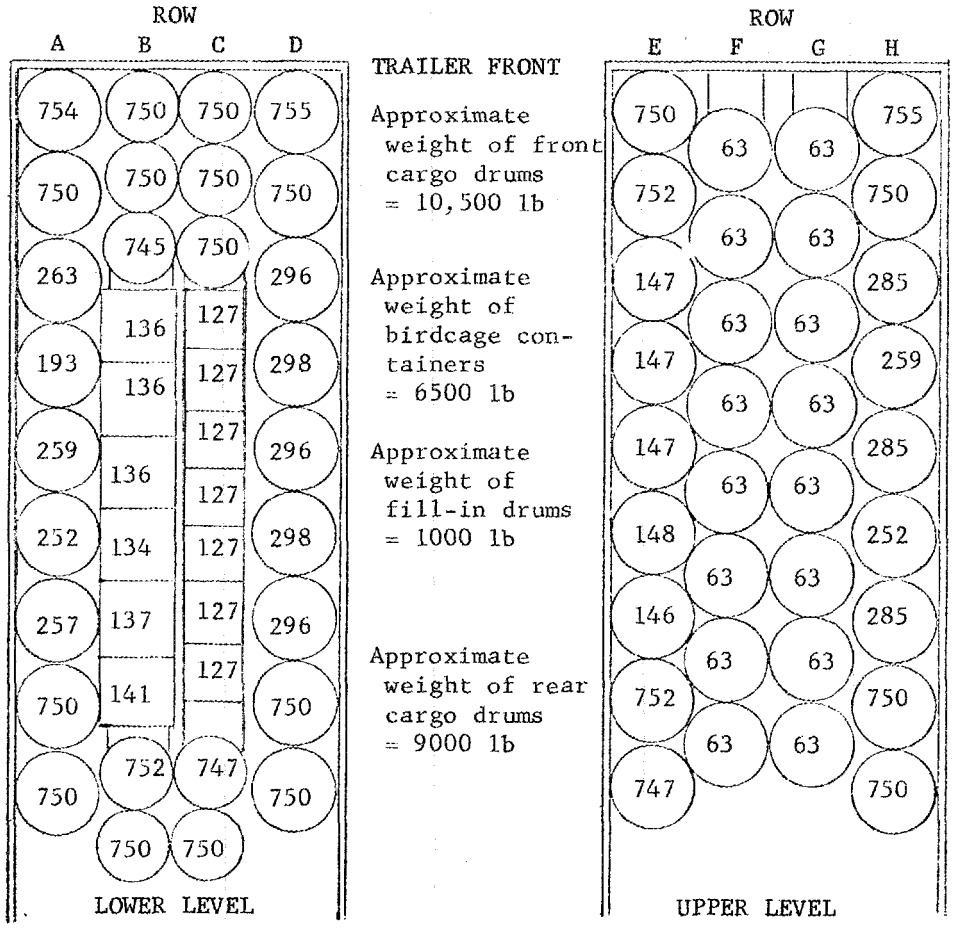

Approximate Weights of Simulated Contents of Birdcage Containers

Row A: 60 lb (except that A-4 had no contents)
Row B: 50 lb
Row C: 35 lb
Row D: 135 lb
Row E: 50 lb
Row H: 20 lb (H-3, H-5, and H-7)

Cargo Weights		Vehicle Weights (curb)	
Lower level,	17,925 lb	Tractor,	7,865 lb
Upper level,	9,115 lb	Trailer,	10,050 lb
Total	27,040 lb	Total	17,915 lb

Total weight of loaded vehicle = 44,955 lb.

Fig. 5.8. Cargo Weights in Semitrailer for Second Test.

test containers, 9000 lb of cargo containers behind the test containers, and an additional 1000 lb for the empty fill-in drums. The radioactive contents of the test containers were simulated by conventional materials such as sand, steel, and lead to approximate the desired weights of these containers, which weighed 6523 lb. The gross weight of the trailer was 27,000 lb. There was no tie-down of the containers to the floor of the trailer.

As measurements were made of the position of each package in the trailer, paint was sprayed on the bed of the trailer around the containers in the lower level to visually indicate the position of these containers prior to impact. The tops of the containers were also marked so that they could be identified with the overhead cameras. Marks were placed on the containers so that their positions relative to the direction of travel could be determined.

5.3 Instrumentation

The initial preparation of the test tractor-trailer combination consisted of instrumenting it with 19 channels of transducers. The instrument plan was the same as that used in the first test, shown in Fig. 4.2, except for the addition of two accelerometers mounted on two different test packages. One accelerometer was placed on the outside box of a Union Carbide Corporation 20-in. birdcage (B-6), and the other was placed on the bird of a USAEC Design KKD-1 birdcage (C-7). Only the front load cells were physically calibrated, and this was done by using a laboratory type of tension-compression tester with a capacity of 600,000 lb.

5.4 Results of Second Test

The procedures used for the second test were as described in Section 3.2 except that the guard rails beside the barrier approach were removed. The operating procedures were successful and produced a near perfect

impact. However, the nominal impact velocity of 45 mph selected for this test was not reached, and the velocity of the tractor was clocked at 41 mph immediately prior to impact. There was no measurable movement of the barrier as a result of the impact (the method of measurement used was not reported).

The cab of the vehicle was completely demolished as a result of the impact, and the fifth wheel also separated from the tractor. As a result of this separation, the semitrailer also struck the barricade and severe damage was inflicted on its forward section. The separation of the fifth wheel from the tractor occurred between the corrugated mounting baseplate and the channels that comprised the frame. The shear pads welded to the frame of the tractor (indicated by arrow A in Fig. 5.9) remained intact, but the front corrugation of the baseplate (indicated by arrow B in Fig. 5.9) deformed in a forward rolling mode that caused the front and rear U-bolts to fail in combined tension and shear.

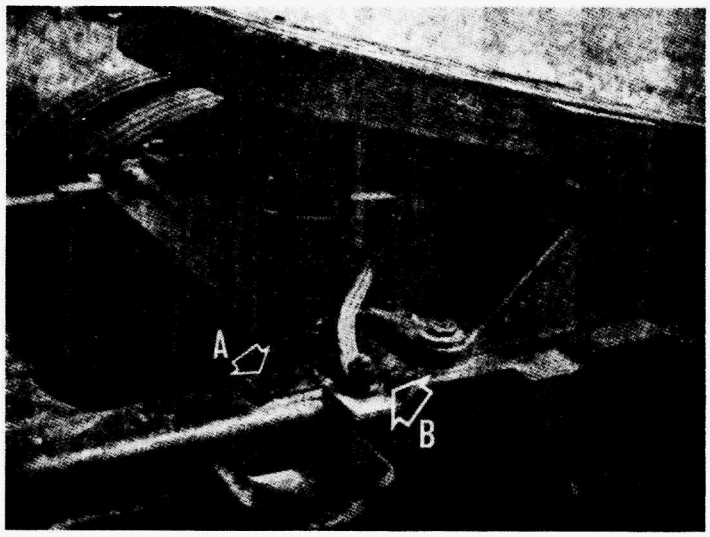

Fig. 5.9. Cab-Behind-Motor Tractor Fifth Wheel Plate Attachment.

5.4.1 Results Recorded By High-Speed Photography

The general behavior of the tractor-trailer combination and its cargo is shown in a sequence of still pictures in Fig. 5.10. These prints were produced from selected frames of 35-mm high-speed motion pictures.

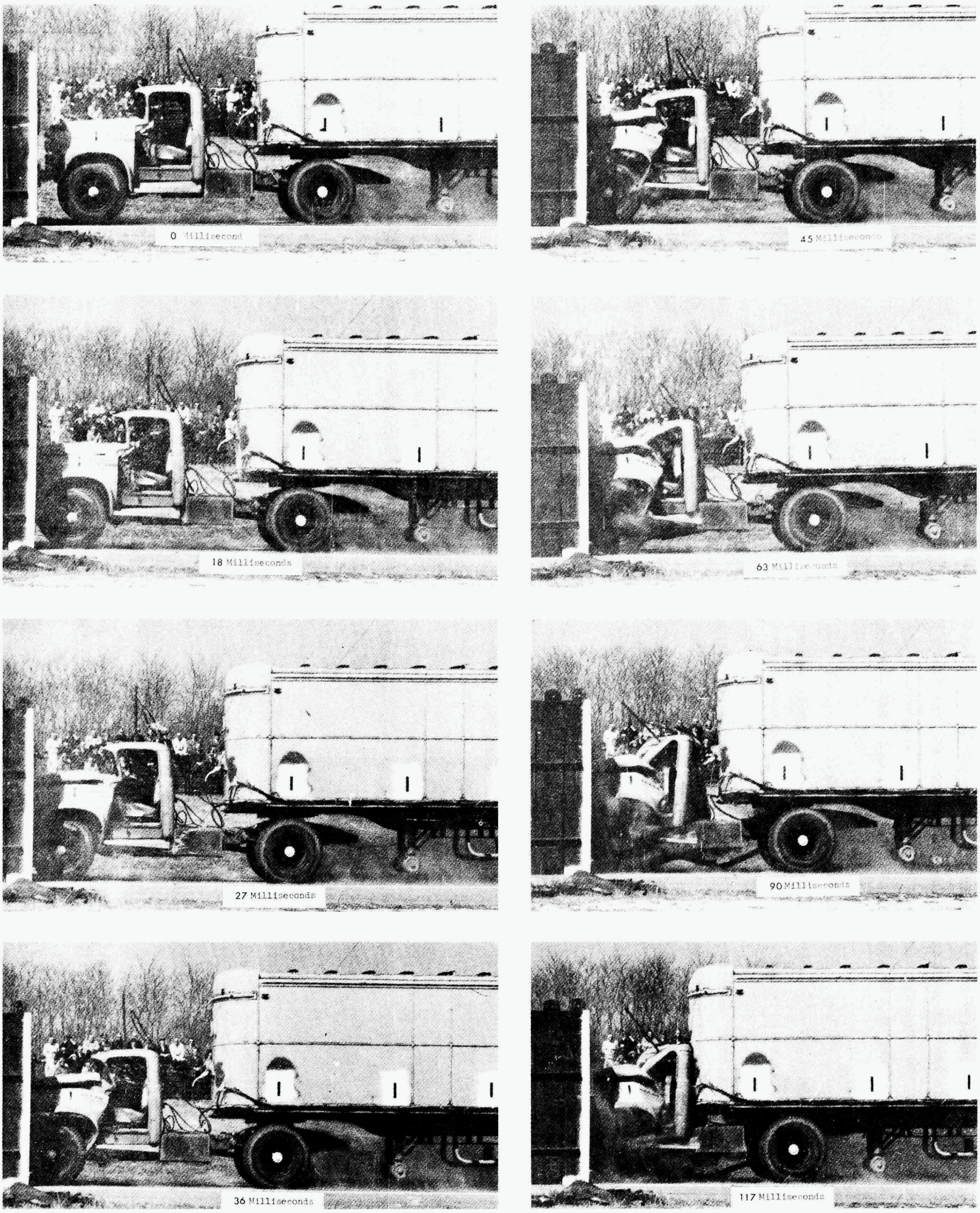

Fig. 5.10. Still Pictures Showing Impact of Test Vehicle Against Barrier at a Velocity of 41 mph in the Second Test.

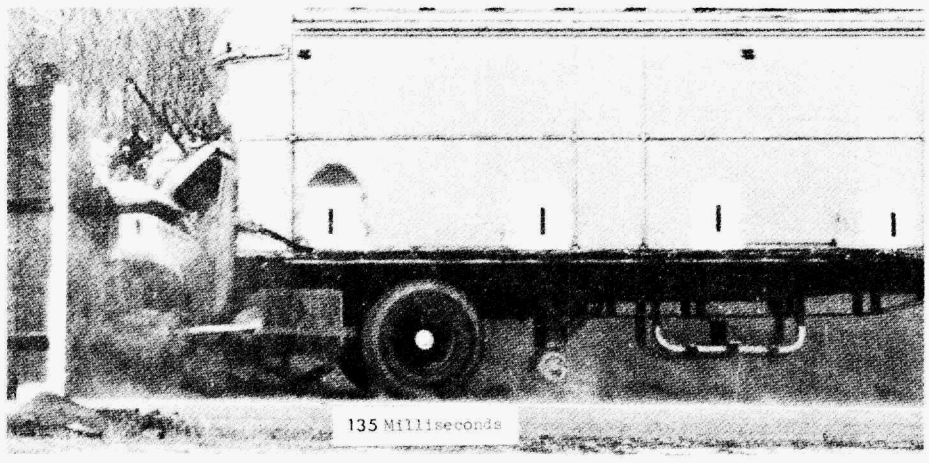

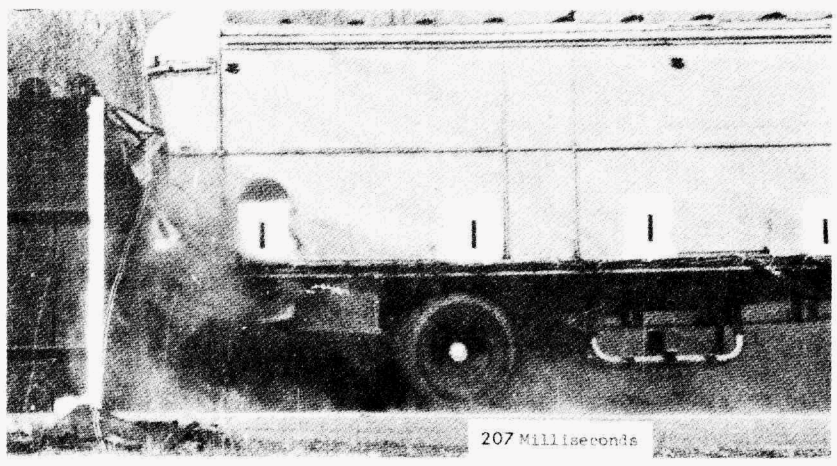

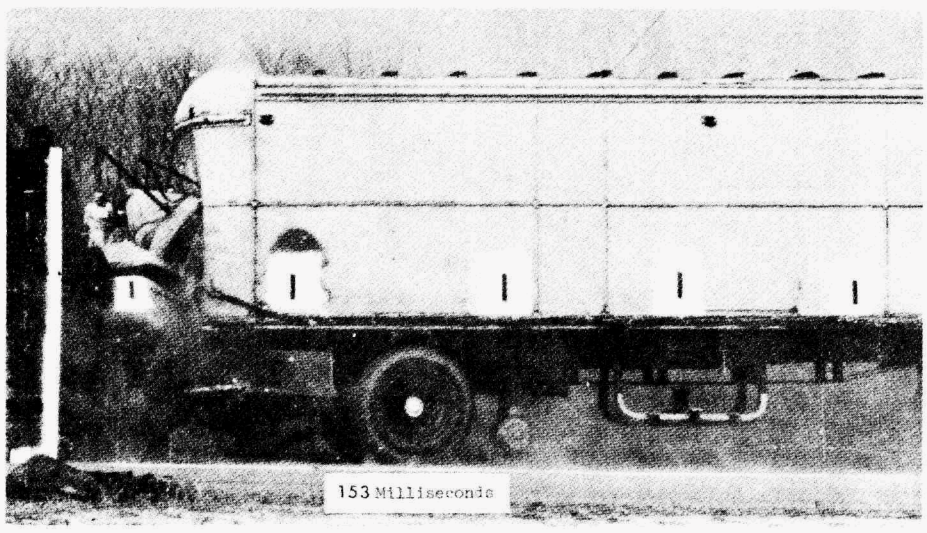

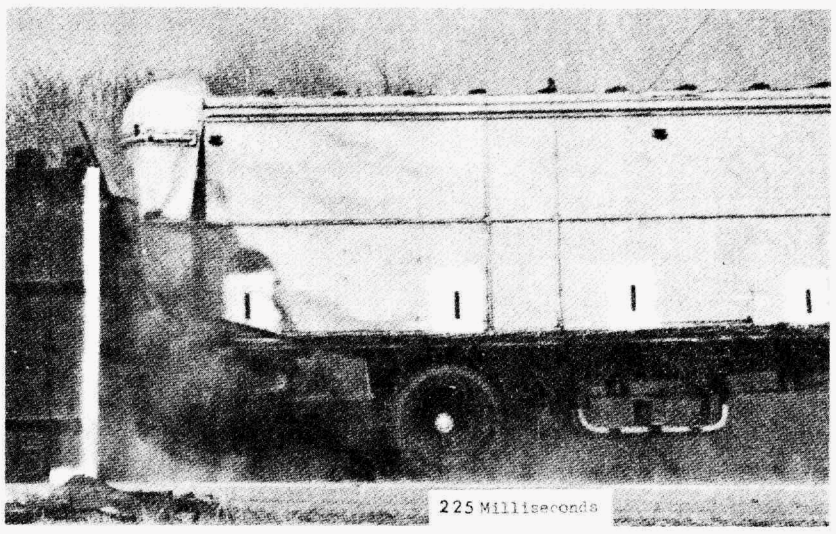

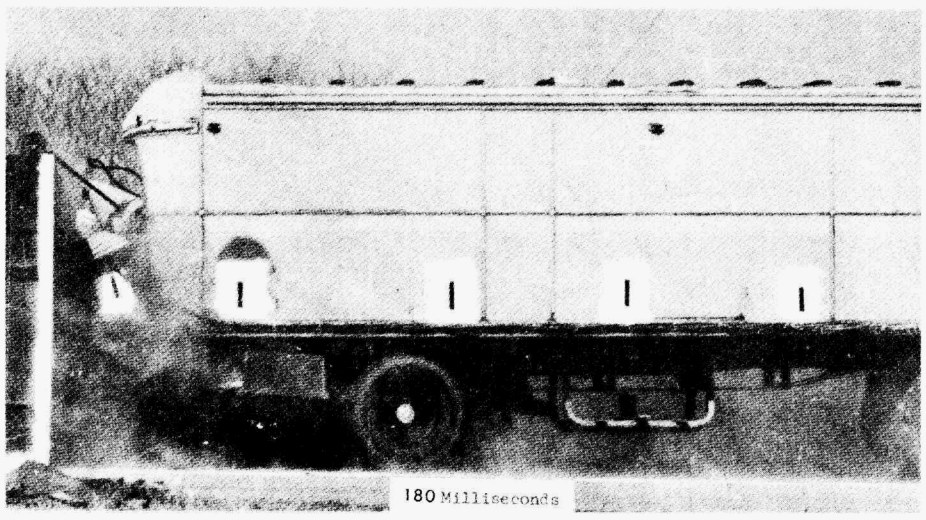

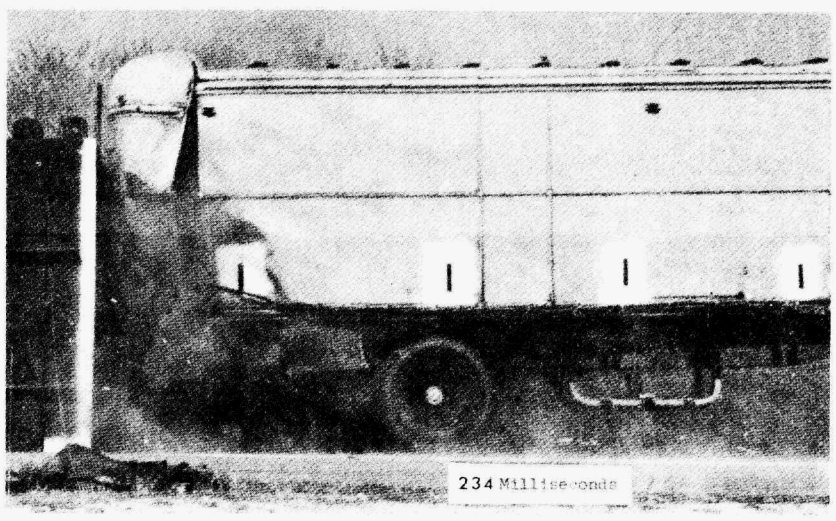

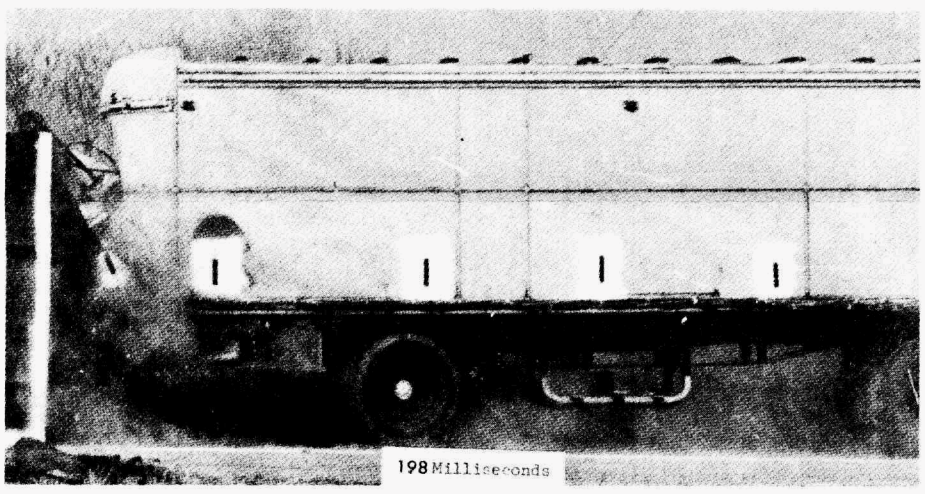

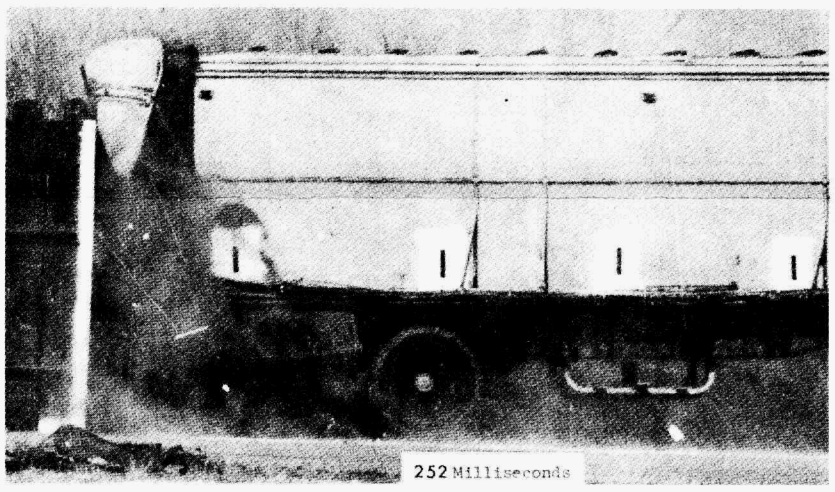

Fig. 5.10 (continued)

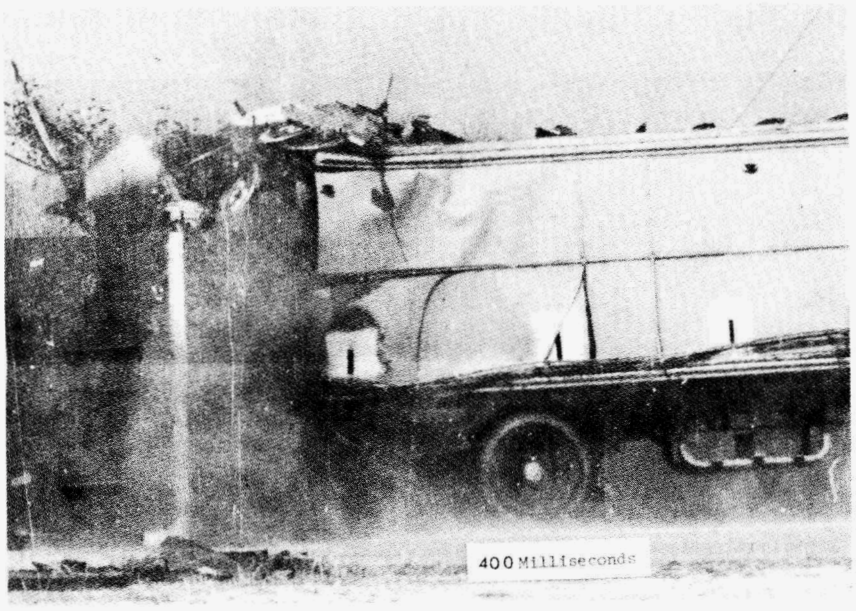

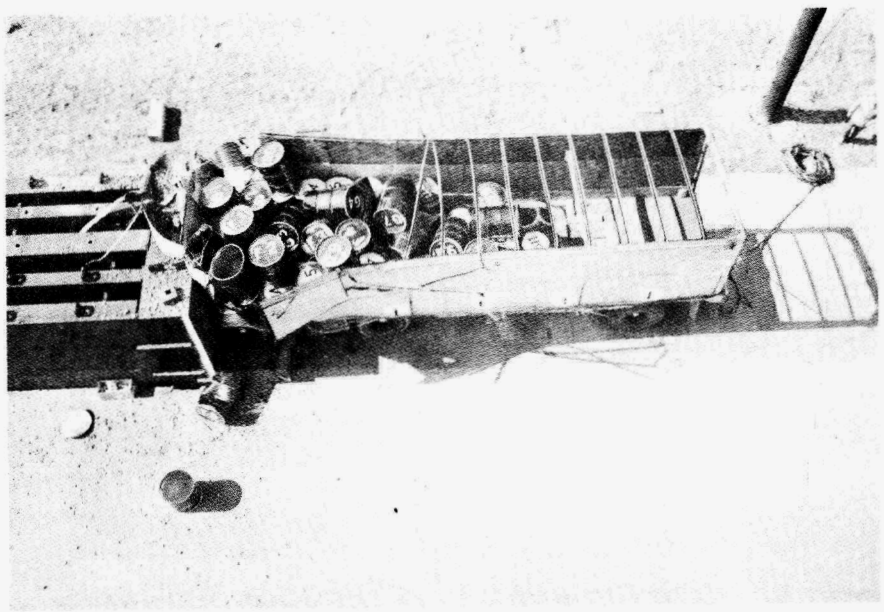

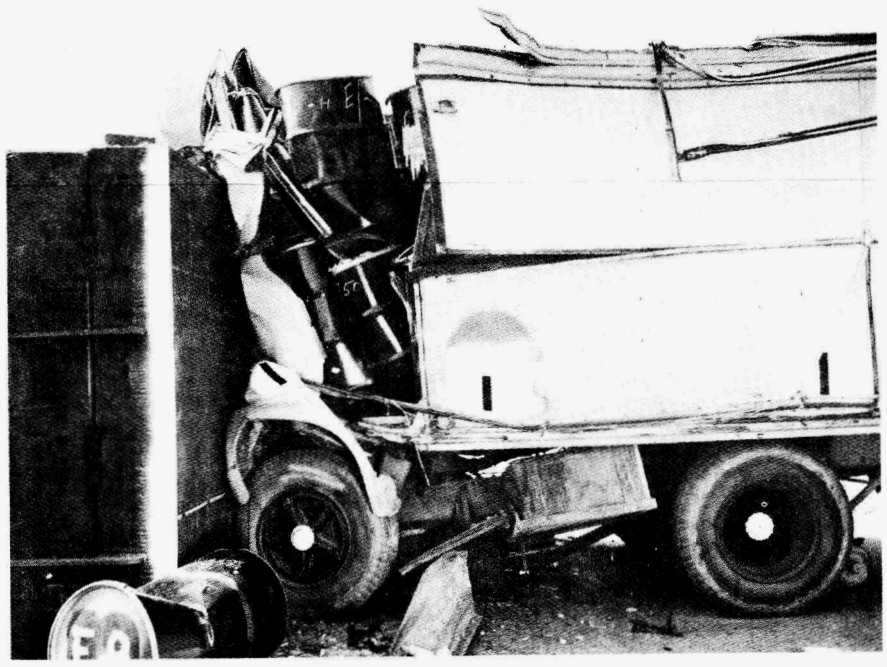

Fig. 5.10 (continued)

The sequence is annotated in terms of elapsed time from the point of load cell contact with the barrier. The photographs show that the tractor and trailer remained a coupled system for about 100 msec, at which time the attachment bolts holding the fifth wheel assembly to the frame of the tractor failed. After failure of the bolts, the trailer became a quasi-free body that caused a secondary impact, and forward motion of the trailer ceased after about 250 msec. The front of the van type of trailer began rupturing at about 220 msec, and this caused partial spillage of the birdcages. An overhead view of the transport system after the 41-mph impact is shown in Fig. 5.11.

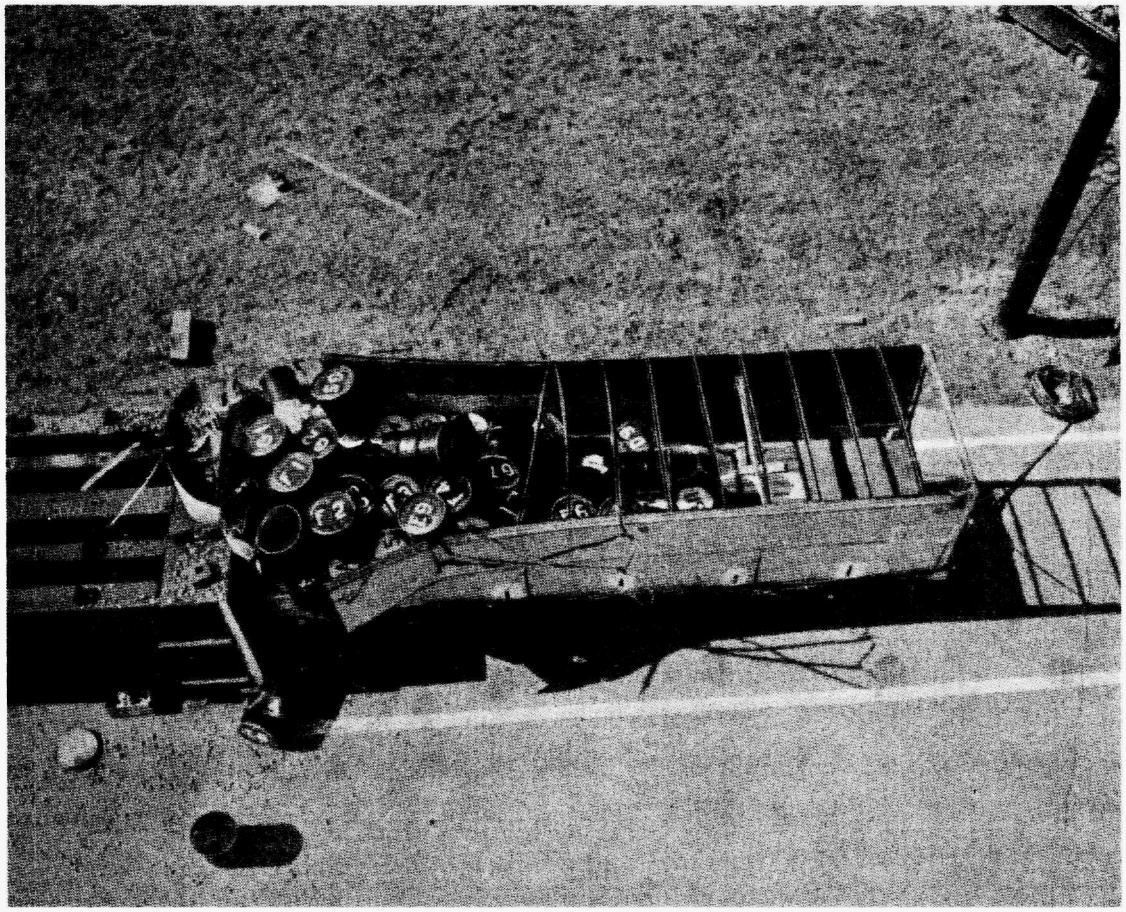

Fig. 5.11. Overhead View of Tractor-Trailer Combination Following the 41-mph Impact With the Barrier in the Second Test.

5.4.2 Measurements Recorded by Instruments

Quantitative measurements of the impact force and axial acceleration based on values manually scaled from the time histories recorded by remote instruments were plotted by applying appropriate scale factors. The force measurements of the front load cells are shown in Fig. 5.12, and the axial acceleration measurements are shown in Fig. 5.13. These quantitative values are included for academic interest, but they are virtually meaningless because

1. the load cells were absorbed within the tractor in less than 18 msec and ceased to measure total force after that time,
2. the transducers located on the tractor were damaged and telemetry cables were severed by the interaction between the tractor and trailer and subsequent separation at the fifth wheel, and
3. the accelerometers selected for fast rise time response and mounted on the various members did not respond to the low-frequency components of acceleration.

5.4.3 Measurements Taken From Photographs

In the absence of other quantitative information, distance-versus-time measurements between the leading reference mark on the trailer and the barrier were determined from the motion-picture frames. These displacement measurements were used to calculate the velocity and acceleration.

The position of a fixed point on the side of the semitrailer over the fifth wheel as a function of time was determined from film reader measurements of a 114-frame/sec 35-mm film taken at a fixed position 200 ft to the side of the barrier. The 35 frames covering the interval from initial impact to the sixth frame after the turning point for rebound were analyzed. A random error of 0.060 ft was expected from the film reader.

The displacement or compression-versus-time data were least-square fitted to a power series of the sixth degree in time, using Gram orthogonal polynomials. These results were then differentiated analytically

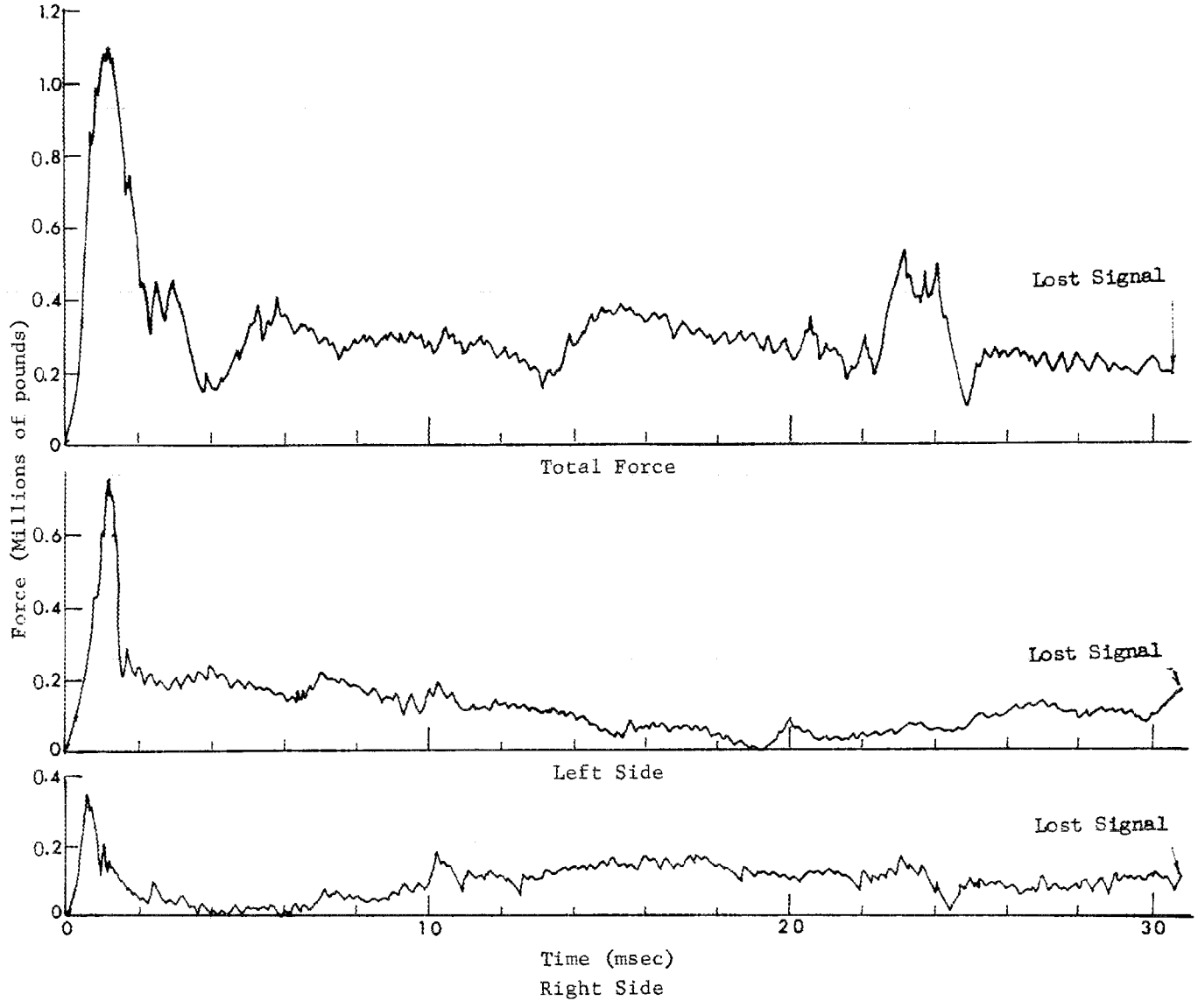

Fig. 5.12. Force Measurements (filtered above 25 KHz) of Front Load Cells Resulting From 41-mph Impact.

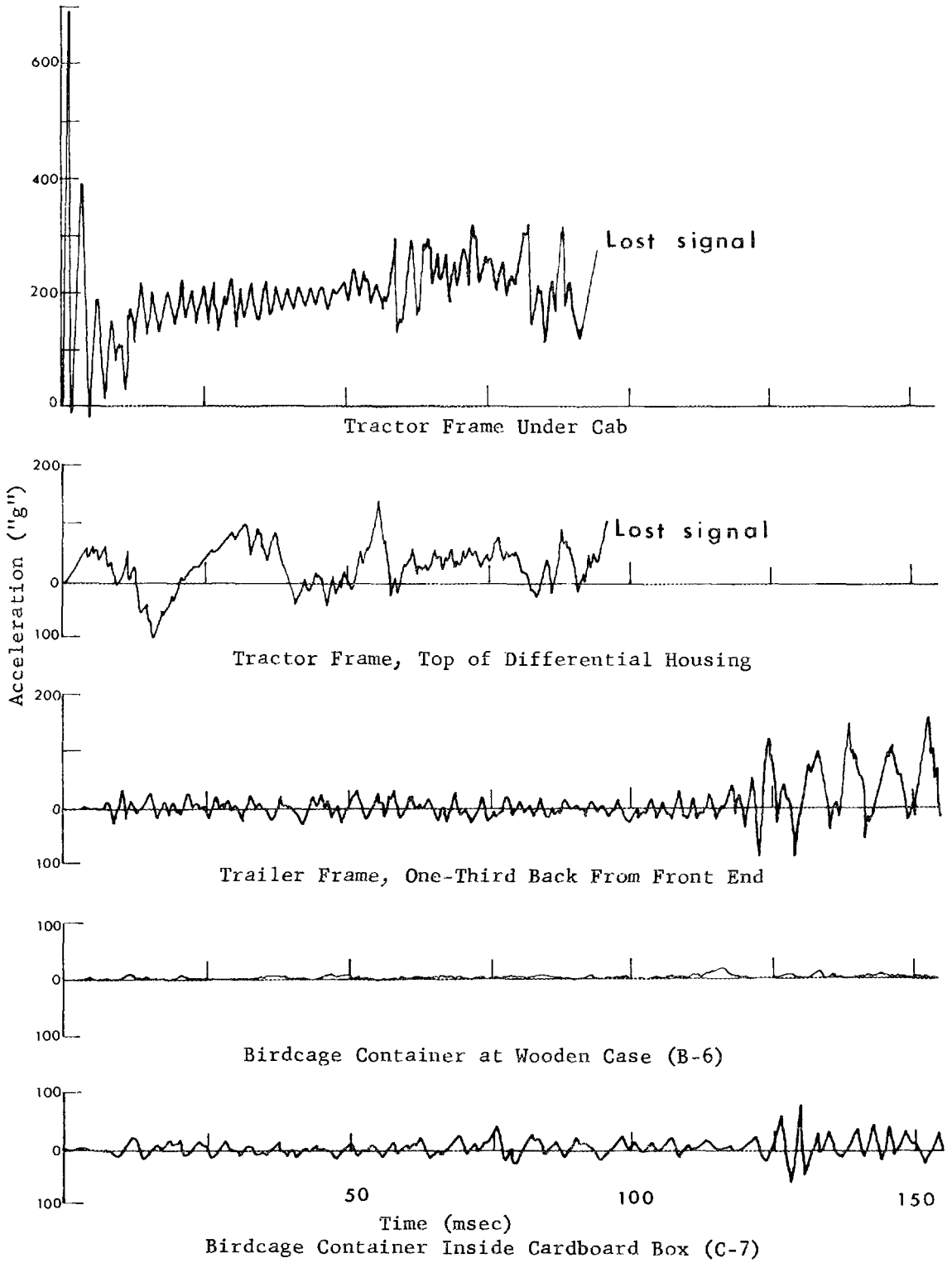

Fig. 5.13. Axial Acceleration Measurements (filtered 5 to 240 Hz Bandpass) on Tractor and Trailer Frames Resulting From 41-mph Impact.

to fit the velocity and acceleration curves. The fit, rms error in the displacement, and the final equations are as follows where t = time in seconds.

The fit = sixth degree

The rms error in Y = 0.016 ft

The displacement in feet

$$Y = 8.10 + 48.96(t - 0.149) - 134.70(t - 0.149)^2 - 1142.09(t - 0.149)^3 - 1138.68(t - 0.149)^4 + 23004.8(t - 0.149)^5 + 57913.5(t - 0.149)^6 .$$

The velocity in ft/sec

$$Y' = 48.96 - 269.40(t - 0.149) - 3426.27(t - 0.149)^2 - 4554.72(t - 0.149)^3 + 115024.0(t - 0.149)^4 + 347481.0(t - 0.149)^5 .$$

The acceleration in ft/sec^2

$$Y'' = 269.40 - 6852.54(t - 0.149) - 13664.16(t - 0.149)^2 + 460096.0(t - 0.149)^3 + 1737405.0(t - 0.149)^4 .$$

The significant dynamic collision conditions derived from the analysis of the high-speed photographs are tabulated below.

Total compression = 10.7 ft
Compression time = 245 msec
Calculated initial velocity = 40.4 mph
Initial acceleration = -6.9 "g"
Minimum acceleration = 0.9 "g"
Maximum acceleration = -19.2 "g"

A negligible amount of energy was absorbed in shearing the fifth wheel, and the impact velocity of the trailer against the barrier was almost the same as the impact velocity of the tractor against the barrier.

The results of the analysis indicate that the displacement of the semitrailer during the first 245 msec of the collision may be described, within the accuracy of the data, by a smooth function of time, as illustrated in Figs. 5.14 and 5.15. This implies that the dynamics of the collision were controlled by a single source of resistance, such as the shearing of the fifth wheel. The distinct minimum in the acceleration at 73 msec after impact, shown in Figs. 5.14 and 5.15, is certainly consistent with such a conclusion. Thus, the fifth wheel sheared shortly

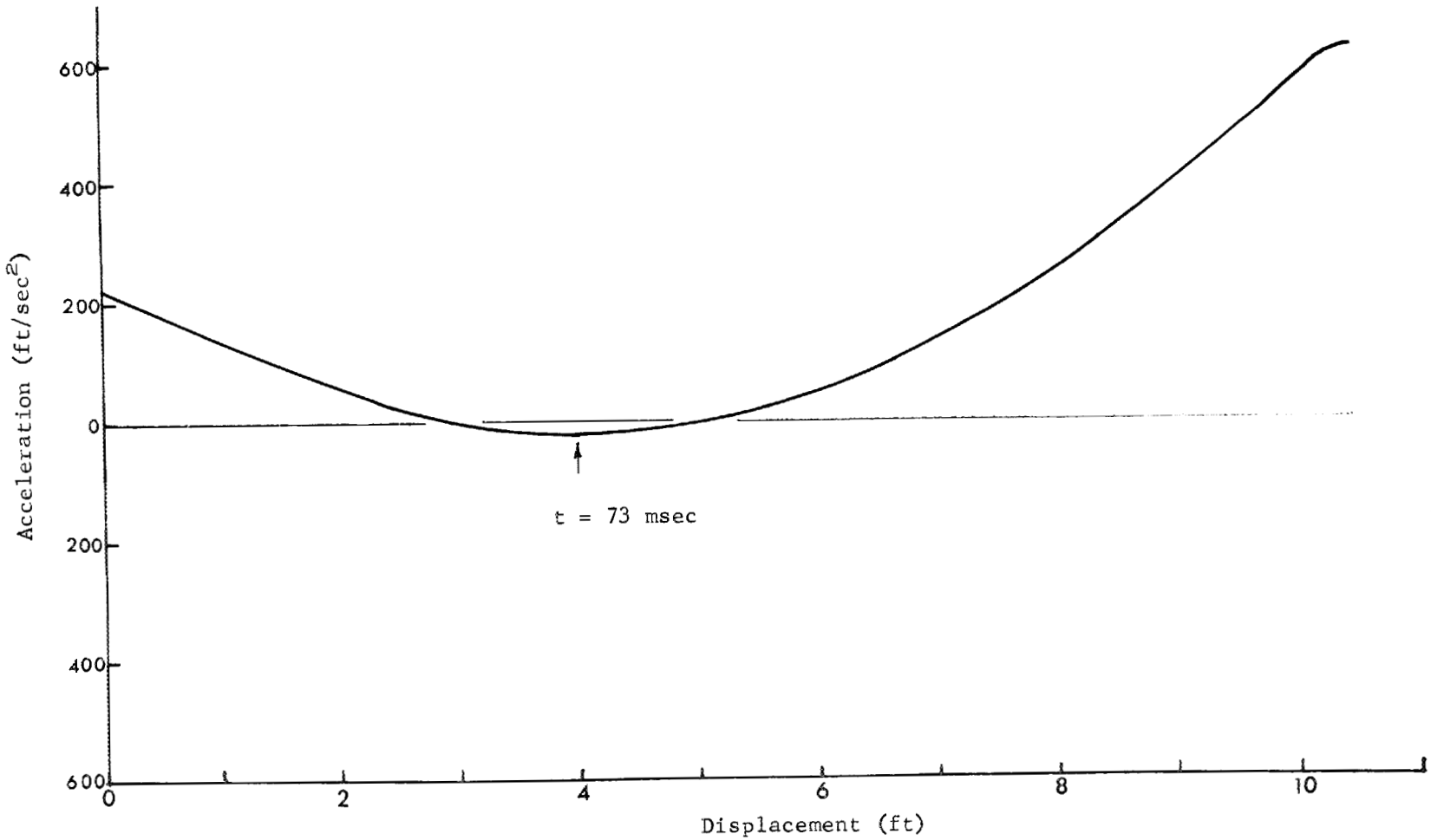

Fig. 5.14. Acceleration as a Function of Displacement of Point Over Fifth Wheel Resulting from the 41-mph Impact.

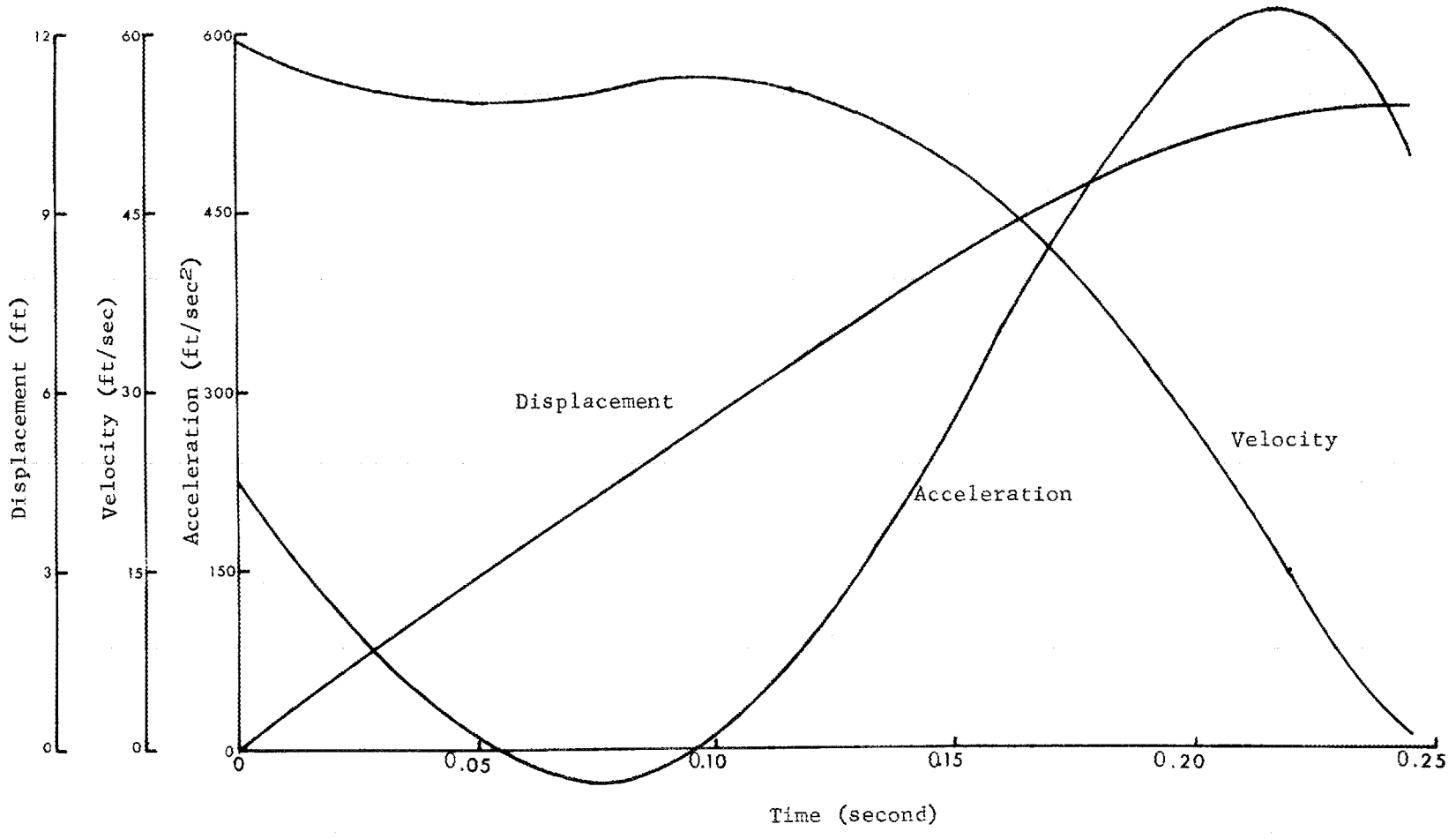

Fig. 5.15. Displacement, Velocity, and Acceleration of Fixed Point Over Fifth Wheel as a Function of Time Resulting from the 41-mph Impact.

after impact and the transmitted force decreased from the initial rigid elastic buildup. At a time 73 msec after impact, the force was essentially zero, indicating complete shear, and then it began to increase rapidly as the accordian effect of crushing the tractor body took place. The force finally decreased upon rebound.

5.4.4 Effect of Impact on Cargo

The interior of the trailer following the 41-mph impact is shown in Fig. 5.16, in which a portion of the upper level of containers has been removed for inspection. All the test containers on the outboard upper level (Rows E and H) were thrown from the trailer as a result of the impact. This included all of the Union Carbide Corporation, Nuclear Division, Y-12 Foamglas containers at positions E-3 to E-7; the three-liter Class-II containers at positions H-3, H-5, and H-7; and the Los Alamos B of E Permit 1736 containers at positions H-4 and H-6. The high-speed motion pictures taken with the overhead cameras showed that the containers in Rows E and H moved forward in a crushing action, then bowed outward, and suddenly burst upward and outward from the trailer to the ground.

The Los Alamos B of E Permit 1736 containers in positions A-5 and A-6 are shown in the damaged array prior to removal from the trailer in Fig. 5.17. Note the loss of vermiculite and drum covers and the failure of the locking ring. The Union Carbide Corporation 20-in. birdcage and the KKD-1 containers are shown in the damaged array prior to removal from the trailer in Fig. 5.18. Five KKD-1 containers were compacted in the array. The damaged containers made of 8-in. Schedule-40 pipe in 55-gallon drums prior to removal from the trailer are shown in Fig. 5.19. Note the overriding of the drums, but despite this, the drum covers remained secured.

Damage to the cargo drums in positions A-1, A-2, D-1, and D-2 on the lower level was similar to the damage received by cargo drums in positions E-1, E-2, H-1, and H-2 on the upper level. On the other hand, the damage to the two Los Alamos B of E 1736 containers in Row H was

Fig. 5.16. Interior of Trailer Following Second Impact Test.

somewhat less than the average damage inflicted on the five Los Alamos containers in Row A.

Fig. 5.17. Los Alamos B of E Permit 1736 Containers (A-5 and A-6) in Damaged Array Before Removal From the Trailer After the 41-mph Impact.

Fig. 5.18. Damaged KKD-1 Containers and Union Carbide Corporation 20-in. Birdcage Containers Before Removal From Trailer After the 41-mph Impact.

Fig. 5.19. Damaged Containers Made of 8-in. Schedule-40 Pipe in 55-Gallon Drums Before Removal From Trailer After 41-mph Impact.

The position of each container in the lower level of the damaged array was determined by measuring the distance from the rear of the van to the rear of each container before it was removed from the trailer for individual measurement and photography. The reference point on each drum was approximately at the midpoint of the outer surface of the drum, and it was selected to avoid discrete dents or bulges not representative of the effective surface of the drum. However, it was not possible to locate the boundary between the two crushed 20-in. birdcages or the boundaries between the five crushed KKD-1 containers. The position of each of these packages was estimated by prorating the combined dimensions in the direction of travel. The lateral position of each package was also noted. A summary of the average dimensions of the damaged containers after the 41-mph impact is given in Table 5.1. The measured positions of the container arrays in the trailer before and after the 41-mph impact are given in Table 5.2.

Table 5.1. Average Container Dimensions After 41-mph Impact[a]

Type of Container	Row	Average Dimension in Direction of Travel of Container: in Array (in.)	Average Dimension in Direction of Travel of Container: Individual (in.)	Average Lateral Dimension of Container (in.)
L. A. B of E 1736[b]	A	12.4	12.9	25.7
UCC 20-in. birdcage	B	7.0[c]		24
KKD-1	C	7.5[c]		20
8-in. pipe in drum	D	18.8	17.0	22.5
UCC Y-12 foamglas	E		20.9	22.7
3-liter Class II	H		19.9	22.3
L. A. B of E 1736[b]	H		15.0	24.9

[a]Original ID of drum-type containers = 22.5 in.

[b]Now designated as DOT Specification ICC-6L.

[c]For two crushed 20-in. birdcages and five crushed KKD-1 containers.

Table 5.2. Measured Positions of Containers in Trailer Before and After 41-mph Impact

	Original Distance From Rear to Near Side of Container	Final Distance From Rear to Near Side of Container	Dimensions of Damaged Package ↕a (in.)	↔b (in.)	Remarks
Row A					
Front wall	26' 2" (314")	28' 10" (346")			
A-1 Cargo (55)	24' 2" (290")	27' 7" (331")			
A-2 Cargo (55)	22' 2" (266")	25' 8" (308")			
A-3 Los Alamos	20' 2" (212")	24' 8" (296")	12	26.2	Top cover off
A-4 Los Alamos	18' 2" (218")	23' 6" (282")	14	24.8	Top cover intact
A-5 Los Alamos	16' 2" (194")	22' 8" (272")	10	27.3	Top cover off
A-6 Los Alamos	14' 2" (170")	21' 7" (259")	13	25.1	Top cover intact
A-7 Los Alamos	12' 2" (146")	20' 6" (246")	13	25.2	Top cover loose
A-8 Cargo (55)	10' 2" (122")	18' 7" (223")	(Original diam		(No visual damage to
A-9 Cargo (55)	8' 2" (98")	16' 2" (194")	= 22 1/2 in.		inner containers)
Row B					
Front wall	26' 2" (314")	28' 6" (342")			
B-1 Cargo (30)	24' 6" (294")	27' 0" (324")			
B-2 Cargo (30)	22' 11"(275")	25' 8" (308")			
B-3 Cargo (30)	21' 3" (255")	24' 5" (293")			
B-4 20" birdcage	19' 2.5" (230.5")	23' 10" (286")	7		Crushed, spacing lost
B-5 20" birdcage	17' 3.5" (207.5")	23' 3" (279")	7	21.5	Crushed, spacing lost
B-6 20" birdcage	15' 4.5" (184.5")	21' 3" (255")	23	21.5	Negligible damage
B-7 20" birdcage	13' 5.5" (161.5")	19' 3" (231")	23	21.5	Negligible damage
B-8 20" birdcage	11' 6.5" (138.5")	17' 3" (207")	23	21.5	Negligible damage
B-9 20" birdcage	9' 7.5" (115.5")	15' 3" (183")	23	21.5	Negligible damage
B-10 Cargo (30)	7' 8" (92")	12' 1" (145")	(Originally		(some steel banding straps
B-11 Cargo (30)	6' 1" (73")	10' 2" (122")	23 by 21.5")		broken B-6 to B-9)
Row C					
Front wall	26' 2" (314")	28' 5" (341")			
C-1 Cargo (30)	24' 6" (294")	27' 5" (329")			
C-2 Cargo (30)	22' 11" (275")	26' 0" (312")			
C-3 Cargo (30)	21' 3" (255")	24' 9" (297")			
C-4 KKD-1	19' 6" (234")	24' 2" (290")	7	20	Crushed, spacing lost
C-5 KKD-1	18' 2" (218")	23' 7" (283")	7	20	Crushed, spacing lost
C-6 KKD-1	16' 10" (202")	22' 11" (275")	8	20	Crushed, spacing lost
C-7 KKD-1	16' 6" (186")	22' 3" (267")	8	20	Crushed, spacing lost
C-8 KKD-1	14' 2" (170")	21' 7" (259")	8	20	Crushed, spacing lost
C-9 KKD-1	12' 10" (154")	20' 3" (243")	16	16	Negligible damage
C-10 KKD-1	11' 6" (138")	18' 11" (227")	16	16	Negligible damage
C-11 Cargo (30)	7' 6" (90")	14' 5" (173")	(Originally		(Some denting of birds C-4
C-12 Cargo (30)	5' 11" (71")	11' 7" (139")	16 by 16 in.)		to C-8, 3 threaded plugs in containment vessel loosened)
Row D					
Front wall	26' 2" (314")	29' 3" (351")			
D-1 Cargo (55)	24' 2" (290")	27' 9" (333")			
D-2 Cargo (55)	22' 2" (266")	26' 1" (313")			
D-3 8" pipe	20' 2" (242")	24' 7" (295")	18	22.5	Top closure intact
D-4 8" pipe	18' 2" (218")	23' 0" (276")	19	22.5	Top closure intact
D-5 8" pipe	16' 2" (194")	21' 5" (257")	19	22.5	Top closure intact
D-6 8" pipe	14' 2" (170")	19' 10" (238")	19	22.4	Top closure intact
D-7 8" pipe	12' 2" (146")	18' 2" (218")	20	22.3	Top closure intact
D-8 Cargo (55)	10' 2" (122")	16' 7" (199")	(Original diam		(no apparent damage to inner
D-9 Cargo (55)	8' 2" (98")	12' 5" (149")	= 22 1/2 in.)		containers)
Row E					
Front wall	26' 2" (314")				
E-1 Cargo (55)	24' 2" (290")				
E-2 Cargo (55)	22' 2" (266")				
E-3 UCC Y-12	20' 2" (242")	All Y-12 Foam-	19.3	23.0	Top closure intact
E-4 UCC Y-12	18' 2" (218")	glas containers	21.0	22.8	Top closure intact
E-5 UCC Y-12	16' 2" (194")	first row upper	21.0	22.5	Top closure intact
E-6 UCC Y-12	14' 2" (170")	layer thrown	21.2	22.7	Top closure intact
E-7 UCC Y-12	12' 2" (146")	from van	21.7	22.6	Top closure intact
E-8 Cargo (55)	10' 2" (122")		(Original diam		(Considerable indenting and
E-9 Cargo (55)	8' 2" (98")		= 22 1/2 in.)		some perforation of inner containers)
Row H					
Front wall	26' (312")				
H-1 Cargo (55)	24' (288")				
H-2 Cargo (55)	22' (264")				
H-3 3-liter	20' (240")	All three 3-	19.0	23.0	Top intact
H-4 Los Alamos	18' (216")	liter and two	15.2	25.2	Top intact
H-5 3-liter	16' (192")	L.A. contain-	19.1	23.2	Top intact
H-6 Los Alamos	14' (169")	ers thrown from	14.9	24.7	Top off, vermiculite lost
H-7 3-liter	12' (144")	van	21.6	23.0	Top intact
H-8 Cargo (55)	10' (120")		(Original diam		
H-9 Cargo (55)	8' (96")		= 22 1/2 in.)		

[a]Measured in the direction of travel

[b]Measured perpendicular to the direction of travel

The individual containers were measured after the 41-mph impact, and these dimensions are given in Table 5.3. The leading edge of the container in the direction of travel is recorded as 0° and was determined from the markings on the containers and a review of the motion pictures taken with the overhead camera. The diameters of the damaged containers in Rows A and D were obtained from inside spacing measurements plus the diameters of the birds, and these measurements do not in all cases match the outside diameter measurements because the two sets of measurements were made at different points on the drums.

Based on a review of the motion pictures taken with the overhead camera and visual inspection of the actual damage done to the containers, it was concluded that the damage inflicted on the test containers thrown from the trailer was essentially the same as that which the containers would have experienced had they remained on the trailer. The maximum "g" force indicated by the accelerometers in the horizontal direction of travel was 55 "g" for the Union Carbide Corporation 20-in. birdcage and 94 "g" for the KKD-1 bird. A general description of the damage done to the individual containers is given in the following paragraphs.

(a) Los Alamos B of E Permit 1736 Containers. The bird of the Los Alamos container consisted of a 6-in.-diameter Schedule-40 steel pipe containment vessel 28 in. long with threaded end caps. The bird was supported by four 0.25-in. steel rod spacers 90° apart and by vermiculite within a steel drum. The drum was an 18-gauge steel 55-gallon Spec. 6J drum with a 16-gauge removable head with one or more corrugations near the periphery. There were seven of these containers on the trailer in positions A-3 to A-7, inclusive, and in positions H-4 and H-6.

After the impact, the drum covers were off the containers at positions A-3, A-5, A-7, and H-6. Closure of the drum covers was effected with a 12-gauge ring with two metal tabs looped over at the ends of the ring to receive a 5/16-in. bolt. These metal tabs opened and the drums lost their covers. Considerable vermiculite was lost from three of the containers even though they remained upright. The average loss of spacing in the direction of travel was greater for these containers than

Table 5.3. Measurements of Individual Containers After the 41-mph Impact

ROW A

CONTAINER Los Alamos B.of E. 1736, A3 to A7

ARRANGEMENT

A9	A8	A7	A6	A5	A4	A3	A2	A1	
55gal	55gal	LA	LA	LA	LA	LA	55gal	55gal	→CAB
750lb	750 lb	257lb	252lb	259lb	198lb	263lb	750lb	754lb	

		INSIDE SPACING (1)				OUTSIDE DIAMETER		
	Location	0°	90°	180°	270°	0°-180°	90°-270°	Remarks
A3	Top	4"	11"	1 3/8"	9 3/8"	13"	26 1/4"	Cover Loose, Rim
	Middle	1 7/8"	9 7/8"	2 1/8"	10 3/4"	10 1/2"	27 1/2"	in Place
	Bottom	1/4"	7 5/8"	2"	10 5/8"	9 3/4"	24 3/4"	
A4	Top	3 7/8"	8"	4 1/4"	9 3/4"	19 1/4"	23 5/8"	Cover Intact, Lock-
	Middle	3 5/8"	9 3/8"	3 1/2"	10 3/4"	14"	26 1/2"	ed with A5
	Bottom	3 3/8"	7 7/8"	3/4"	9 1/4"	8 3/8"	24 1/4"	
A5	Top	1 7/8"	11 3/4"	2 1/8"	11 1/8"	10"	28 7/8"	Cover Off, Rim
	Middle	3 3/4"	10 5/8"	1 1/2"	10 7/8"	13 1/2"	28 1/8"	Failed, Locked to
	Bottom	3 5/8"	8 3/8"	1"	9 1/2"	11 1/4"	24 3/4"	A4,
A6	Top	4 5/8"	9 3/4"	5"	9 3/8"	17 1/4"	24 1/8"	Cover Intact, Bolt
	Middle	4"	10 1/8"	3"	9 3/4"	14 3/4"	26 5/8"	Bent
	Bottom	4"	9 1/8"	0"	9 5/8"	10 5/8"	24 1/2"	
A7	Top	5"	9"	3 1/4"	9 1/4"	15 1/8"	24 5/8"	Cover Loose, Rim
	Middle	4 1/2"	10"	2 3/8"	9 5/8"	14 1/8"	26 5/8"	Failed
	Bottom	3 3/8"	9"	1 3/8"	9 1/8"	12 5/8"	24 3/8"	

(1) Drum to Face of Bird.

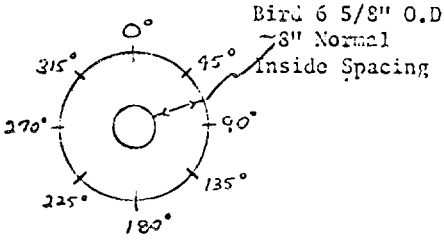

Remarks:

Cargo Drums:

A1, Cover Off, Crushed 25"x17"
A2, Cover Off, Crushed 25"x13"
A8, Intact, Slight Bulge at Bottom
A9, Intact

Test Containers:

A3 to A7, Average Outside Diameters after test - 12.9" x 25.7"

Table 5.3 (continued)

ROW B
CONTAINER UCC 20-in.
BIRDCAGE B4 to B9

B-11	B-10	B-9	B-8	B-7	B-6	B-5	B-4	B-3	B-2	B-1	
30gal 750#	30gal 752#	O.R.20" 141#	O.R.20" 137#	O.R.20" 134#	O.R.20" 136#	O.R.20" 136#	O.R.20" 136#	30gal 745#	30gal 750#	30gal 750#	→CAB

CONTAINER	REMARKS
B4	Bird Detached from Frame, Broken Welds
B5	Bird Resting on Side of Box, Broken Welds
B6	No Apparent Damage
B7	No Apparent Damage
B8	One Box Strap Broke, No Other Apparent Damage
B9	Nails Pulled from Box, No Other Apparent Damage

Cargo Drums: B-1, Cover Off, Crushed 18"x13"
B-2, Cover OK, Crushed 18"x13"
B-3, Cover OK.
B-10, Intact
B-11, Intact

ROW C
CONTAINER DOW KKD-1,
C-4 to C-10

ARRANGEMENT

C-12	C-11	C-10	C-9	C-8	C-7	C-6	C-5	C-4	C-3	C-2	C-1	
30gal 750#	30gal 747#	KKD-1 127#	KKD-1 127#	KKD-1 127#	KKD-1 127#	KKD-1 127#	KKD-1 127#	KKD-1 127#	30gal 750#	30gal 750#	30gal 750#	→CAB

CONTAINER	REMARKS
C-4	Welds Cracked, Frames Bent, Birds Struck and Dented
C-5	Same as C4
C-6	Same as C4
C-7	Same as C4
C-8	Same as C4
C-9	Front Frame Bent Inward - 1/2" at Top, 2" at Bottom
C-10	No Apparent Damage

Cargo Drums: C-1, Cover OK, Crushed 18"x13"
C-2, Cover OK, Top 1/4 Pushed in 4" by C3
C-3, Cover Off, Crushed 20"x13"
C-11, Intact
C-12, Intact

Table 5.3 (continued)

ROW D

CONTAINER 8-in. pipe D3 to D7

ARRANGEMENT

D9	D8	D7	D6	D5	D4	D3	D2	D1	
55gal 750#	55gal 750#	O.R.8" 296#	O.R.8" 298#	O.R.8" 296#	O.R.8" 298#	O.R.8" 296#	55gal 750#	55gal 755#	→ CAB

		INSIDE SPACING(1)				OUTSIDE DIAMETER		
	Location	0°	90°	180°	270°	0°-180°	90°-270°	Remarks
D3	Top	6"	7"	4 1/8"	6 7/8"	19 1/2"	22 1/4"	Cover OK, Dent Below Lid, Bottom Buldged
	Middle	3 1/8"	7"	2 1/8"	7 1/8"	14 5/8"	22 5/8"	4" Down and Turn at 215°, Spacers Bent,
	Bottom	0"	6 3/4"	0"	6 7/8"	7 1/2"	22 3/4"	Welds Cracked
D4	Top	5 ½"	7"	3 ½"	7"	18 1/8"	22 3/4"	Cover OK, 8" Opening
	Middle	3 3/4"	7"	2 3/4"	7"	15 1/2"	22 1/2"	Below Lid at 150°,
	Bottom	3"	6 7/8"	2 ¼"	6 5/8"	13 5/8"	22 3/8"	Spacers Bent, Welds Cracked
D5	Top	5 3/4"	7"	4 3/4"	7"	18 3/4"	22 3/4"	Cover OK, 8" Opening
	Middle	4 3/4"	7"	4 1/2"	7"	18"	22 5/8"	Below Lid
	Bottom	4 1/8"	7 1/8"	4"	6 3/4"	15 3/4"	22"	
D6	Top	4 3/4"	6 7/8"	4 7/8"	6 7/8"	19"	22 3/4"	Cover OK
	Middle	3 3/4"	7"	4 5/8"	6 7/8"	17 5/8"	22 1/8"	
	Bottom	3 3/4"	6 7/8"	4 1/2"	7"	17 3/8"	22 1/2"	
D7	Top	6 3/4"	7"	6 3/4"	7"	22 1/4"	22 1/2"	Cover OK
	Middle	6"	7"	6"	7"	20 3/8"	22 3/8"	
	Bottom	5"	6 7/8"	4 3/4"	6 3/4"	17 1/4"	22"	

(1) Drum to Face of Bird.

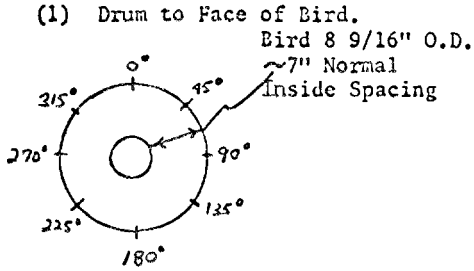

Remarks:

Cargo Drums:

D1, Cover Loose, Crushed 27"x16"
D2, Cover Off, Crushed 28"x16"
D8, Cover Off, Crushed 24"x15"
D9, Intact

Test Containers:

D3 to D7, Average Outside Diameters after test - 17" x 22.5"

Table 5.3 (continued)

ROW E
CONTAINER UCC Y-12
Foamglas
E3 to E7

ARRANGEMENT

E9	E8	E7	E6	E5	E4	E3	E2	E1	
55gal 747#	55gal 752#	Y-12 146#	Y-12 148#	Y-12 147#	Y-12 147#	Y-12 147#	55gal 752#	55gal 750#	→CAB

		OUTSIDE DIAMETER				REMARKS
	Location	0°-180°	45°-225°	90°-270°	135°-315°	E3 to E7 Thrown from Van
E3	Top	21 1/4"	22 1/2"	22 3/4"	22 3/4"	Cover OK, 1 1/2" Buldge at Bottom,
	Middle	20 3/4"	22 1/2"	23"	23 1/2"	Inner Container Seam Split at 30°,
	Bottom	17 1/4"	19 3/4"	23 1/4"	24"	Not Able to Remove from Cavity
	Top	22 1/8"	22 3/8"	22 3/4"	22 3/4"	Cover OK, Slight Binding of Inner
E4	Middle	22 7/8"	20 7/8"	22 7/8"	22 1/2"	Container, Seam Opened, Cavity
	Bottom	18"	20 3/4"	22 5/8"	22 5/8"	6 3/4" x 6 1/8"
	Top	21 3/8"	22 1/2"	22 1/2"	22 7/8"	Cover OK, Inner Container Dented,
E5	Middle	21 3/4"	22 3/8"	22 5/8"	22 7/8"	Bottom Seam Parted 1/2", Cavity
	Bottom	19 3/4"	20 3/8"	22 1/2"	23"	6 7/8" x 5 7/8"
	Top	22"	22 1/2"	22 7/8"	22 1/2"	Cover OK, Cavity Dented All Around,
E6	Middle	21 1/2"	22 5/8"	22 5/8"	23"	Inner Container Seam Parted at 160°
	Bottom	19"	23"	22 5/8"	23"	
	Top	22"	22 5/8"	22 5/8"	22 5/8"	Cover OK, Inner Container Lid Loose
E7	Middle	21 1/8"	22 3/4"	22 3/4"	22 3/4"	All Around
	Bottom	22"	22 5/8"	22 1/2"	22 1/2"	

Cavity - 6 5/8" O.D.

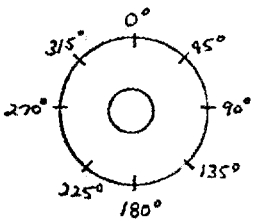

Remarks:
Cargo Drums:
E1, Cover Off, Crushed 29"x12"
E2, Cover Off, Crushed 24"x16"
E8, Intact
E9, Intact
Test Containers:
E3 to E7, Average Outside Diameters after test - 20.9"x 22.7"

Table 5.3 (continued)

ROW H

CONTAINER Dow L-3, H3, 5 &7; Los Alamos B. of E. 1736, H4 & 6

ARRANGEMENT

H9	H8	H7	H6	H5	H4	H3	H2	H1	
55gal 750#	55gal 750#	L-3 285#	LA1736 252#	L-3 285#	LA1736 259#	L-3 285#	55gal 750#	55gal 755#	→CAB

		OUTSIDE DIAMETER				REMARKS
	Location	0°-180°	45°-225°	90°-270°	135°-315°	H3 to H7 Thrown from Van
H3	Top	22"	22 3/4"	22 1/2"	22 1/4"	Cover Intact
	Middle	15 3/8"	25 7/8"	17 3/4"	15 1/2"	
	Bottom	19 1/2"	20 3/4"	22 1/4"	18"	
	Top	21 7/8"	21 7/8"	22 1/2"	22 1/2"	Cover Intact
H5	Middle	18 3/4"	23 1/2"	24 1/2"	23 1/4"	
	Bottom	16 5/8"	22 1/4"	22 1/2"	19 3/4"	
	Top	18 7/8"	-	23"	-	Cover Intact
H7	Middle		No Change			
	Bottom		No Change			
	Top	18 1/2"	20 1/2"	23 1/2"	23 3/4"	Cover Intact - Maximum
H4	Middle	15"	20 1/4"	25 1/2"	25"	Damage on Bottom
	Bottom	12"	-	26 1/2"	-	
	Top	13 1/2"	21"	26"	25"	Cover Off, Vermiculite
H6	Middle	14 1/2"	-	25"	-	Spilled
	Bottom	16 1/2"	-	23"	-	

Dow L3 - Bird 5 1/2" O.D.

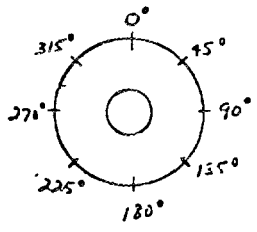

Remarks:

Cargo Drums:

H1, Cover Off, Crushed 28"x14"
H2, Cover Off, On Ground, Crushed 25"x19"
H8, Neglible Damage
H9, Neglible Damage

Test Containers:

H3, 5 & 7 - Average Outside Diameters after test - 19.9" x 22.3"
H4 & H6 - Average diameters after test - 15" x 24.9"

for the other drum types of containers tested. The containers at the positions A-4 and A-5 are shown locked together as a result of the impact in Fig. 5.20, and an inside view of container A-4 is shown in Fig. 5.21. A view of the inside of container A-5 is also shown in Fig. 5.22.

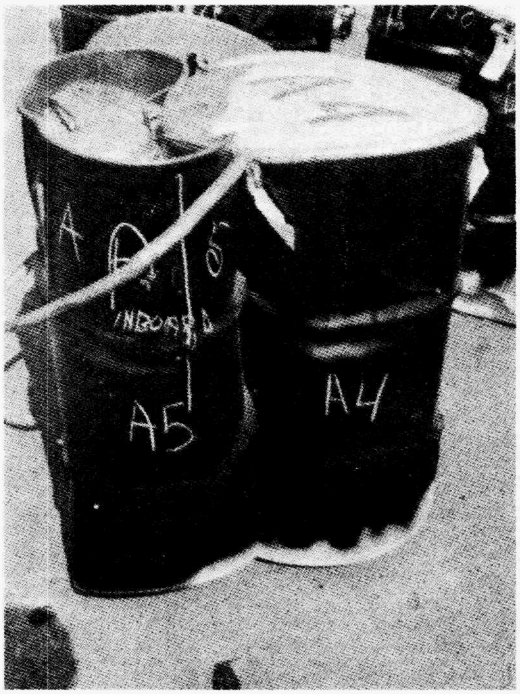

Fig. 5.20. Los Alamos Containers A-4 and A-5 Locked Together After 41-mph Impact.

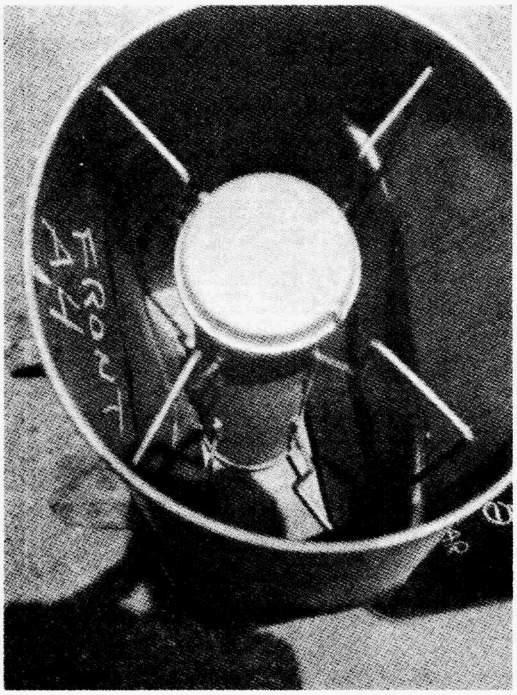

Fig. 5.21. View of Inside of Los Alamos Container A-4 After 41-mph Impact.

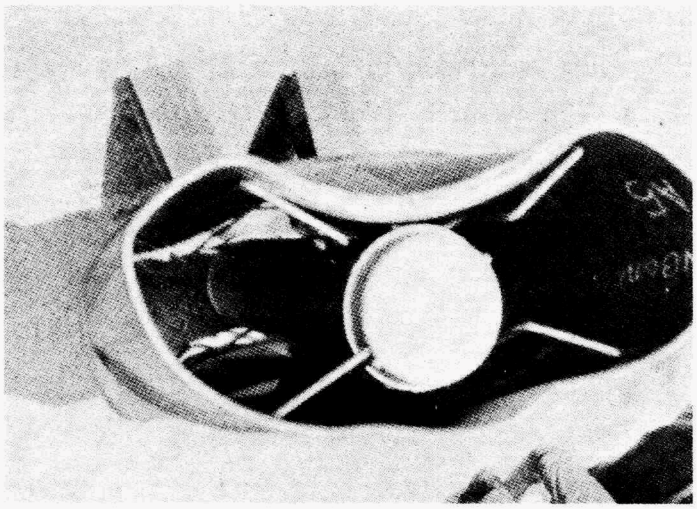

Fig. 5.22. View of Inside of Los Alamos Container A-5 After 41-mph Impact.

The Los Alamos drums showed considerable distortion as a result of the 41-mph impact. The average outside dimensions of the damaged containers at positions A-3 to A-7, inclusive, were 12.9 by 25.7 in. The containers at positions H-4 and H-6 were thrown from the trailer, and their average outside dimensions were 15 by 24.9 in. However, the containment vessels appeared undamaged as a result of the impact. The outside view of container H-4 is shown in Fig. 5.23, and a view of the

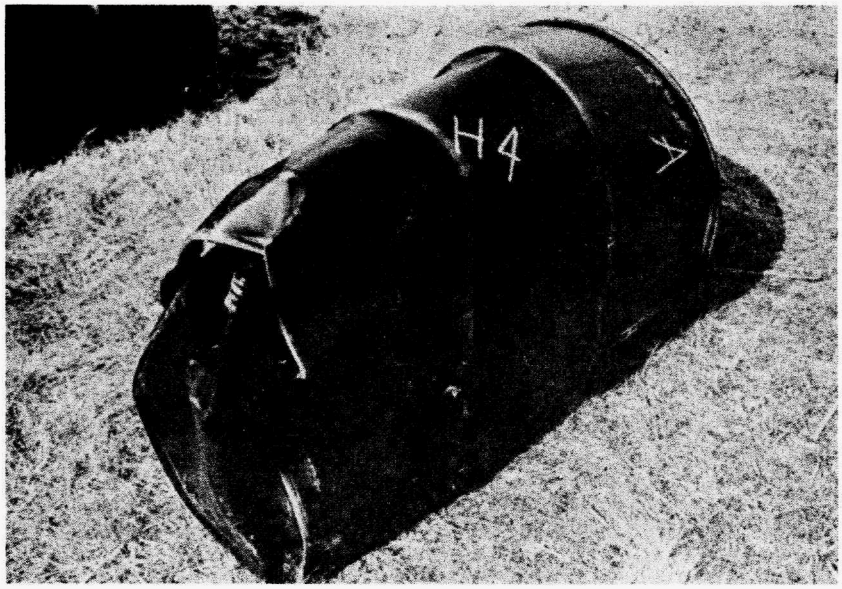

Fig. 5.23. Outside of Los Alamos Container H-4 After Being Thrown From Trailer as a Result of the 41-mph Impact.

inside of container H-4 is shown in Fig. 5.24. It should be noted that the vermiculite had been removed from the containers before the photographs shown in Figs. 5.21, 5.22, and 5.24 were taken.

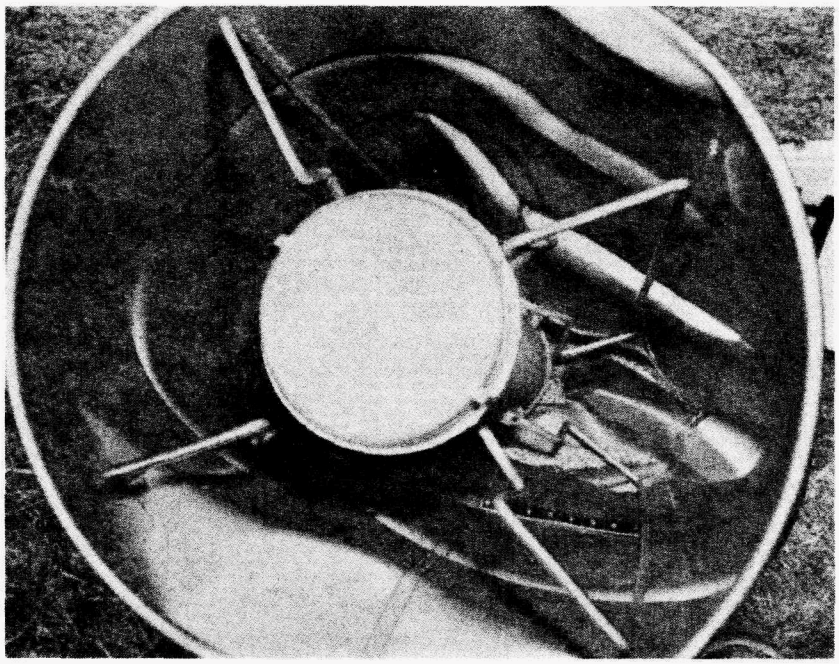

Fig. 5.24. View of the Inside of Los Alamos Container H-4 After the 41-mph Impact.

(b) Union Carbide Corporation 20-in. Birdcage. The containment vessel (bird) of the Union Carbide Corporation, Nuclear Division, 20-in. birdcage consisted of a steel pot with a diameter of 10 in., an inside height of 5 in., and a flanged cover. The bird was welded to a 20- by 20-in. steel frame made up of 1 1/2 x 1 1/2 x 1/8-in. angles and enclosed within a steel-banded 1/2-in.-thick plywood box. Six of these containers were in line on the trailer in positions B-4 through B-9.

After the 41-mph impact, containers B-4 and B-5 were crushed with loss of all spacing between the containment vessels. The bird was detached from the frame of container B-4, as is shown in Fig. 5.25 with the outer plywood box removed. The 20-in. birdcage at position B-5 is shown in Fig. 5.26 with a portion of the plywood box removed. The containers at positions B-6 through B-9 showed negligible damage with no loss of spacing.

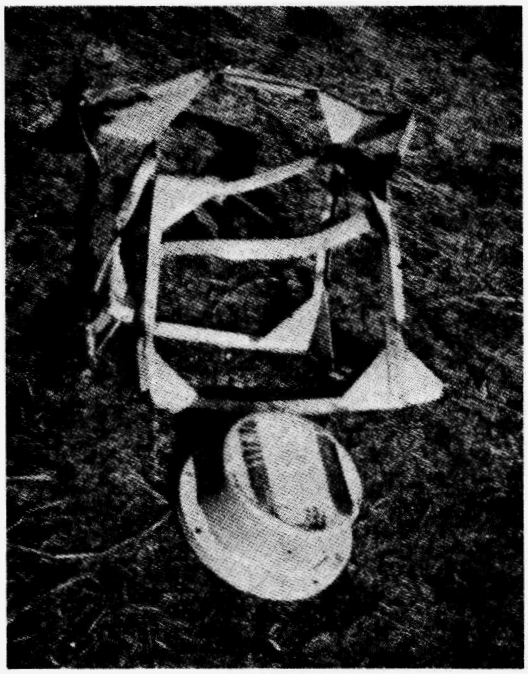

Fig. 5.25. Union Carbide Corporation 20-in. Birdcage B-4 With Outer Plywood Box Removed After 41-mph Impact.

Fig. 5.26. Union Carbide Corporation 20-in. Birdcage B-5 With a Portion of the Outer Plywood Box Removed After 41-mph Impact.

(c) USAEC Design KKD-1 Birdcage. The bird or containment vessel in the USAEC Design KKD-1 birdcage was comprised of a 5-in.-diameter Schedule-120 steel pipe 11 1/2 in. long with a threaded plug and stainless steel O-ring gasket within a pressure-cooker type of container also sealed with a stainless steel O ring gasket. The bird was supported by a frame of 3/4-in.-diameter 16-gauge steel tubing, and this 25 in. high by 16 in. square frame was enclosed within a corrugated cardboard box banded with steel straps. There were seven of these containers in line on the trailer in positions C-4 through C-10.

As a result of the 41-mph impact, containers C-4, C-5, C-6, C-7, and C-8 were crushed with loss of all spacing between the containment vessels. There was no loss of spacing or apparent damage to containers C-9 and C-10. Some denting of the birds was noted, and the threaded plugs of the containment vessels in three of the damaged containers could be loosened by hand. However, the plugs on the containment vessels of these containers were not examined for tightness prior to the impact test. The KKD-1 containers after removal from the trailer following the impact are shown in Fig. 5.27.

(d) Eight-Inch-Pipe-Inside-Drum Containers. The containment vessel in the drum container was an 8-in.-diameter Schedule-40 steel pipe 24 in. long. This pipe was supported by two tiers of 1 1/4 x 1 1/4 x 3/16-in. steel angles 60° apart and a 3- by 1/4-in. bearing band spot-welded to the steel drum. This 55-gallon drum was of 18-gauge steel and had a 16-gauge cover. Five of these containers were in line on the trailer in positions D-3 through D-7.

After the 41-mph impact, all of these test containers retained their covers. The drum closure was effected by a 12-gauge ring with drop-forged lugs, one of which was threaded to receive a 5/8-in.-diameter bolt. The average outside dimension of the damaged containers in the direction of travel was 17 in., and the average lateral dimension was 22.5 in. The outside of the 8-in.-pipe-in-drum container in position D-3 is shown after the impact in Fig. 5.28. The locking ring has been unbolted in this picture. An inside view of this container with the cover removed is shown in Fig. 5.29.

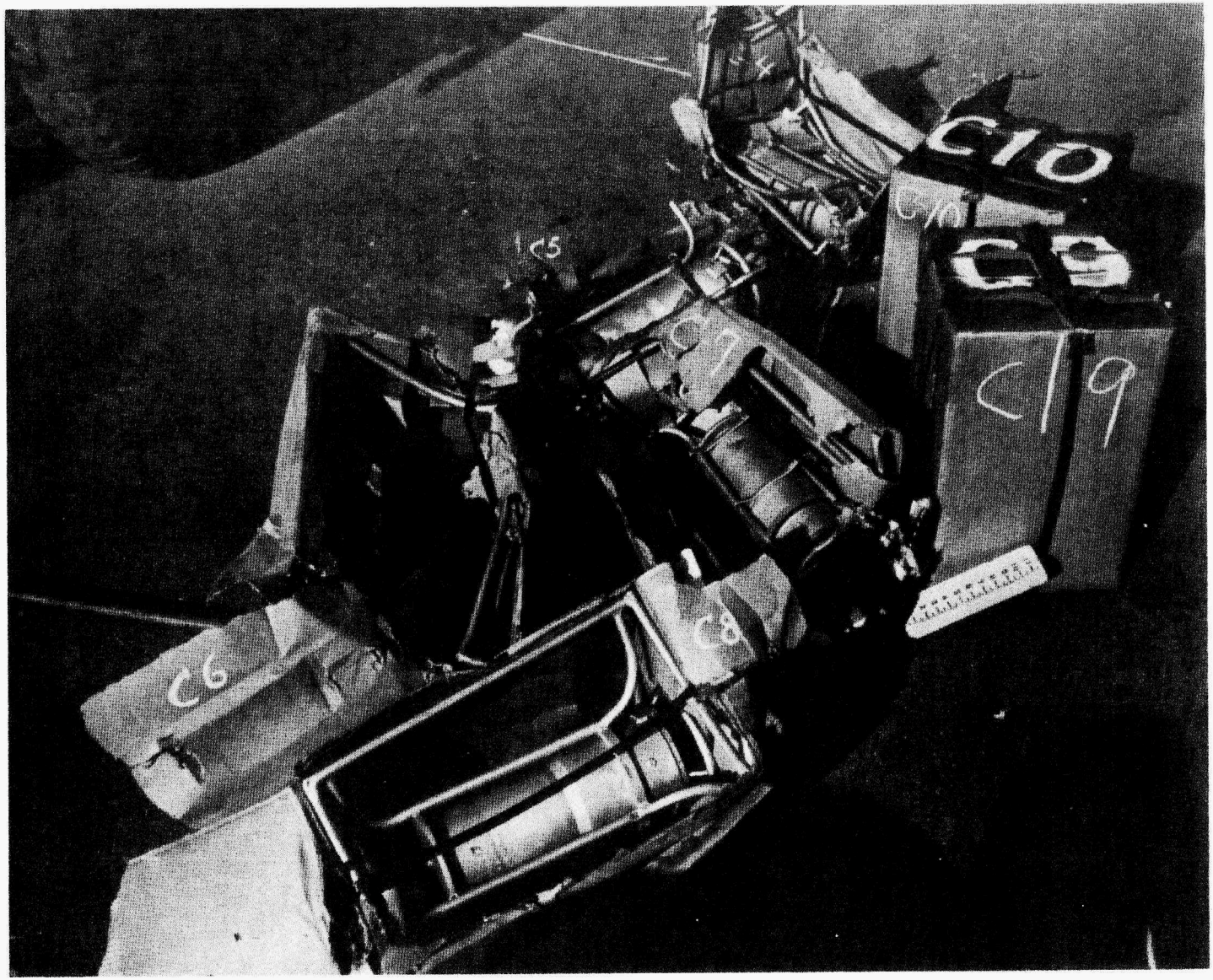

Fig. 5.27. USAEC Design KKD-1 Containers After Removal From the Trailer Following 41-mph Impact.

Fig. 5.28. Outside View of Container Comprised of 8-in. Pipe in 55-Gallon Drum in Position D-3 After 41-mph Impact.

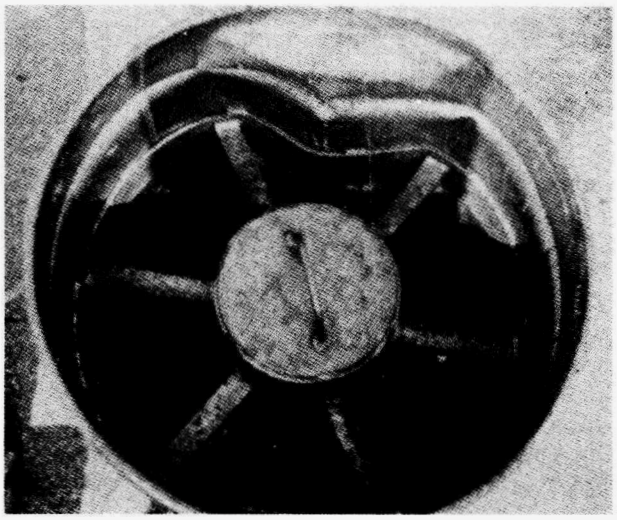

Fig. 5.29. View of Inside of Container D-3 After the 41-mph Impact.

(e) Union Carbide Corporation Y-12 Foamglas Containers. The "bird" or containment vessel of the Union Carbide Corporation, Nuclear Division, Y-12 Foamglas container was comprised of a hermetically sealed 6 3/16-in.-diameter number-12 tinned-steel can inner container 8 3/4 in. long within a 6 5/8-in.-diameter tinned-steel sleeve 9 in. long. This containment vessel was supported with cemented blocks of foamglas inside a 16-gauge drum 22 in. long with an inside diameter of 22.5 in. Five of these containers were in line on the trailer in positions E-3 through E-7.

As a result of the 41-mph impact, all of these test containers were thrown from the trailer. One such container is shown in Fig. 5.30.

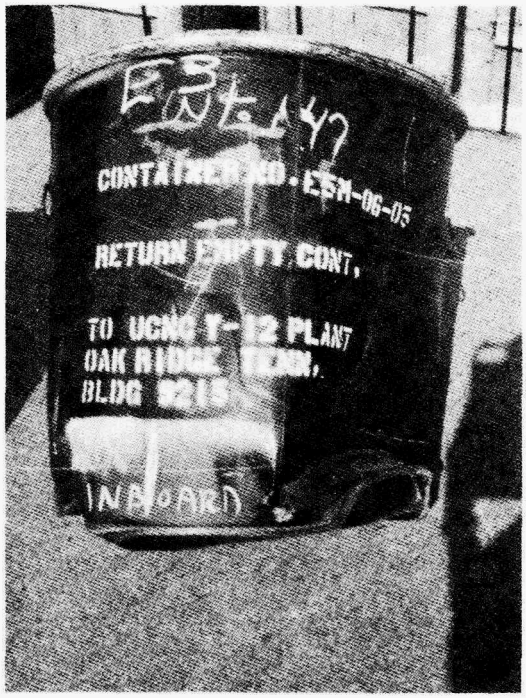

Fig. 5.30. Outside of Union Carbide Corporation Y-12 Foamglas Container E-3 Thrown From Trailer as a Result of the 41-mph Impact.

Despite being thrown out of the trailer, all of the drum covers were retained. The drum closure on these containers was effected by a 12-gauge ring with drop-forged lugs, one of which was threaded to receive a 5/8-in.-diameter bolt. The sleeves and inner containment vessels in the containers were indented, as shown in Fig. 5.31, and some were punctured by sharp corners of the foamglas blocks. The seals were

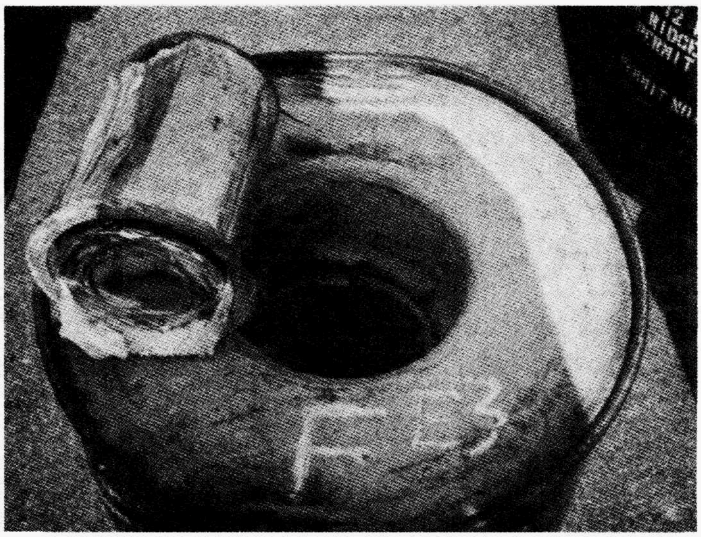

Fig. 5.31. View of Inside of Union Carbide Corporation Y-12 Foamglas Container E-3 With Containment Vessel Removed After 41-mph Impact.

broken on all of the inner containers. The average outside dimension of the damaged containers in the direction of travel was 20.9 in., and the average lateral dimension was 22.7 in.

(f) Three-Liter Class-II Containers. The containment vessel of the 3-liter Class-II container consisted of a 5-in.-diameter Schedule-80 steel pipe with a flanged closure gasketed with a stainless steel O-ring. The vessel was supported with 3/4-in.-OD 16-gauge steel tubing and vermiculite within a 16-gauge 55-gallon drum. Additional support for the heavy flanged top was provided in some of the containers by incorporating a square steel angle frame between the containment vessel and the drum. Three such containers were in positions H-3, H-5, and H-7 on the trailer.

As a result of the 41-mph impact, all of the 3-liter Class-II containers were thrown from the trailer but the drums retained their covers. The drum closure was effected by a 12-gauge ring with drop-forged lugs, one of which was threaded to receive a 5/8-in.-diameter bolt. No damage to any containment vessel was noted. The average outside dimension of the damaged containers in the direction of travel was 19.9 in., and the average lateral dimension was 22.3 in. A view of the outside of the H-3 container after it was thrown from the trailer is shown in Fig. 5.32, and a view of the inside of this container is shown in Fig. 5.33.

Fig. 5.32. Outside of 3-Liter Class-II Container H-3 After It Was Thrown From the Trailer as a Result of the 41-mph Impact.

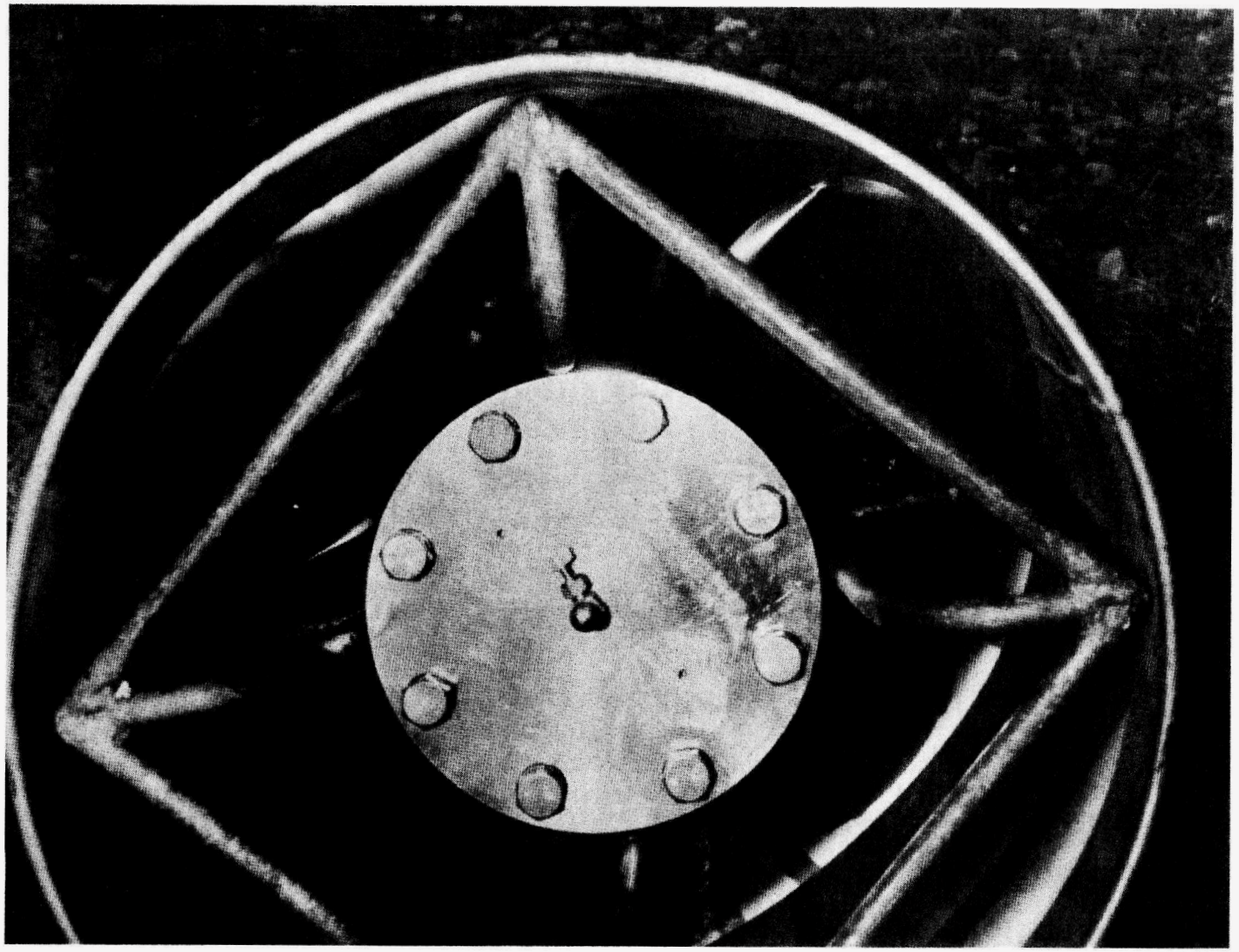

Fig. 5.33. View of the Inside of the 3-Liter Class-II Container H-3 After It Was Thrown From the Trailer as a Result of the 41-mph Impact.

6. TEST NUMBER THREE

The third test was a low-speed nondestructive collision against the barrier by a tractor-trailer combination with an irradiated-fuel shipping cask as the cargo. A velocity of 4 mph was selected as the impact velocity of the vehicle in this test, which was conducted to evaluate the effectiveness of the instrumentation and to obtain quantitative measurements for the mathematical model.

6.1 Test Vehicle

The commercial cab-over-motor tractor and flatbed semitrailer shown in Fig. 6.1 were used in the third test. The tractor was a 1959 Ford

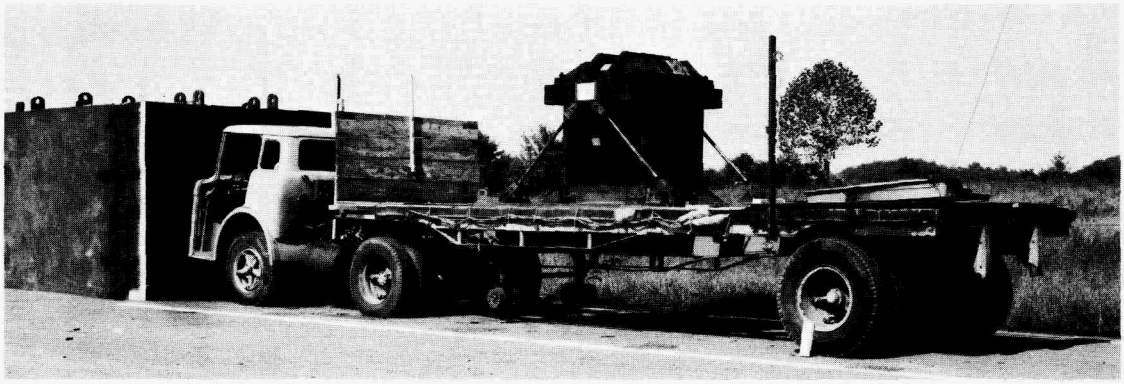

Fig. 6.1. Tractor and Flatbed Trailer Used in Third Test.

Model C-700 with a gross vehicle weight of 3500 lb. The trailer was a 1956 flatbed single-axle Kentucky Manufacturing Company Model CP-28 with a rated capacity of 12 tons. Both the tractor and the semitrailer were measured and analyzed to determine the cross-sectional areas of their structural members and the physical properties of their materials. These physical properties are given in Table 6.1.

The tractor frames consisted of two longitudinal members braced laterally by crossbeams. In addition, the attachments of the fifth wheel and the motor and transmission block provided considerable lateral

Table 6.1. Physical Properties of Materials of the Tractor and Trailer Used in the Third Impact Test

Source of Test Specimen	Yield Point[a] (psi)	Hardness RHN "B"	Ultimate Strength (psi)	Elastic Modulus (10^6 psi)	Elongation (%)
Tractor frames					
Top flange between	42,700	68/68	56,350	31.0	25.0
rear wheel and cab	41,200	67/68	54,050	31.3	29.0
Middle of beam,	42,000	68/68	53,850	30.7	26.0
side above rear wheel	41,860	68/68	56,120	31.4	27.0
Semitrailer frames					
Center left side	40,670	66/66	60,140	28.0	34.0
Center right side	41,840	75/74	65,850	30.0	31.0
Outside left side	37,410	57/57	48,620	36.2	36.0
Outside right side	37,410	56/57	48,620	31.9	41.0

[a]All specimens exhibited a dropping load while the straining rate continued constant at this point.

stiffening. The frame had connections with the motor block, front and rear axles, and the fifth wheel. A schematic layout and the cross-sectional properties of the main frame members of the tractor are given in Fig. 6.2. The foremost point of the tractor frame was reinforced for this test by the addition of lateral stiffness between the two frame members. A piece of 5 x 5 x 5/16-in. H-beam was welded between the two frame members about 10 in. in front of the forward rear spring hanger to add lateral stiffness.

The semitrailer frame was constructed like a gridwork with heavy longitudinal members. A schematic layout and the cross-sectional properties of the main frame members of the trailer are shown in Fig. 6.3. The semitrailer was prepared for this test by removing most of the wood platform, and the existing cross members were strengthened by welding an additional angle on top of them. This served the dual purpose of adding strength and of bringing the top flange of the cross member flush with the side rails of the trailer to accommodate the cask baseplate. The cask baseplate was a 96- by 89.5-in. steel plate 1.5 in. thick welded directly to the partially rebuilt trailer frame. This enhanced the grid-like structure of the trailer frame.

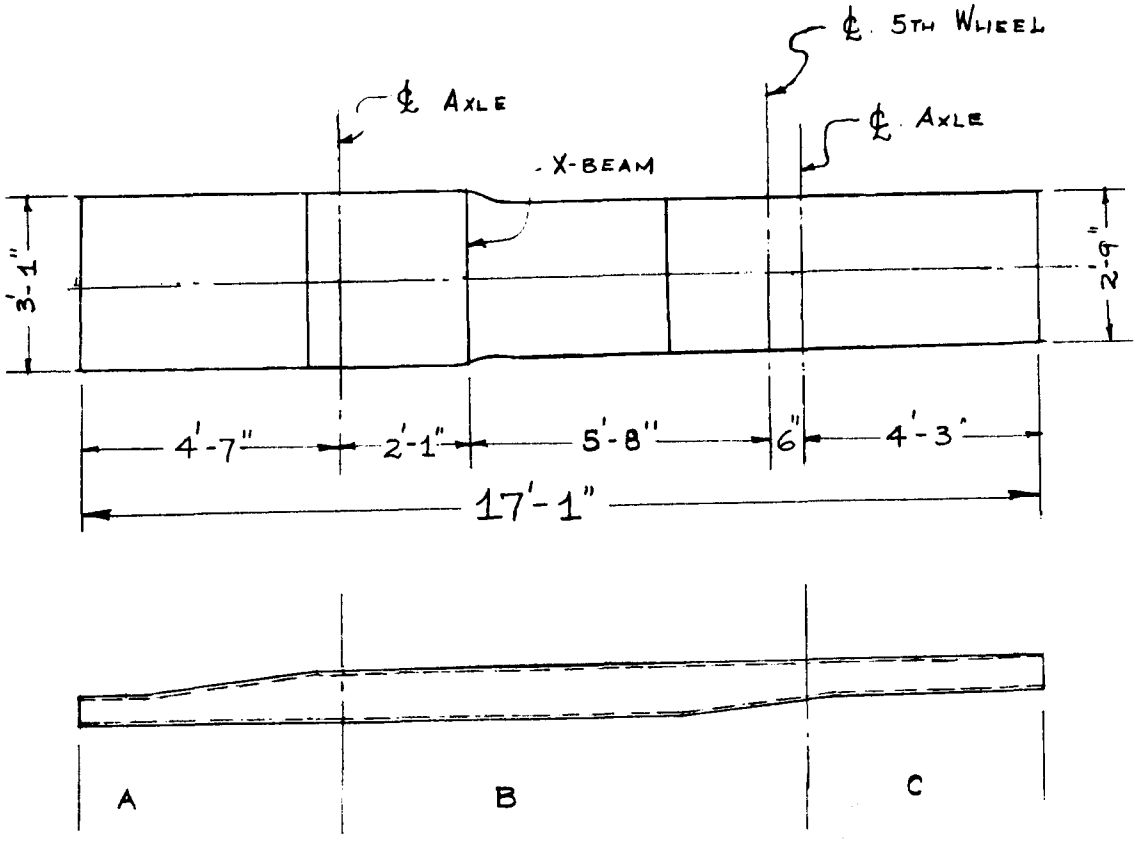

Channel Cross-Sectional Properties for Each Beam

Location	Overall Dimensions (in.)	A ($in.^2$)	I_{yy} ($in.^4$)	Z_{yy} ($in.^3$)
A	4-1/2 x 3 x $\frac{5}{32}$	1.53	5.2	2.3
B	9-1/2 x 3 x $\frac{1}{4}$	3.75	47.3	10.0
C	5-1/2 x 3 x $\frac{5}{32}$	1.68	8.2	3.0

Fig. 6.2. Details of the Framing of the Tractor Used in the Third Impact Test.

Preliminary calculations indicated that the cask trunnions had a combined strength of 400,000 lb and the major dimension of the semi-trailer kingpin through which impact forces would be transmitted would withstand 400,000 lb in shear. The hinge pin in the fifth wheel assembly was modified by removing the bushings and replacing the existing

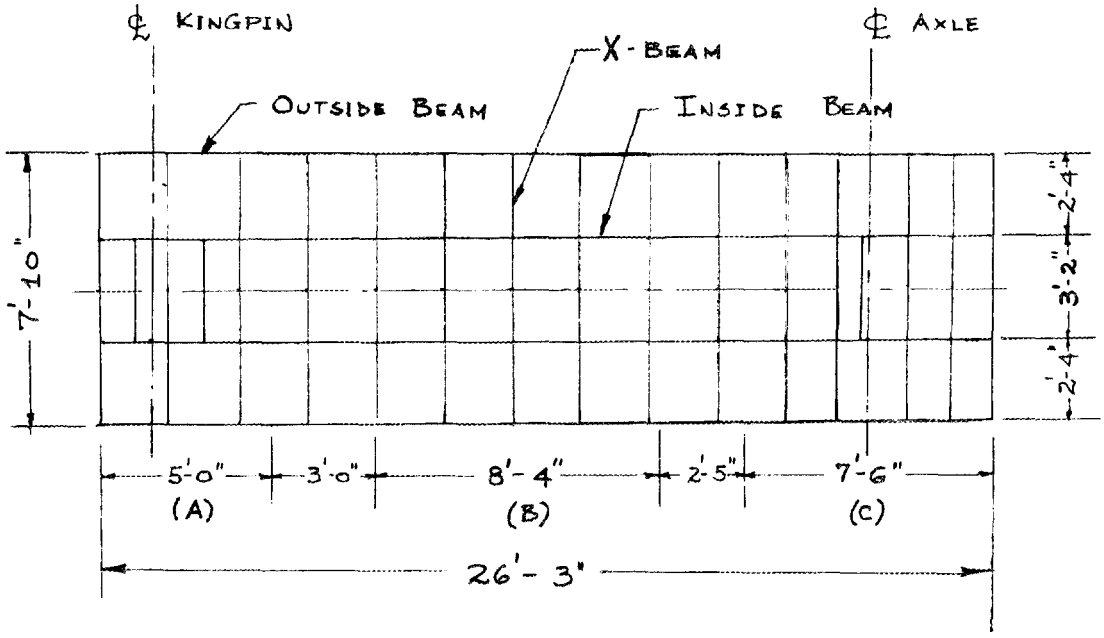

Channel Cross-Sectional Properties for Each Beam

Location		Overall Dimensions (in.)	A (in.^{2})	I_{yy} (in.^{4})	Z_{yy} (in.^{3})
A	Outside	$7 \times 2\frac{1}{2} \times \frac{1}{4}$	2.88	20.0	5.7
	Inside	$7\frac{5}{8} \times 3\frac{1}{4} \times \frac{5}{16}^{+}$	5.44	55.6	14.6
B	Outside	$10 \times 2\frac{1}{2} \times \frac{1}{4}$	3.63	47.6	9.5
	Inside	$11\frac{5}{8} \times 3\frac{1}{4} \times \frac{5}{16}$	5.47	99.7	17.2
C	Outside	$7 \times 2\frac{1}{2} \times \frac{1}{4}^{+}$	3.81	32.7	9.4
	Inside	$9\frac{1}{8} \times 3\frac{1}{4} \times \frac{5}{16}^{+}$	5.91	83.0	18.2

Fig. 6.3. Details of the Framing of the Trailer Used in the Third Impact Test.

1.115-in.-diameter pin with a 1.404-in.-diameter pin. The larger pin had an area of 1.545 in.^{2} that gave a 6.18-in.^{2} area in the four-point shear configuration used. The fifth wheel on this vehicle was also

restrained by U-bolts, but the design was compromised by the use of a 4-in. I-beam as a spacer between the baseplate and the tractor frame on each side. This design was reinforced by the addition of about ten linear inches of weld to each outer side of the junction between the baseplate and the spacer. A total of about 80 linear inches of weld was applied to the junctions between the spacer and the frame. This 80-in. section was divided into 20 in. of weld between the inside and outside junctions on each side of the tractor.

6.2 Vehicle Cargo

The cargo on the flatbed semitrailer consisted of a carbon-steel 15-ton LMF cask which was typical of irradiated-fuel casks except for its shape. This cask was essentially a rectangular box (almost cubical) with a bolt-on cover. The cask was 5 ft high and it weighed approximately 30,000 lb. The cavity for containing fuel elements was formed in the main body by an inner steel shell separated from the outer shell by 8 1/2 in. of lead shielding. Vertical cooling fins were spaced at 2-in. intervals around the periphery of the outer shell. Trunnions were located on the cask for the purpose of tie-down, and the cask was used without a crash frame.

This decontaminated cask was provided by the E. I. du Pont de Nemours Company Savannah River Plant, and an AEC license (No. 19-294-17) authorizing its possession for this test was obtained. The cask was mounted on the flatbed semitrailer as shown in Fig. 6.4, and the detailed design of the cask tie-down is shown in Fig. 6.5. The weight distribution for the empty and loaded tractor-semitrailer combination is given in Table 6.2.

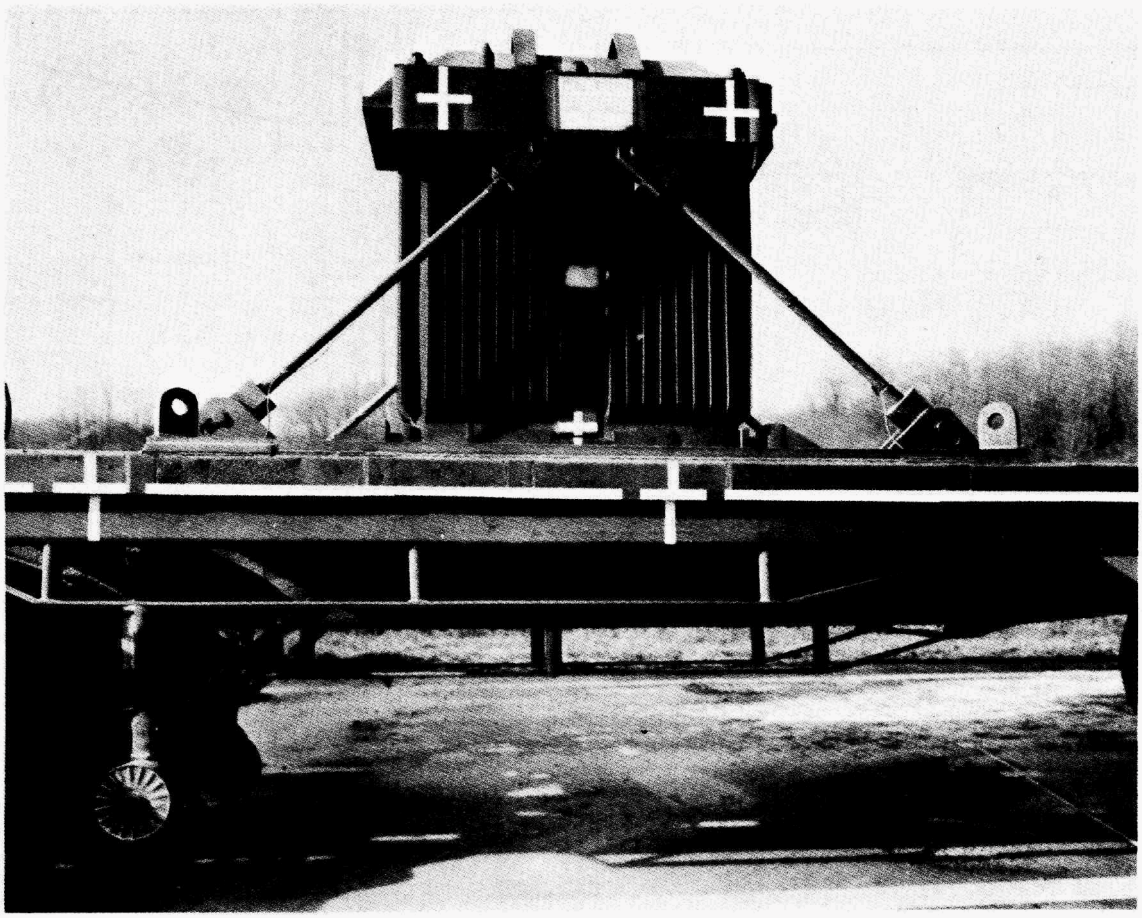

Fig. 6.4. Fifteen-Ton Cask Mounted on Flatbed Semitrailer for the Third Impact Test.

Table 6.2. Weight Distribution on Modified Tractor-Trailer Rig When Empty and When Loaded for the Third Test

Wheel Location	Weight of Tractor		Weight of Semitrailer	
	Empty (lb)	Loaded (lb)	Empty (lb)	Loaded (lb)
Right front	2250	2620		
Left front	2345	2760		
Right rear	2360	10270	2380	10250
Left rear	2390	10210	2340	10550
Total weight				
Empty, lb	14,065			
Loaded, lb	46,660			

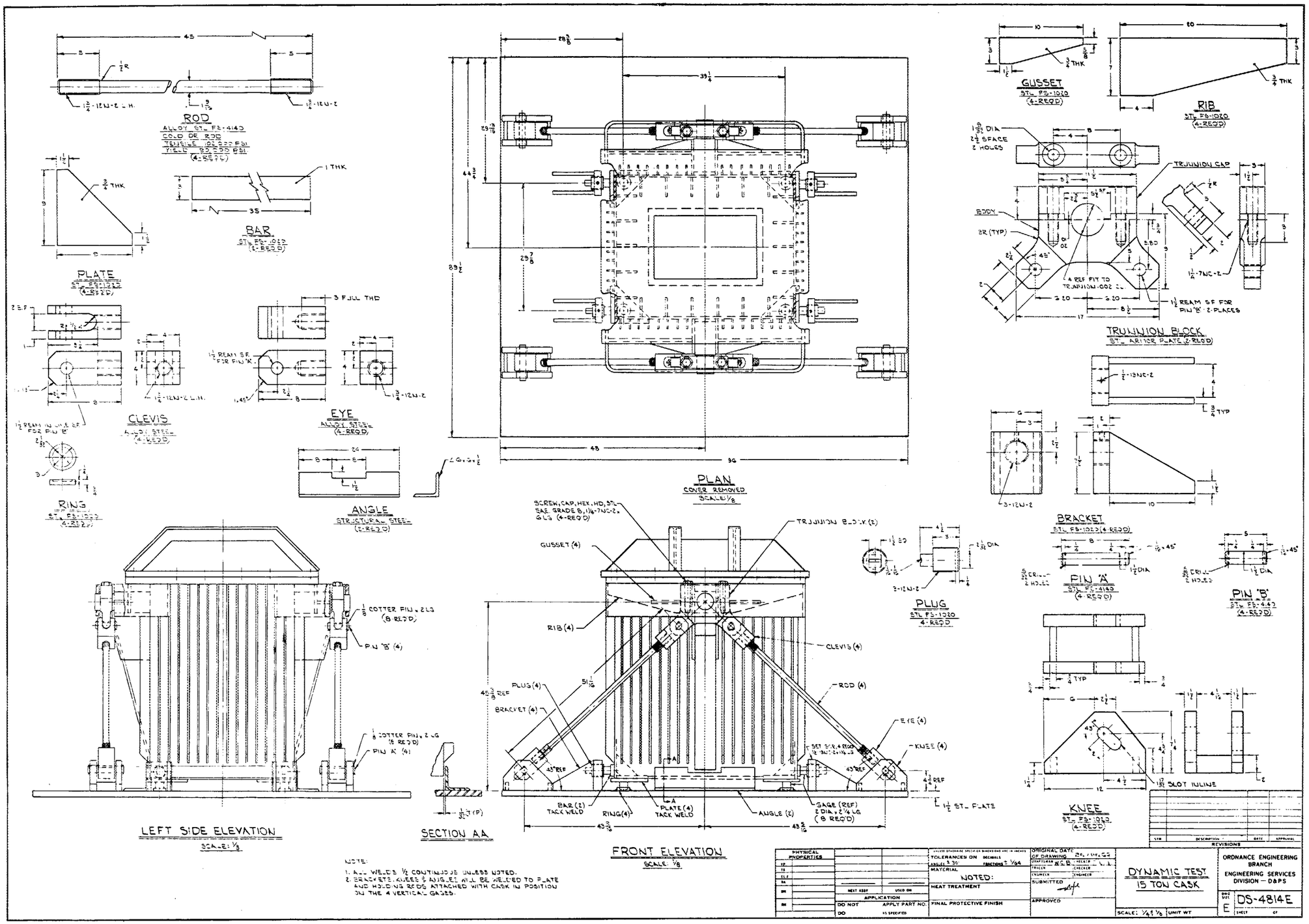

Fig. 6.5. Design of 15-Ton Cask Tie-Down to Trailer.

6.3 Instrumentation

Since this was the first test in which detailed quantitative measurements were to be made, the test vehicle was instrumented with 38 data channels in accordance with the instrumentation plan shown in Figs. 6.6 and 6.7. Most of the rationale behind this plan was based on the requirements of the mathematical model. In addition to the instrumentation placed on the cask and transport vehicle, a series of pre-impact investigations were made to calibrate the load cells under and around the cask, to determine force-deflection characteristics of the tractor and trailer suspensions, and to determine the load-deflection characteristics of the trailer frame. The data from these investigations were for use in the mathematical model and are documented in The Franklin Institute Research Laboratories final report F-B2397 entitled "Analysis for the Longitudinal Vehicle Collision Test of Joint AEC-DA Pilot Study" that was prepared for the Development and Proof Services, Aberdeen Proving Ground, and included in the original Joint AEC-DA Advisory Committee report published in November 1967.

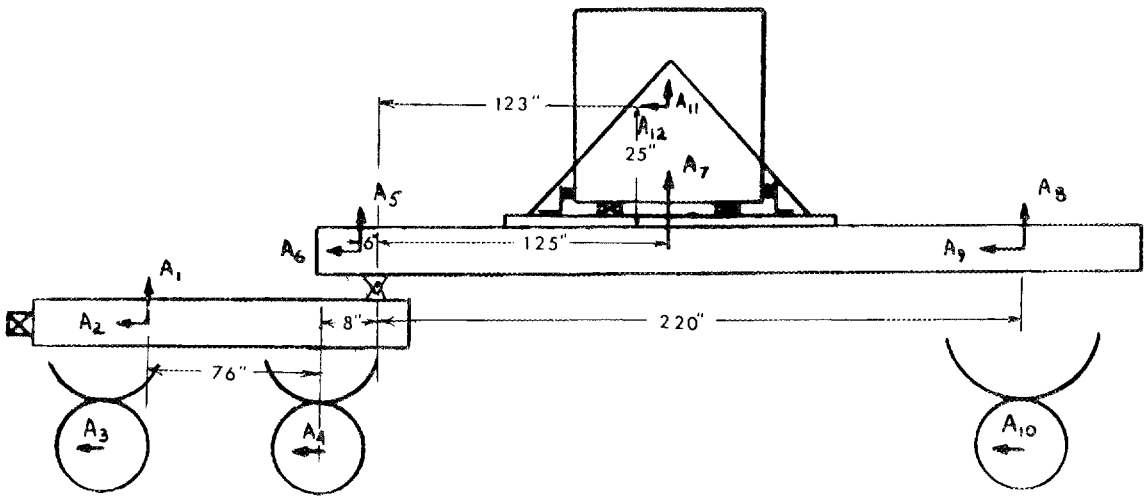

		No. of Channels
A_1	- Tractor Frame, Front, Vertical	1
A_2	- Tractor Frame, Front, Horizontal	1
A_3	- Tractor, Front Axle Assy, Horizontal	1
A_4	- Tractor, Rear Axle Assy, Horizontal	1
A_5	- Trailer Frame, Front, Vertical	1
A_6	- Trailer Frame, Front, Horizontal	1
A_7	- Trailer Frame, Under Cask, Vertical	1
A_8	- Trailer Frame, Rear, Vertical	1
A_9	- Trailer Frame, Rear, Horizontal	1
A_{10}	- Trailer, Rear Axle Assy, Horizontal	1
A_{11}	- Cask, Center of Gravity, Vertical	1
A_{12}	- Cask, Center of Gravity, Horizontal	1
	Total	12

Fig. 6.6. Location of Accelerometers on the Cask and Transport Vehicle for the Third Impact Test.

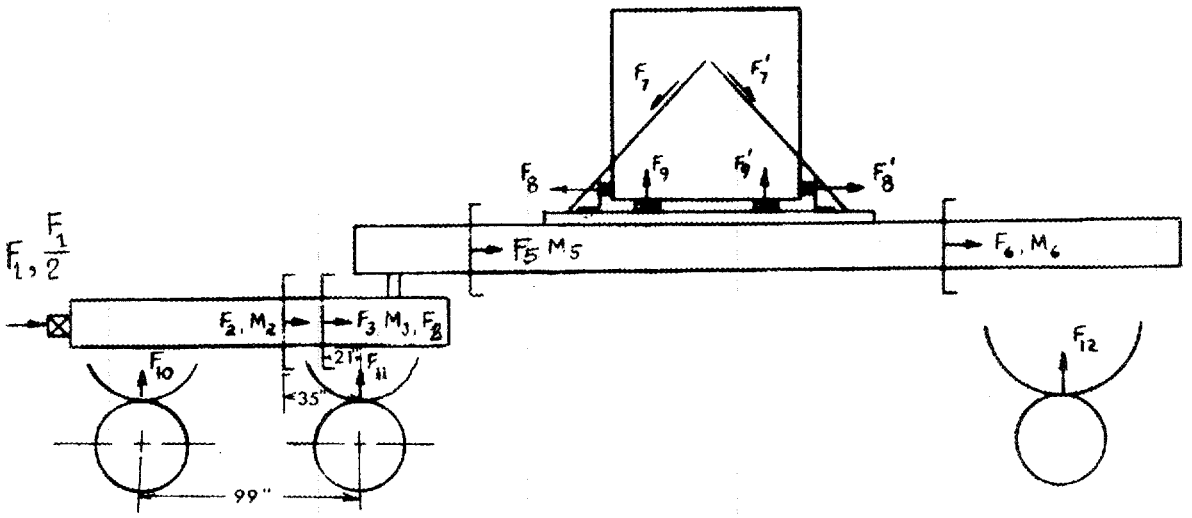

	No. of Channels
F_1, $\frac{F_1}{2}$ - Input Two load cells connected to record the total force of impact and the force of impact in the right frame member as shown.	2

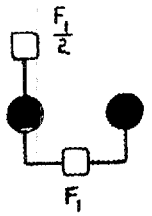

F_2, M_2 - Tractor Frame, Rear Front of forward spring attachment. Strain gages to measure sums and differences of strain in the flanges of the left and right frame members separately as shown.	4

Fig. 6.7. Location of Load Cells and Strain Gages on the Cask and Transport Vehicle for the Third Impact Test.

No. of Channels

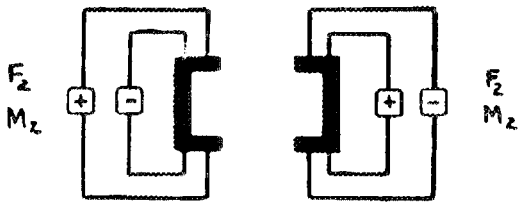

F_3, M_3, F_4 - Tractor Frame, Rear 3
Rear of forward spring attachment. Strain gages to measure the sum and difference of strains in the flanges of the left member (F_3, M_3) and difference of strains in the flanges of both frame members (F_4) as shown.

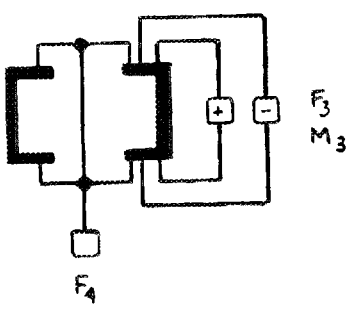

F_5, M_5 - Trailer Frame, Front 4
Between kingpin plate and beginning of nonuniform frame section. Strain gages to measure the sums and differences of strain in the flanges of both the main and side frame members as shown.

F_6, M_6 - Trailer Frame, Rear 4
Front of forward spring attachment. Strain gages mounted the same as for F_5, M_5 as shown.

Fig. 6.7. (continued)

No. of Channels

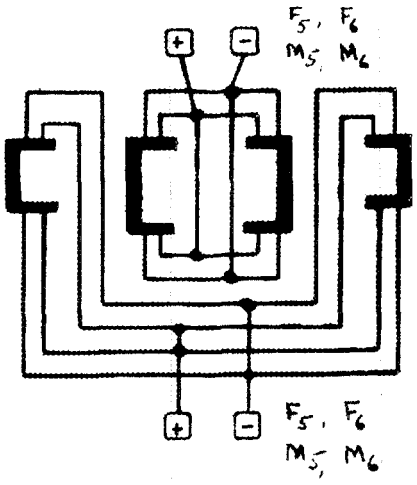

F_7, F'_7 -	Cask, Tie Rods, Front and Rear Straining gages or load cells to measure the force in the front and rear rods separately as shown.	2
F_8, F'_8 -	Cask, Lower, Front and Rear Load cells to measure the horizontal force between the front and rear of the cask and the cask restraining lips as shown.	2
F_9, F'_9 -	Cask, Base, Front and Rear Load cells to measure the vertical force between the front and rear of the cask and the baseplate as shown.	2

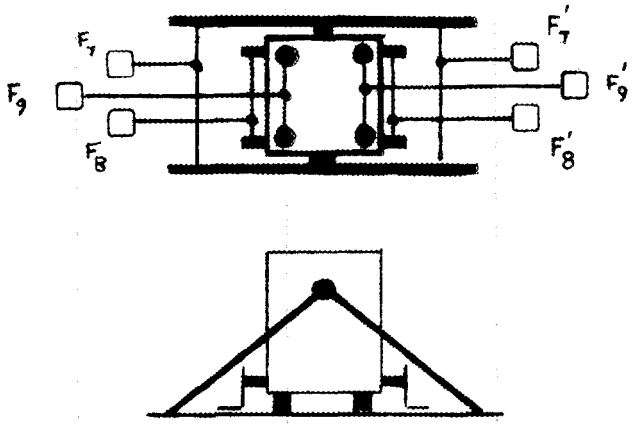

Fig. 6.7. (continued)

		No. of Channels
F_{10} -	Tractor, Front Springs Vertical force summed for both springs as shown.	1
F_{11} -	Tractor, Rear Springs Same as F_{10} as shown.	1
F_{12} -	Trailer, Springs Same as F_{10} as shown.	1
	Total	26

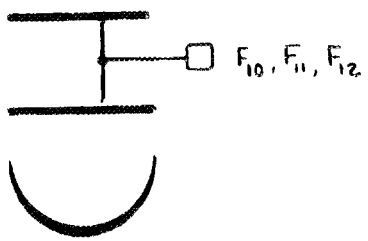

Fig. 6.7. (continued)

6.4 Results of Third Test

The test vehicle was remotely guided to impact against the barrier, and the velocity of the vehicle was clocked at 4 mph immediately prior to the impact. During the impact, the frame of the tractor buckled at a point in front of the fifth wheel, as shown in Figs. 6.8 and 6.9. The yield of the frame members of the tractor in the bending mode occurred immediately ahead of the I-beam spacers for the fifth wheel and slightly behind the front spring hanger for the rear suspension of the tractor, as shown in Fig. 6.9. The extent of this rotation was measured as being about 10.5°. Slight lateral bowing was found in the left frame member about 10 in. behind the base of the load cells. This bowing occurred just behind the reinforcement applied to the front of the tractor frame. This deformation was insignificant when compared with the pronounced buckling that occurred ahead of the fifth wheel.

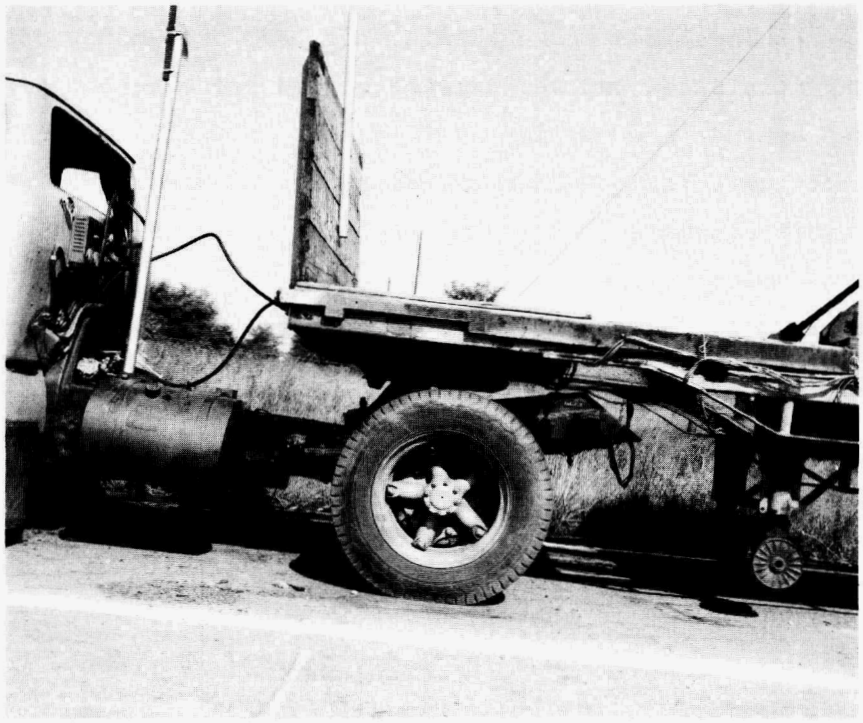

Fig. 6.8. Buckled Frame of Tractor Resulting From the 4-mph Impact.

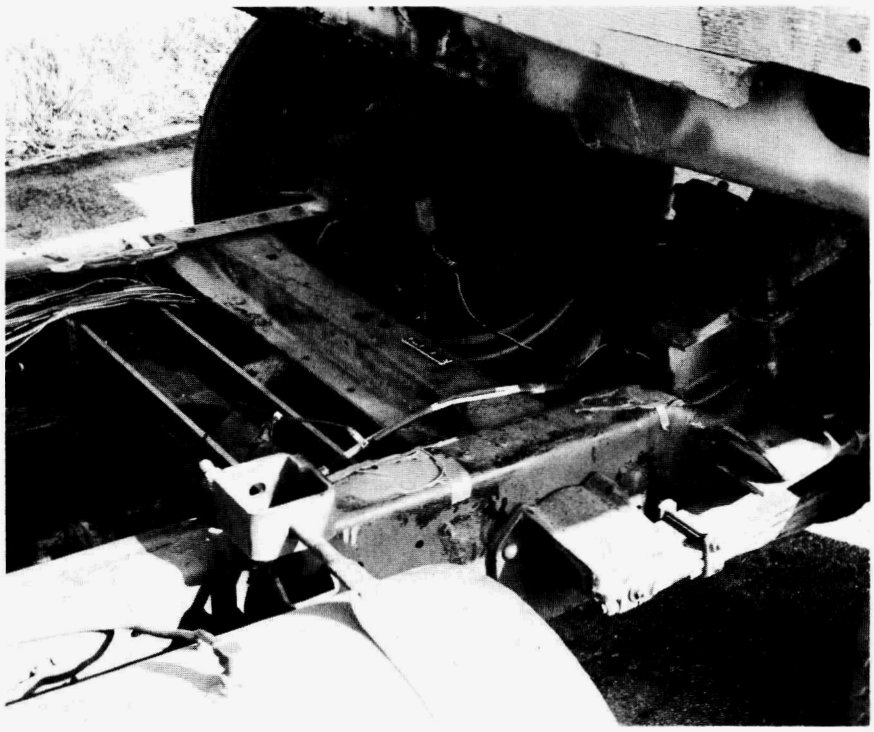

Fig. 6.9. Damage Done to Tractor Frame Immediately Ahead of I-Beam Spacers for Fifth Wheel as a Result of the 4-mph Impact.

Even after localized strengthening, the cab-over-motor tractor was weaker than anticipated and was damaged beyond economical repair by the 4-mph impact against the barrier. It was not possible to use this tractor in the fourth test, as had originally been planned. However, there was no observable damage done to the semitrailer or the cask as a result of the 4-mph impact.

The test data recorded on magnetic tape were digitized, processed through a computer where scale factors were applied, and were then plotted. These plots are shown in Figs. 6.10 through 6.25, and they were used in the evaluation of the mathematical model. The total force measured on the load cells indicated a maximum of 75,000 lb. However, with respect to quantitative measurements, the validity of the values measured on the load cells shortly after impact may be suspect because tension forces were indicated by cells mechanically arranged to measure only compressive forces. On data channel B-1 shown in Fig. 6.10, this phenomenon appears to be a zero shift while there is no specific rationalization for channel B-2. The effects of permanent deformation are reflected in the measurements of the tractor-frame force and moment. The measurements of the forces in the cask tie-down appear reasonable in terms of value and in behavior correlation with time.

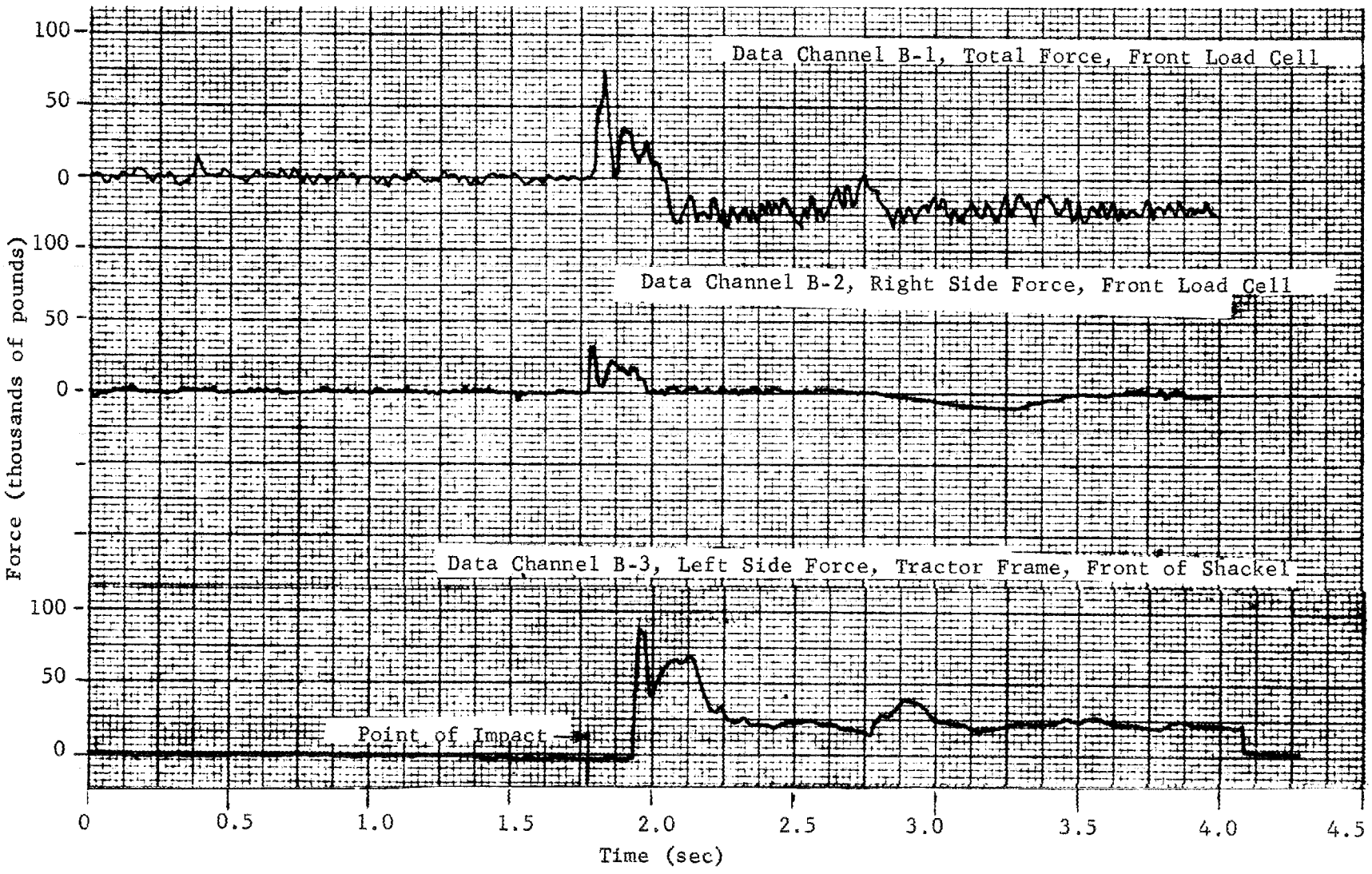

Fig. 6.10. Force Measurements as a Function of Time for the 4-mph Impact.

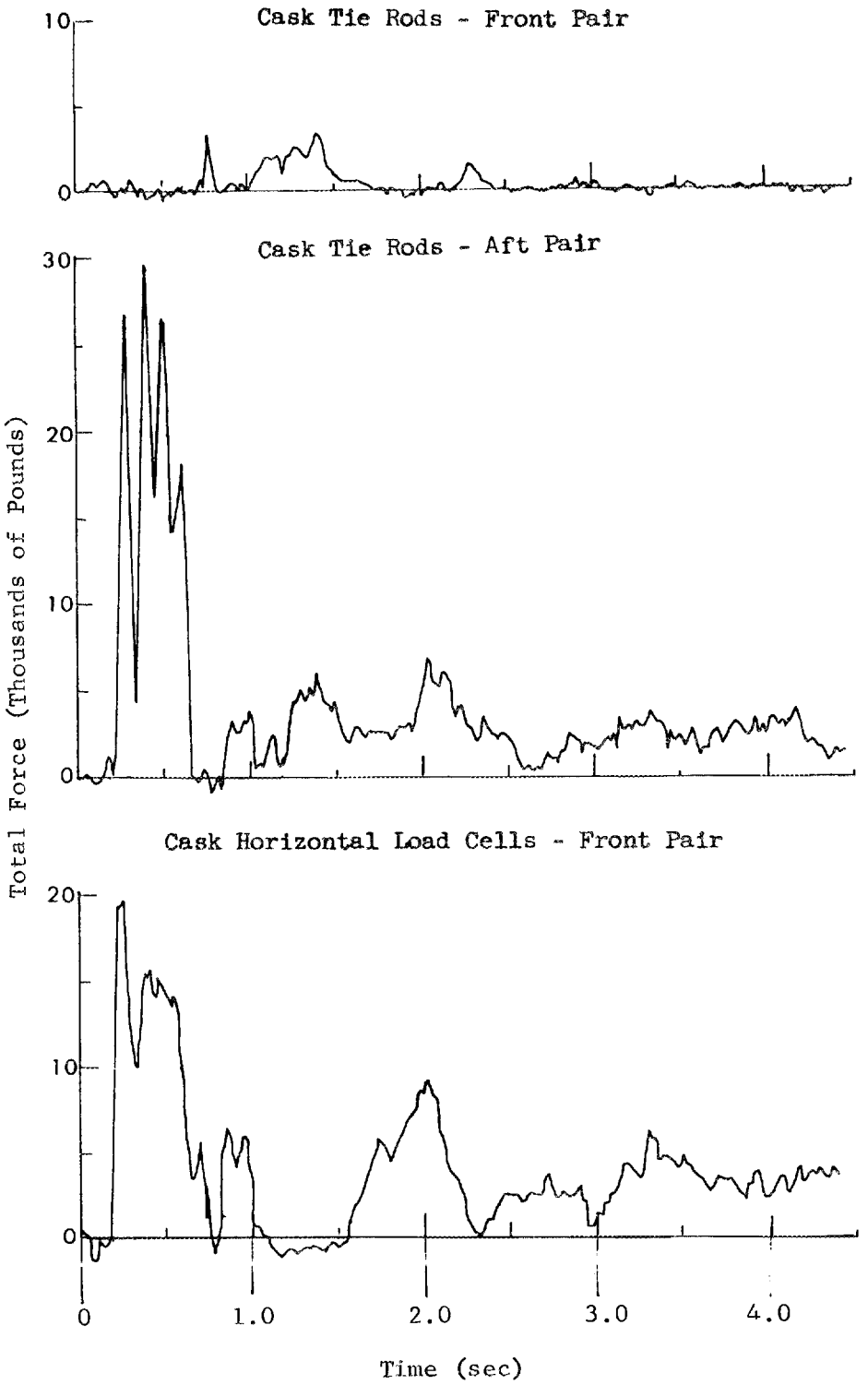

Fig. 6.11. Force Measurements of Cask Tie Rods and Horizontal Load Cells as a Function of Time for the 4-mph Impact.

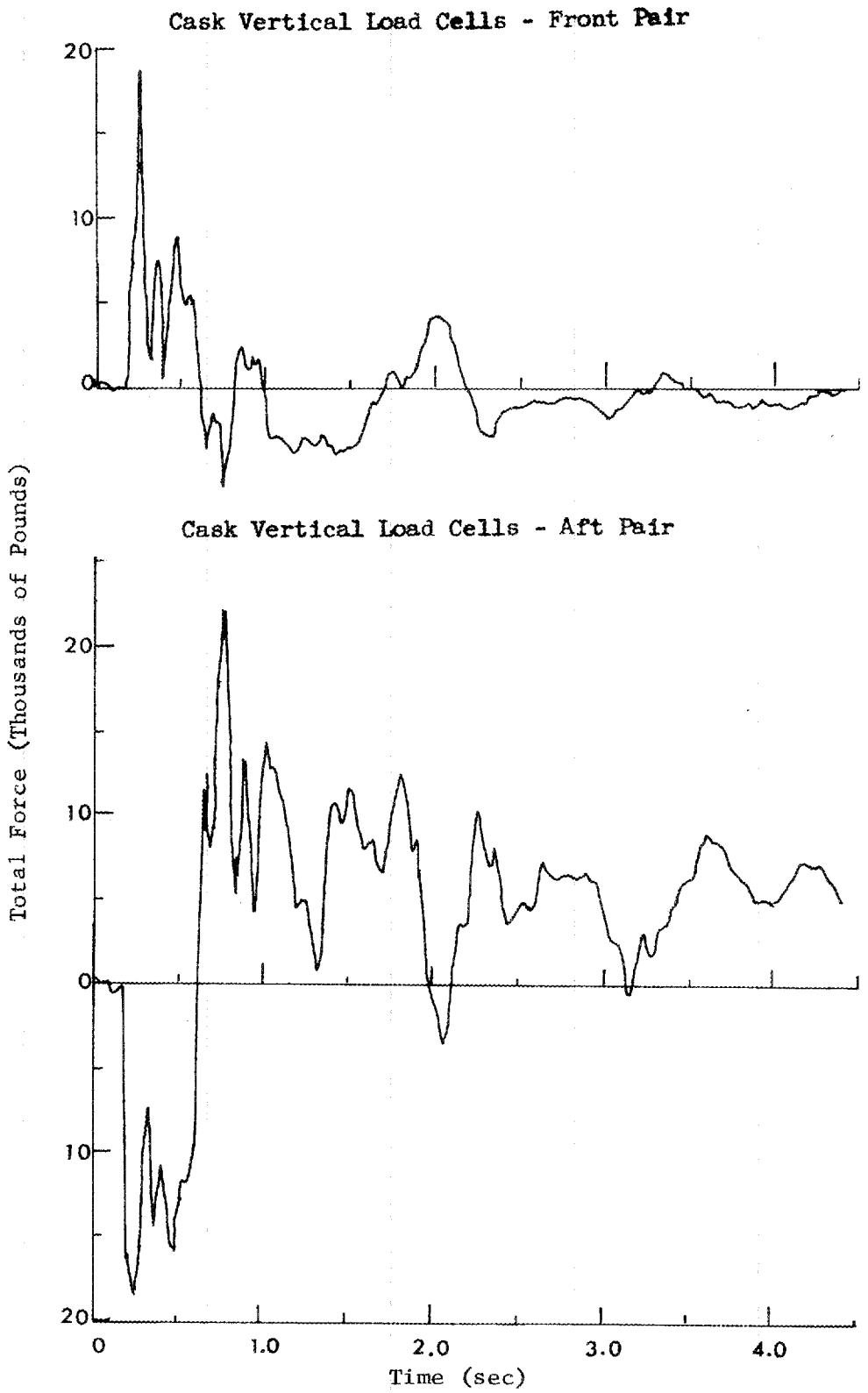

Fig. 6.12. Force Measurements of Cask Vertical Load Cells as a Function of Time for the 4-mph Impact.

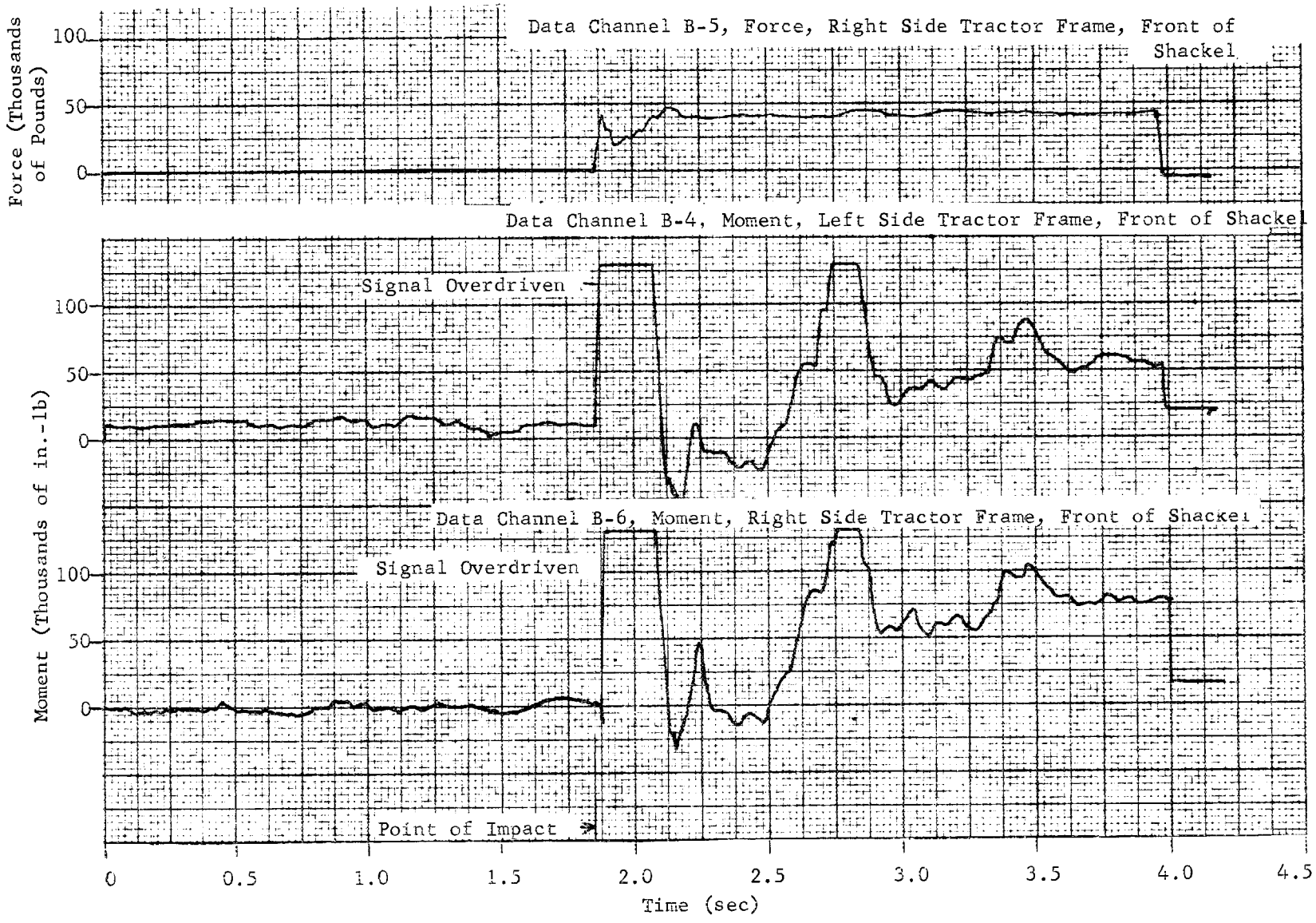

Fig. 6.13. Force and Moment Measurements on Tractor Frame as a Function of Time for the 4-mph Impact.

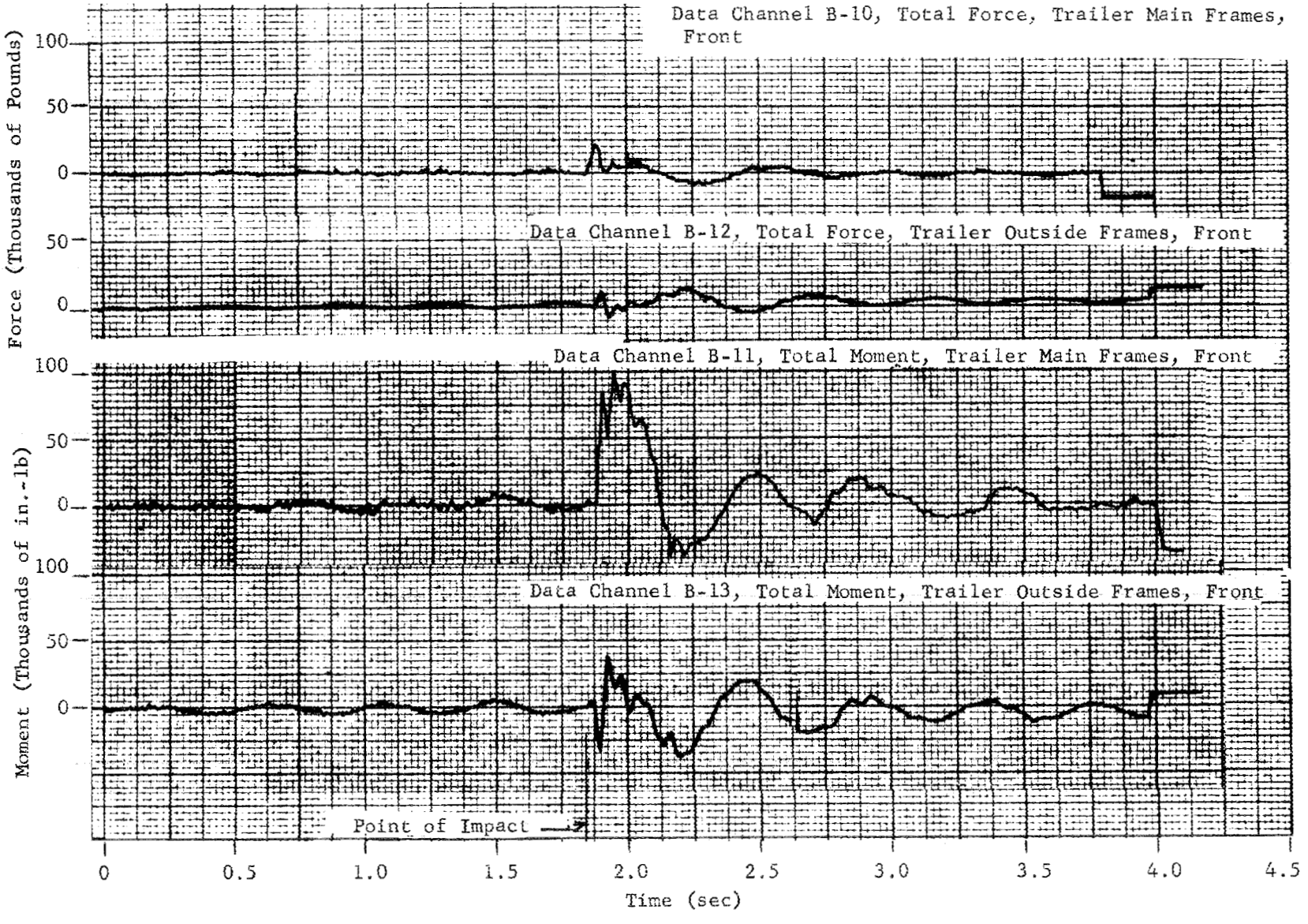

Fig. 6.14. Force and Moment Measurements on Trailer Frames as a Function of Time for the 4-mph Impact.

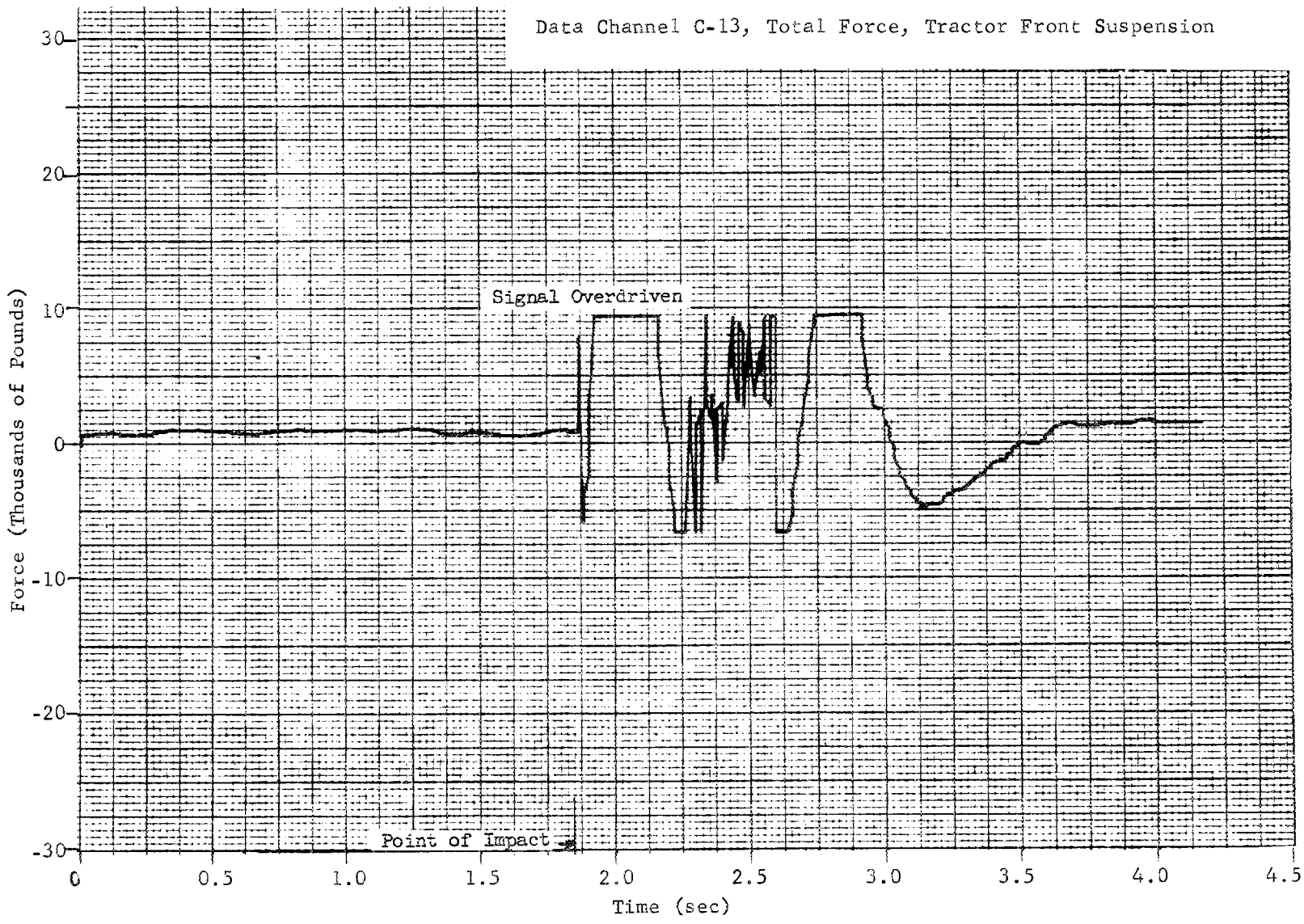

Fig. 6.15. Total Force Measured on Front Suspension of Tractor as a Function of Time for 4-mph Impact.

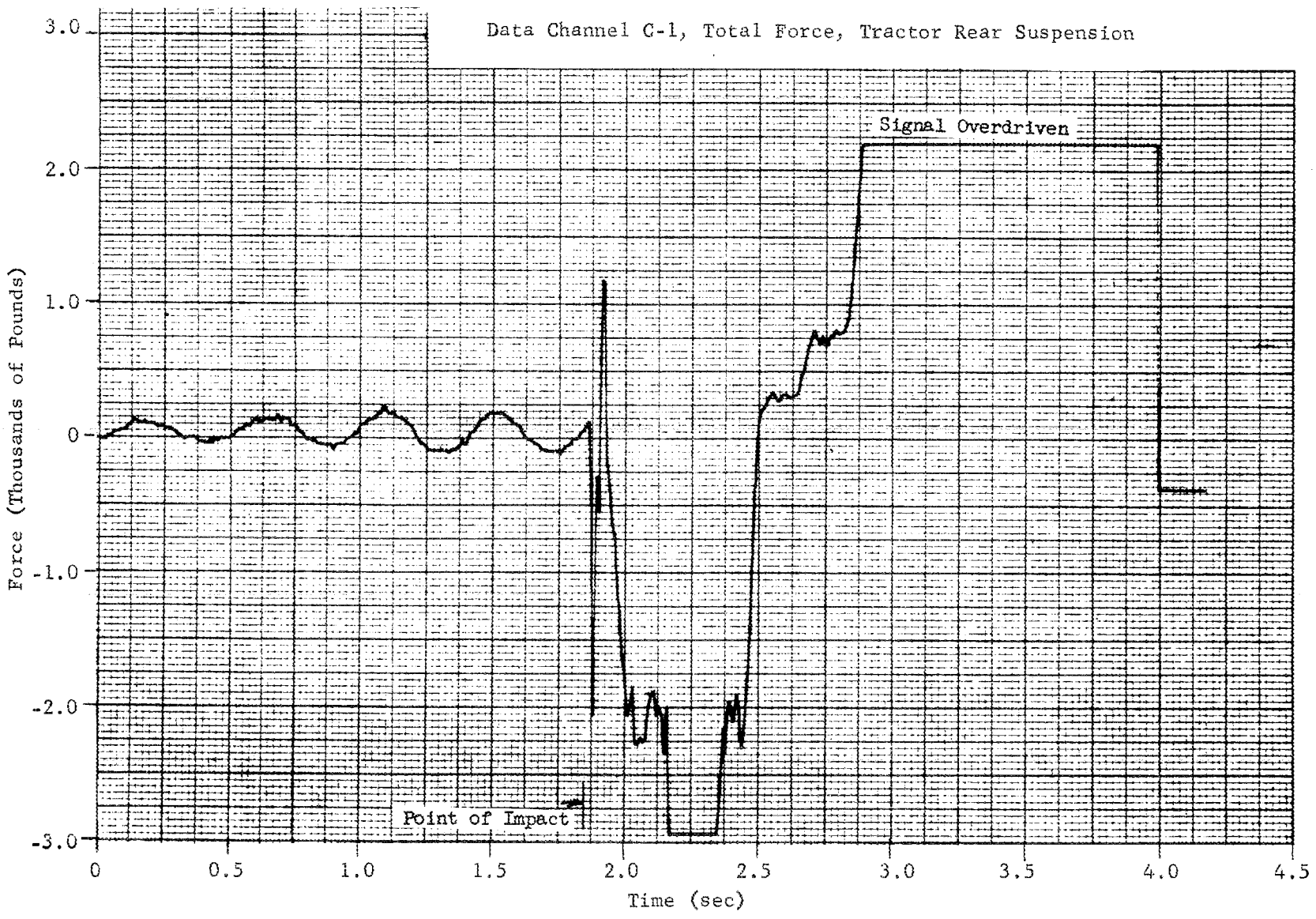

Fig. 6.16. Total Force Measured on Rear Suspension of Tractor as a Function of Time for the 4-mph Impact.

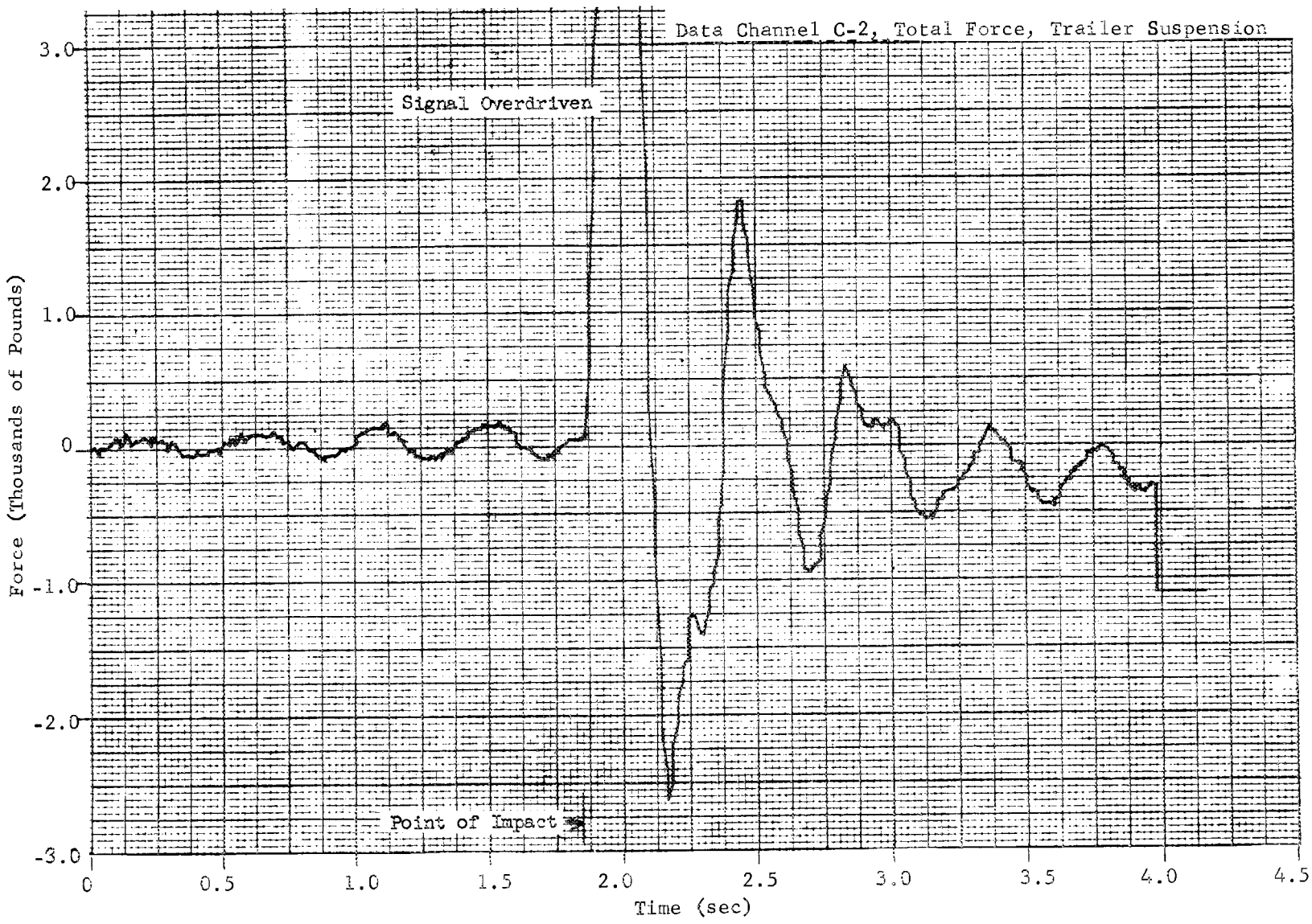

Fig. 6.17. Total Force Measured on Trailer Suspension as a Function of Time for the 4-mph Impact.

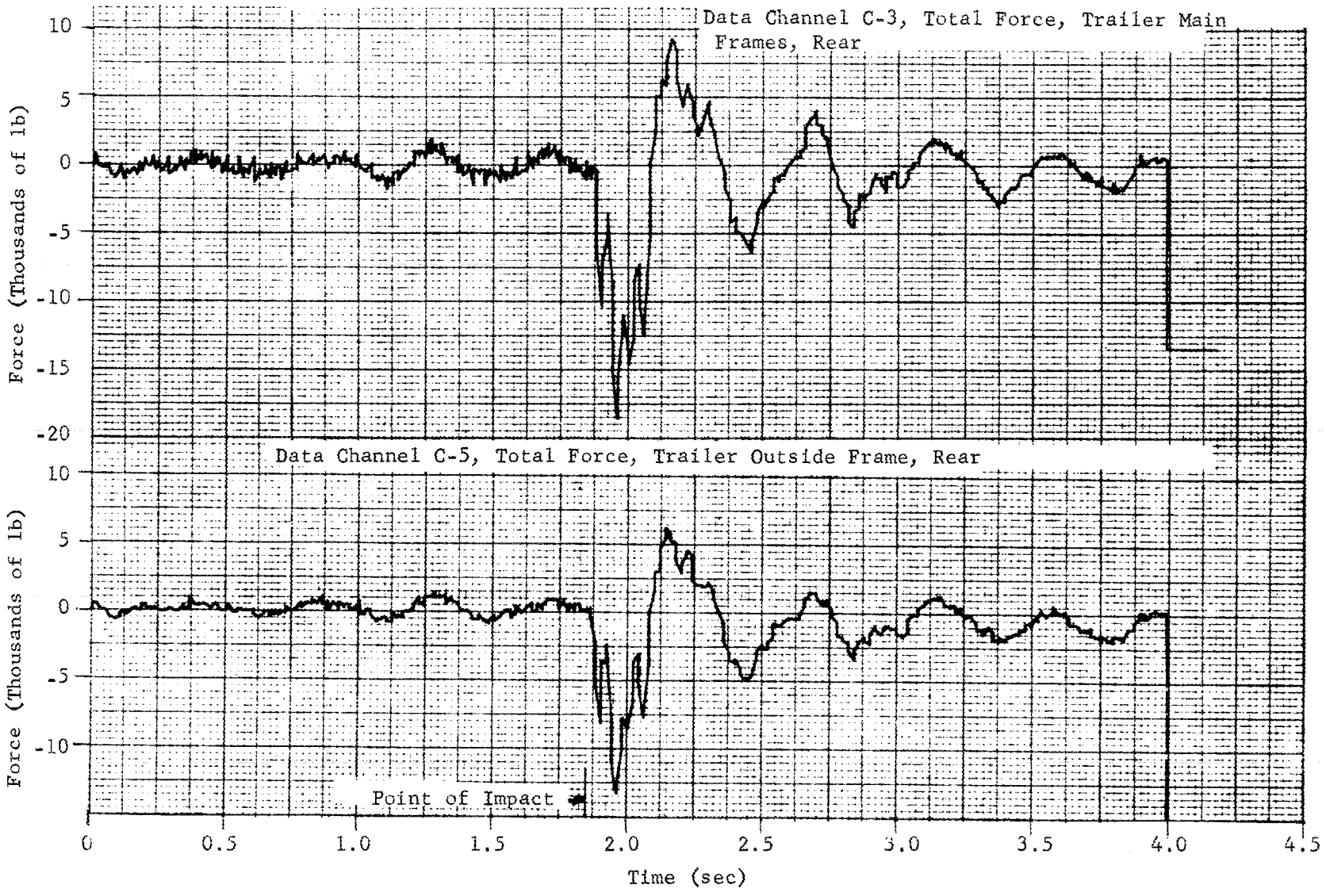

Fig. 6.18. Total Force Measured on Rear Main Frames and Outside Frame of Trailer as a Function of Time for the 4-mph Impact.

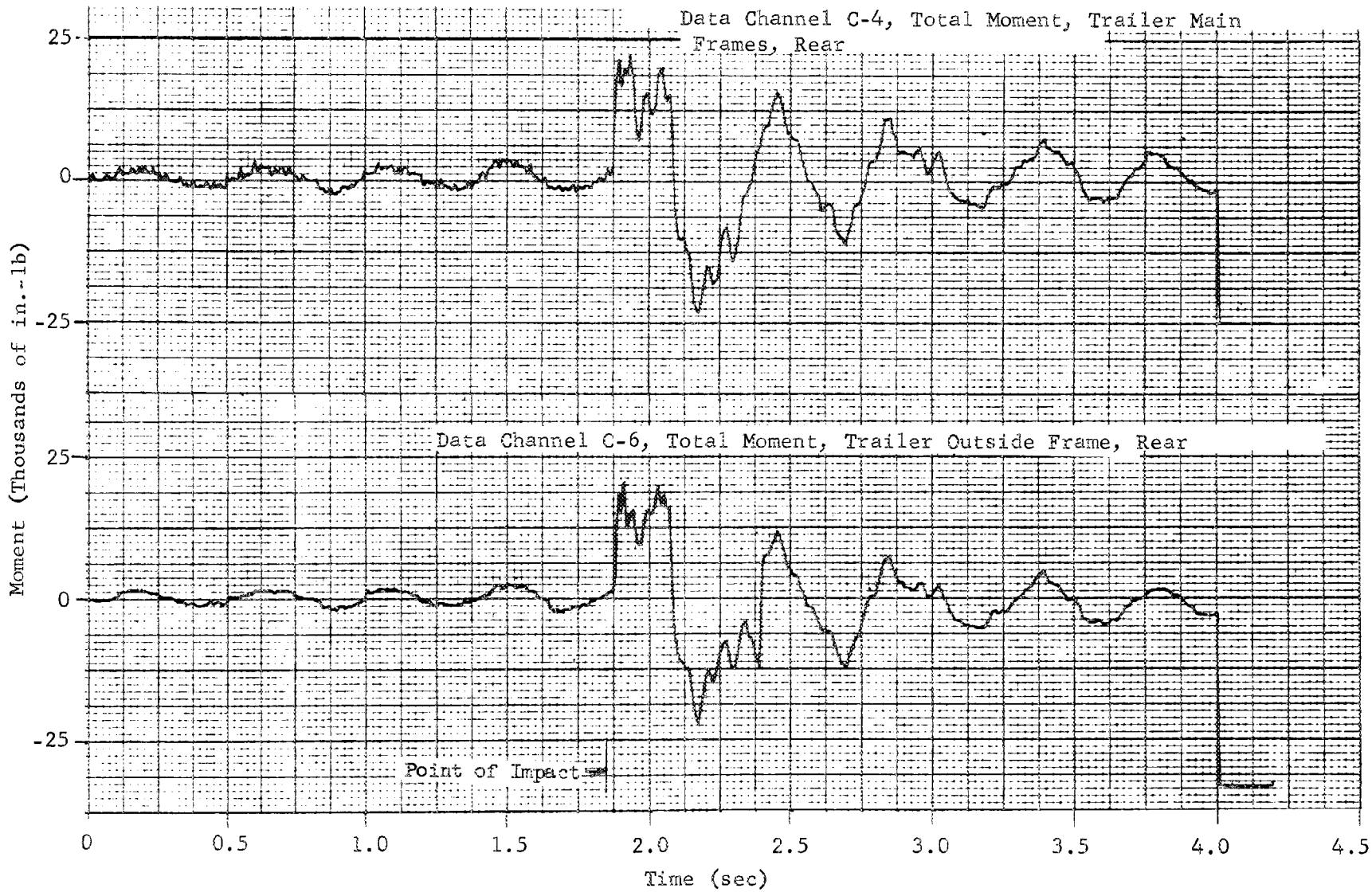

Fig. 6.19. Total Moment Measured on Rear Main Frames and Outside Frame of Trailer as a Function of Time for the 4-mph Impact.

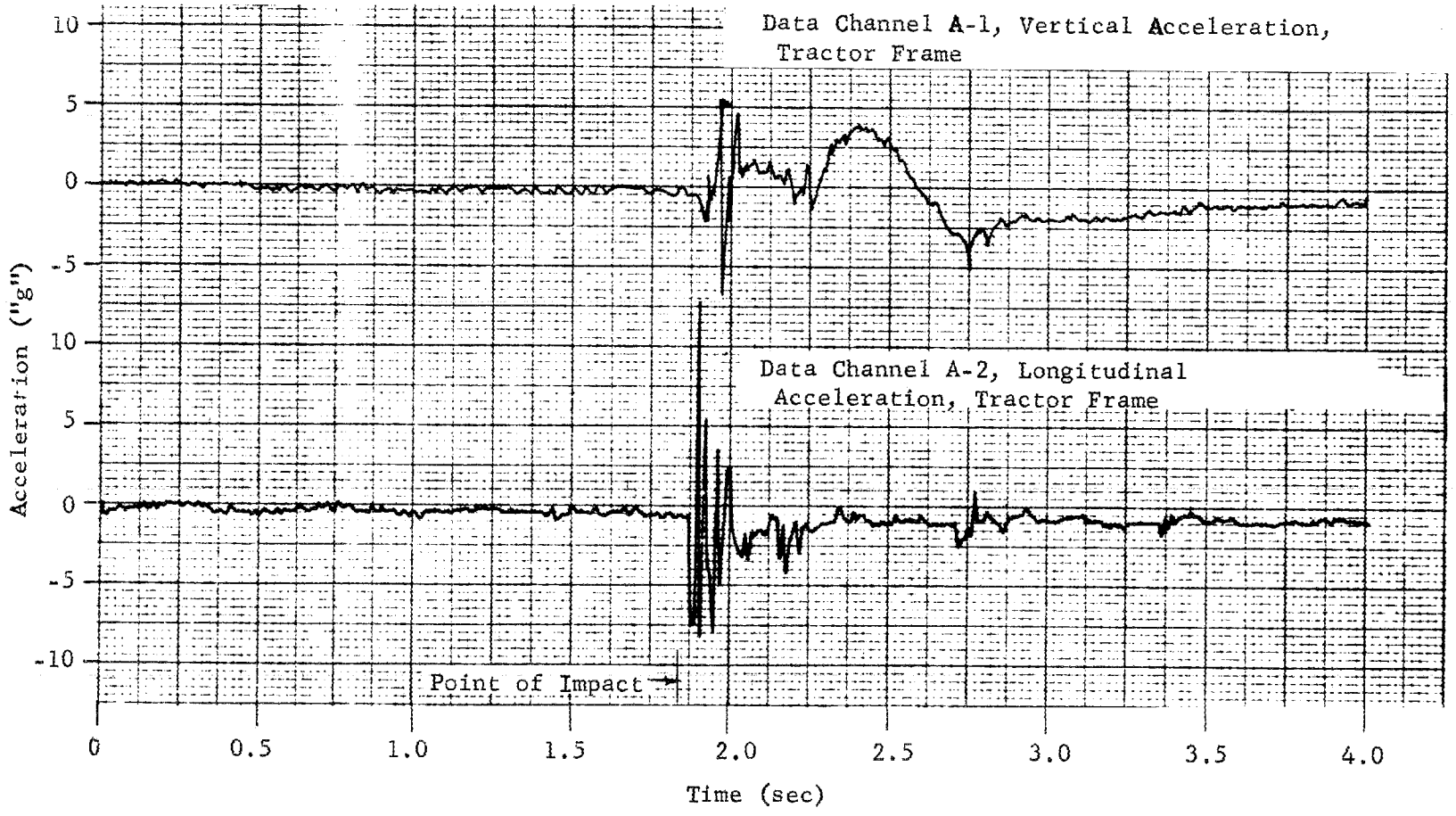

Fig. 6.20. Vertical and Longitudinal Acceleration Measured on Trailer Frame as a Function of Time for the 4-mph Impact.

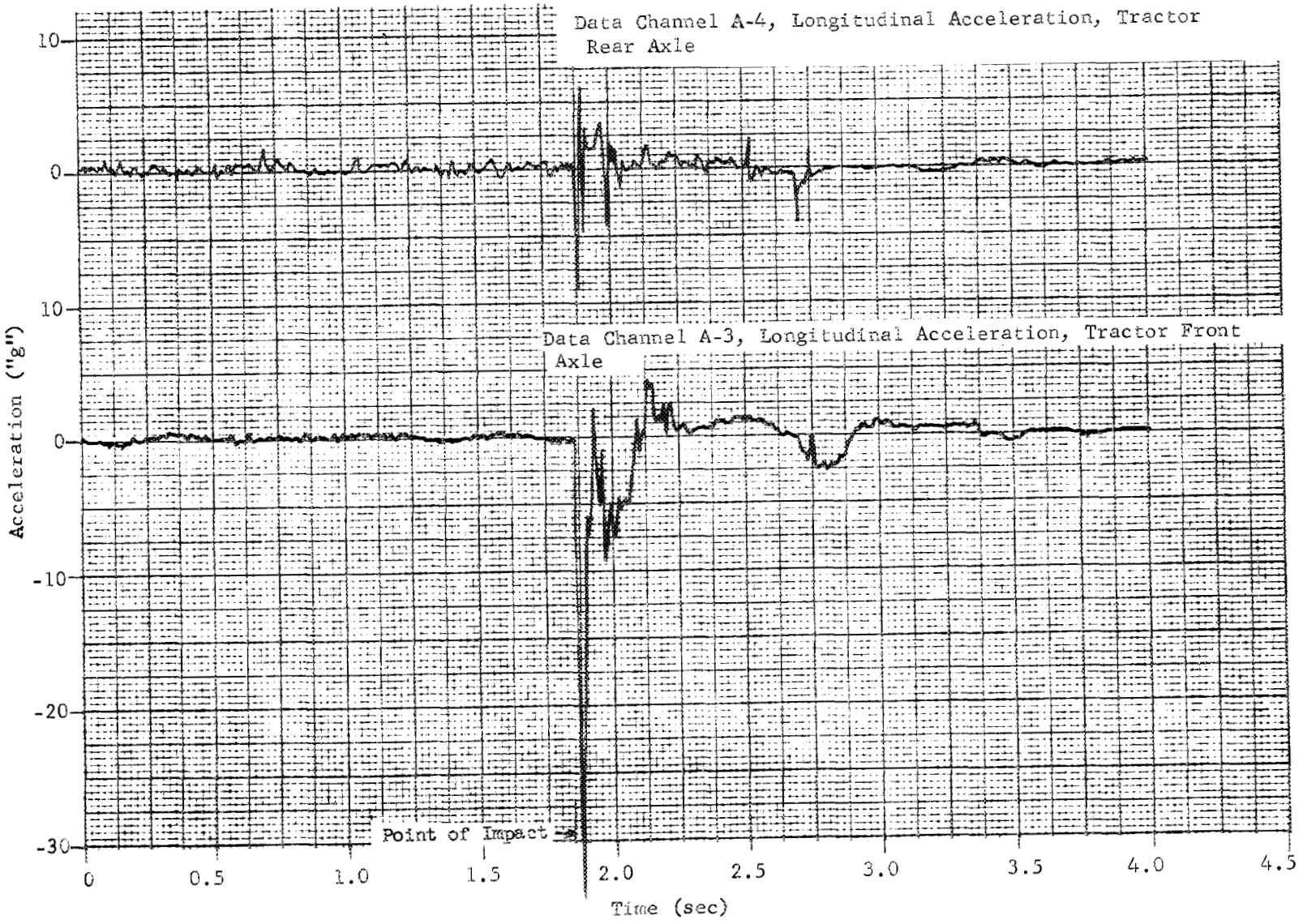

Fig. 6.21. Longitudinal Acceleration Measured on Front and Rear Axles of Tractor as a Function of Time for the 4-mph Impact.

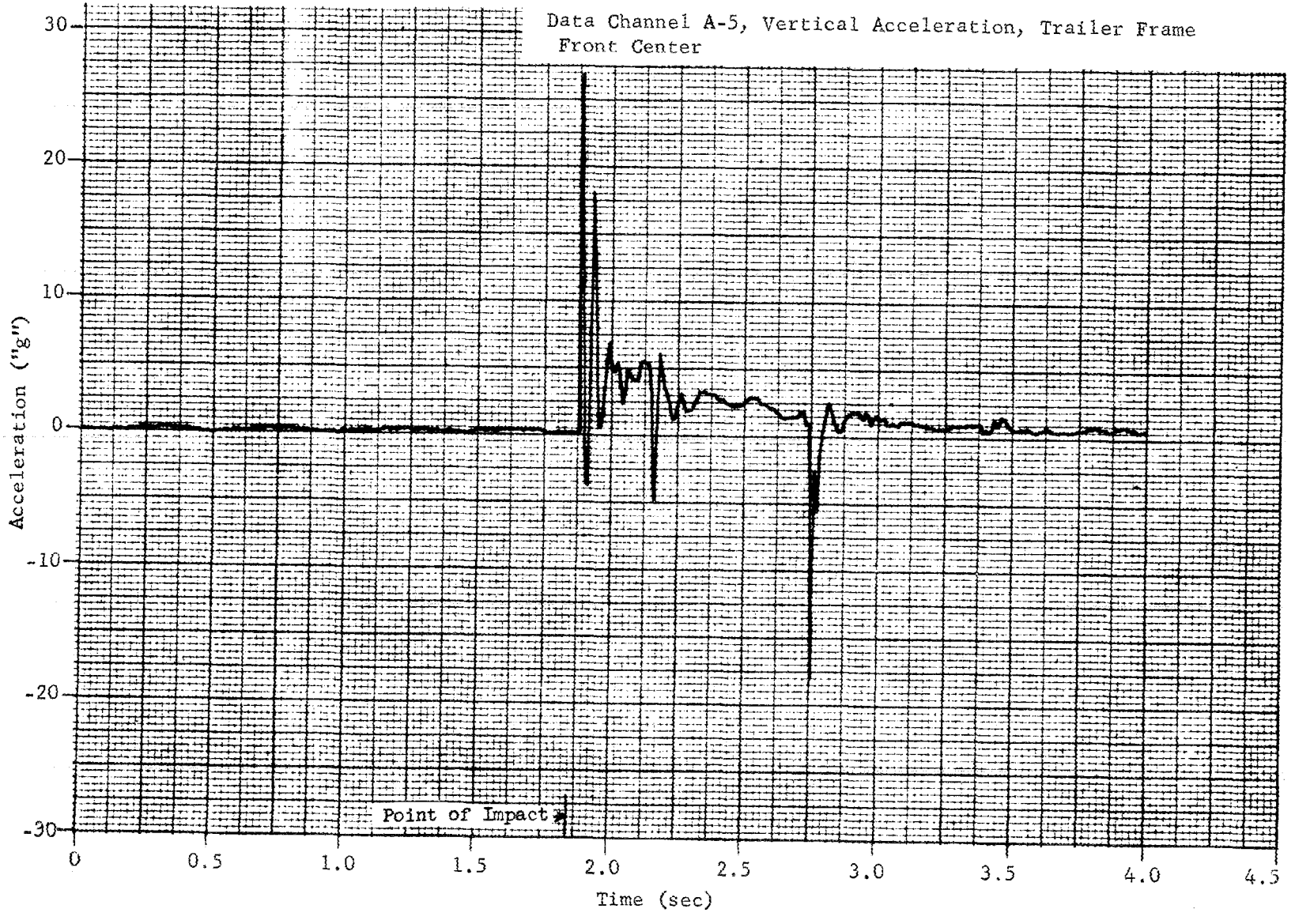

Fig. 6.22. Vertical Acceleration Measured on Front of Trailer Frame as a Function of Time for the 4-mph Impact.

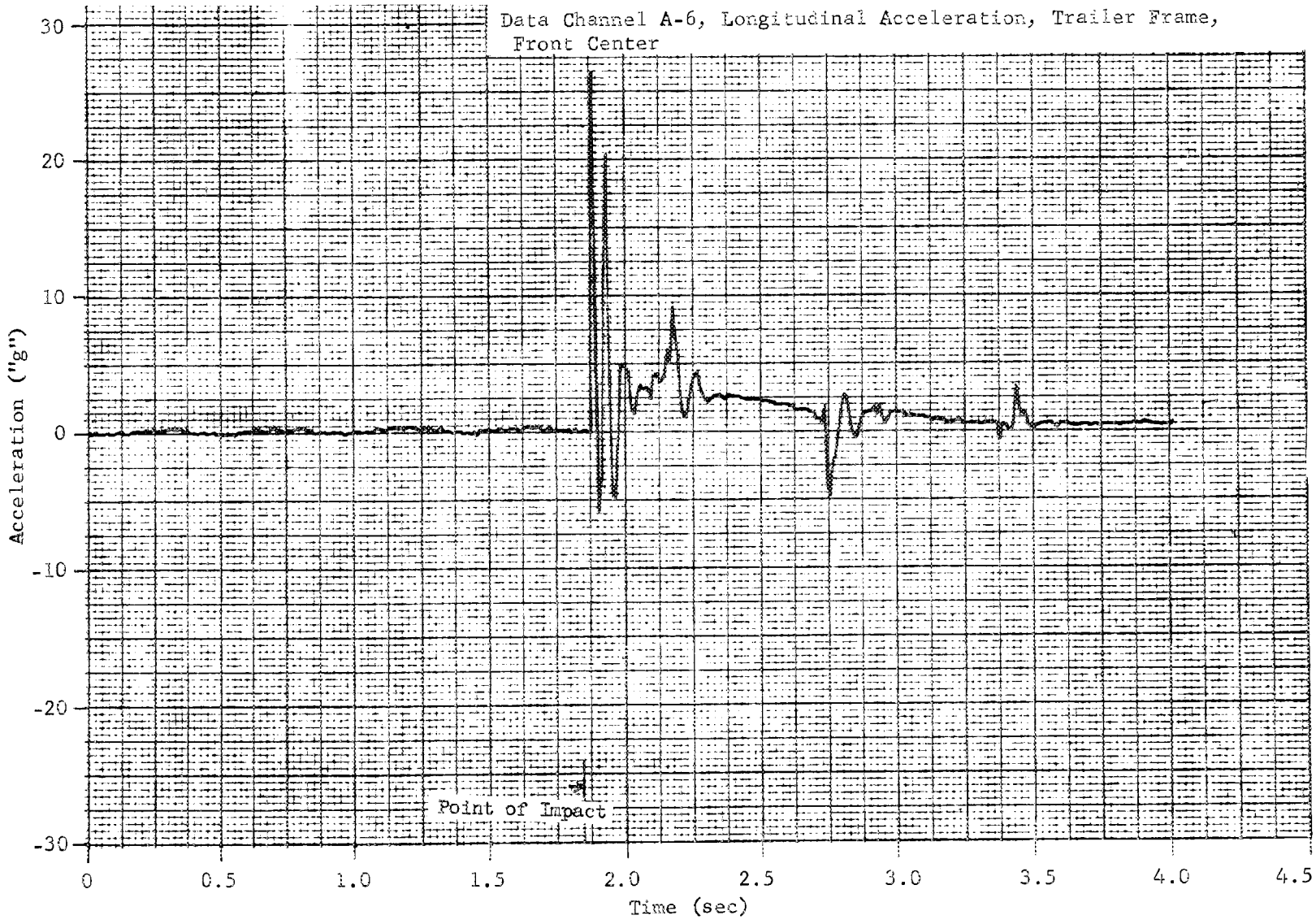

Fig. 6.23. Longitudinal Acceleration Measured on Front of Trailer Frame as a Function of Time for the 4-mph Impact.

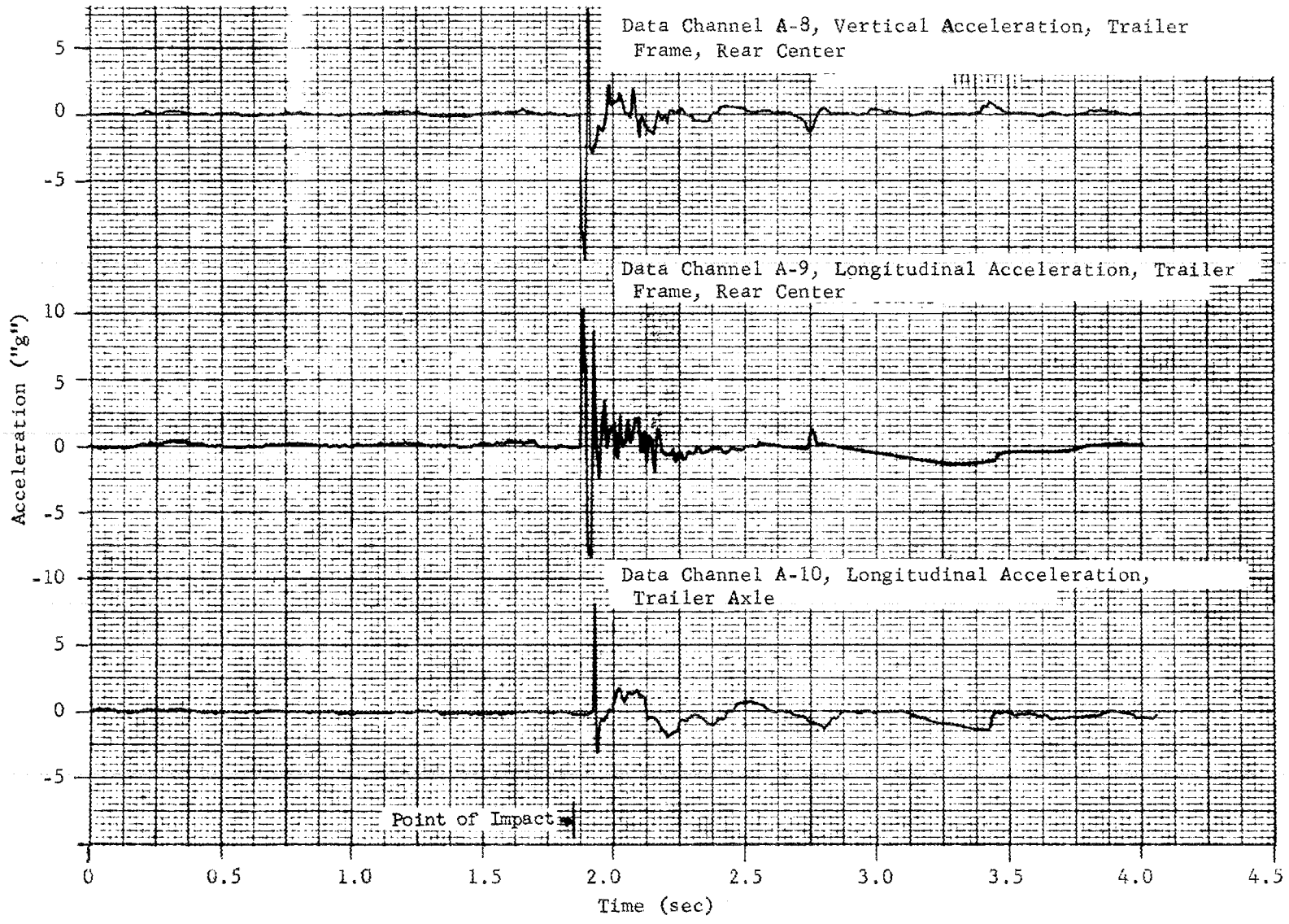

Fig. 6.24. Vertical and Longitudinal Acceleration Measured on Rear of Trailer Frame and Longitudinal Acceleration Measured on Trailer Axle as a Function of Time for the 4-mph Impact.

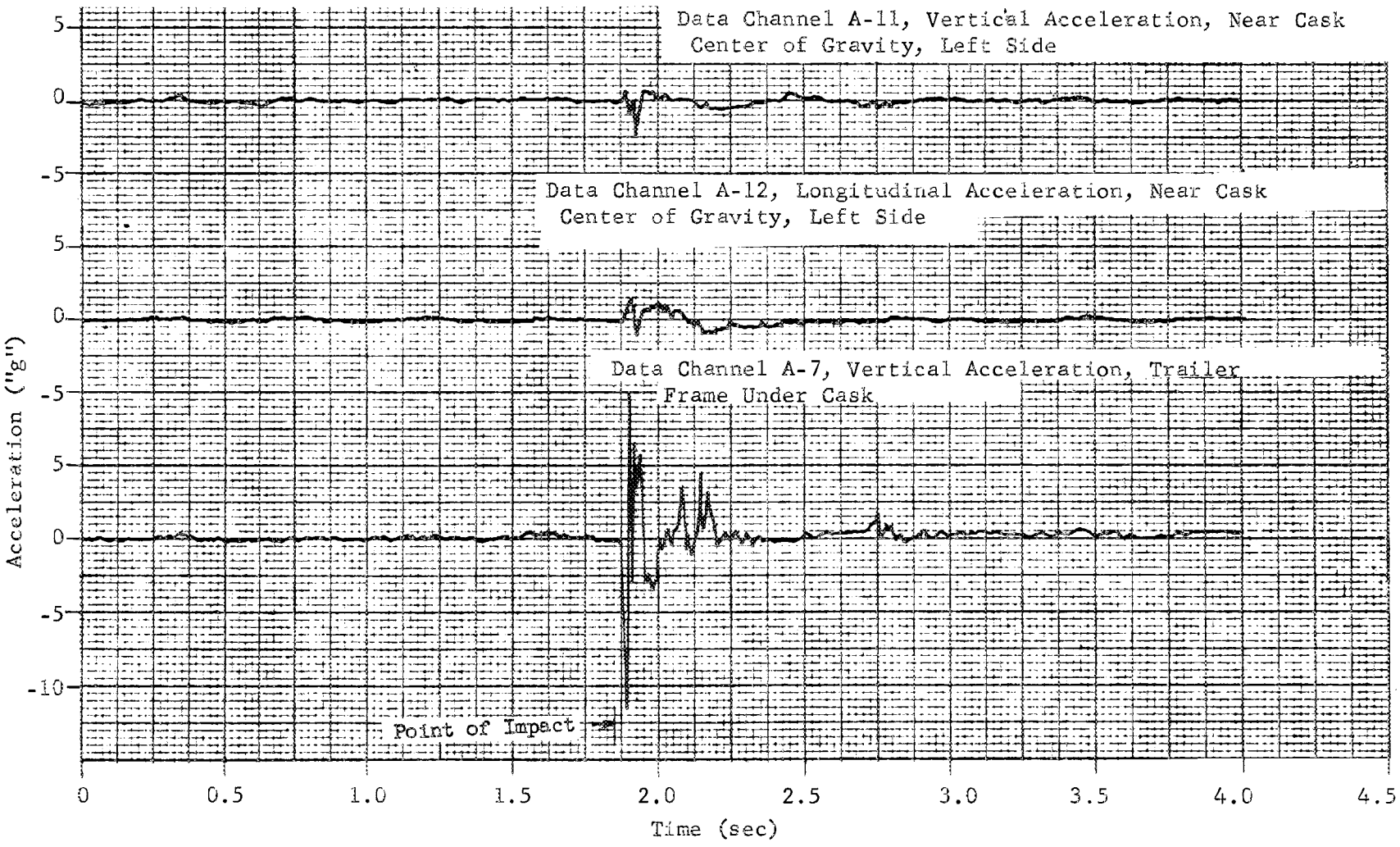

Fig. 6.25. Vertical and Longitudinal Acceleration Measured Near the Cask Center of Gravity on Left Side and Vertical Acceleration Measured on Trailer Frame Under Cask as a Function of Time for the 4-mph Impact.

7. TEST NUMBER FOUR

A nominal velocity of 28 ± 3 mph was selected as the vehicle speed upon impact with the barrier for the fourth test, which was conducted with the same semitrailer and 15-ton cask used in the third test. The fourth test was made to investigate the behavior of the cask transport vehicle during a destructive high-speed collision and to quantify this behavior to the extent possible.

7.1 Test Vehicle

It was originally intended that the cab-over-motor tractor used in the third test would also be used in the fourth test. Since the tractor was damaged beyond economical repair in the third test and because of its obvious weakness in the low-speed impact, the decision was made to use another type of tractor in the relatively high-speed test. A 2.5-ton 6-by-6 M275 military tractor was selected to pull the semitrailer with the cask in the fourth test. This tractor-trailer combination is shown in Fig. 7.1, and the physical features of the M275 tractor are compared with those of the cab-over-motor tractor used in the third test in Table 7.1.

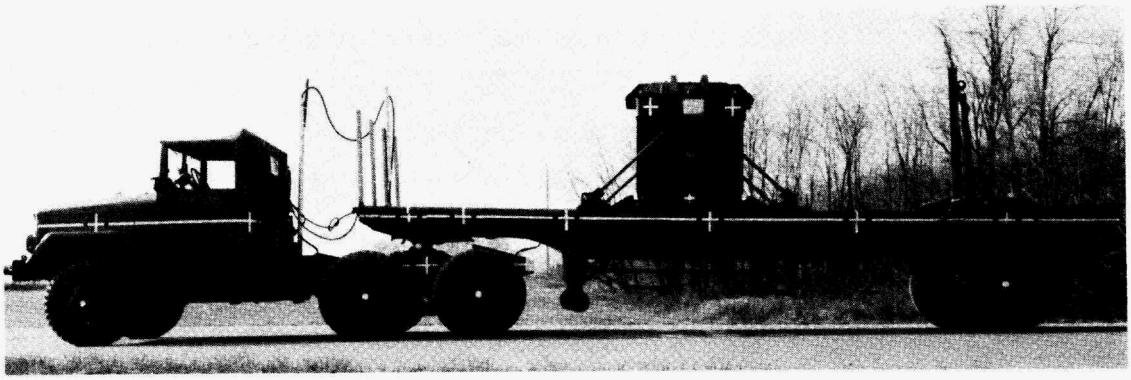

Fig. 7.1. Tractor and Flatbed Semitrailer Used in Fourth Test.

Table 7.1. Physical Features of Tractor Used in the Fourth Test Compared With Those of Tractor Used in the Third Test

Physical Characteristics	M275 Tractor Used in Fourth Test	Cab-Over-Motor Tractor Used in Third Test
Total frame area where gages were installed, in.^{2}	8.2	7.0
Frame configuration	Parallel Channels	Bowed around motor, variable channel depth
Distance from fifth-wheel pin to top of flange, in.	5	10
Average yield strength of frame, psi	35,000	42,000

The total strength of the two tractor frames was nearly equal: 294,000 lb for the cab-over-motor tractor comapred with 286,000 lb for the M275 military tractor, with a slight balance in favor of the cab-over-motor tractor. However, the parallel configuration of the frame rails and the 50% reduction in the moment about the fifth wheel on the military tractor was considered to offset the slight difference between the frame strength of the two vehicles.

Since this was to be the final test in the series, particular consideration was given to the frame members and connections to ensure, insofar as practicable, structural continuity and integrity compatible with the selected impact velocity. Attention was also directed toward seeing that the test vehicle would satisfy certain physical requirements intended to ensure that

1. the tractor-semitrailer fifth-wheel connection would provide sufficient strength to eliminate premature separation of the semitrailer from the tractor,
2. the 15-ton cask would not separate from the semitrailer during impact,
3. the cask tie-down would respond as a rigid restraint system, and
4. the collision impact would be made at such a velocity that instantaneous destruction of possible overturn of the semitrailer would be avoided.

To meet these physical requirements, certain modifications were made on the tractor. The fifth-wheel connection to the tractor frame was strengthened by replacing the ten original 5/8-in.-diameter bolts with 3/4-in.-diameter SAE-Grade-8 bolts. This substitution was made one bolt at a time, and the tolerance was obtained by reaming the holes in a force fit. The front bumper of the tractor was strengthened to support the load cells by welding a 1-in.-thick plate across its face.

The flatbed semitrailer, cask, and cask tie-down were the same used in the third test. The two cask tie-down trunnions and four tie rods were designed to a calculated strength of 200,000 lb per trunnion and 150,000-lb yield strength per tie rod. A 1.5-in.-thick spreader plate, extending nearly one-third the length of the semitrailer, was welded to the frame of the trailer to distribute the weight of the cask. This plate also served to reinforce the frame of the trailer considerably and to increase its stiffness ratio. The physical characteristics of the principal elements of the transport system are tabulated below, and other physical properties and dimensions of the tractor are shown in Fig. 7.2.

	Cross Section Area (in.^{2})	Moment of Inertia I_{xx} (in.^{4})	Section Modulus Z_{xx} (in.^{4})
Tractor frame	8.2	58.4	29.2
Trailer frame	164.6	6440.0	222.7

A study of the static loading and deflection of members of the tractor and trailer was made by The Franklin Institute Research Laboratories for use in the mathematical. The total weight of the loaded test vehicle was 50,670 lb, and a summary of the weight distribution on the test vehicle is given in Table 7.2.

To evaluate the effects of the impact on the fuel tank of the tractor, the tank was drained of fuel and partially filled with colored water. Fuel to propel the tractor was supplied from an auxiliary can with a capacity of 5 gallons that contained only two gallons of gasoline. Fire-fighting equipment was also on standby during the fourth impact test.

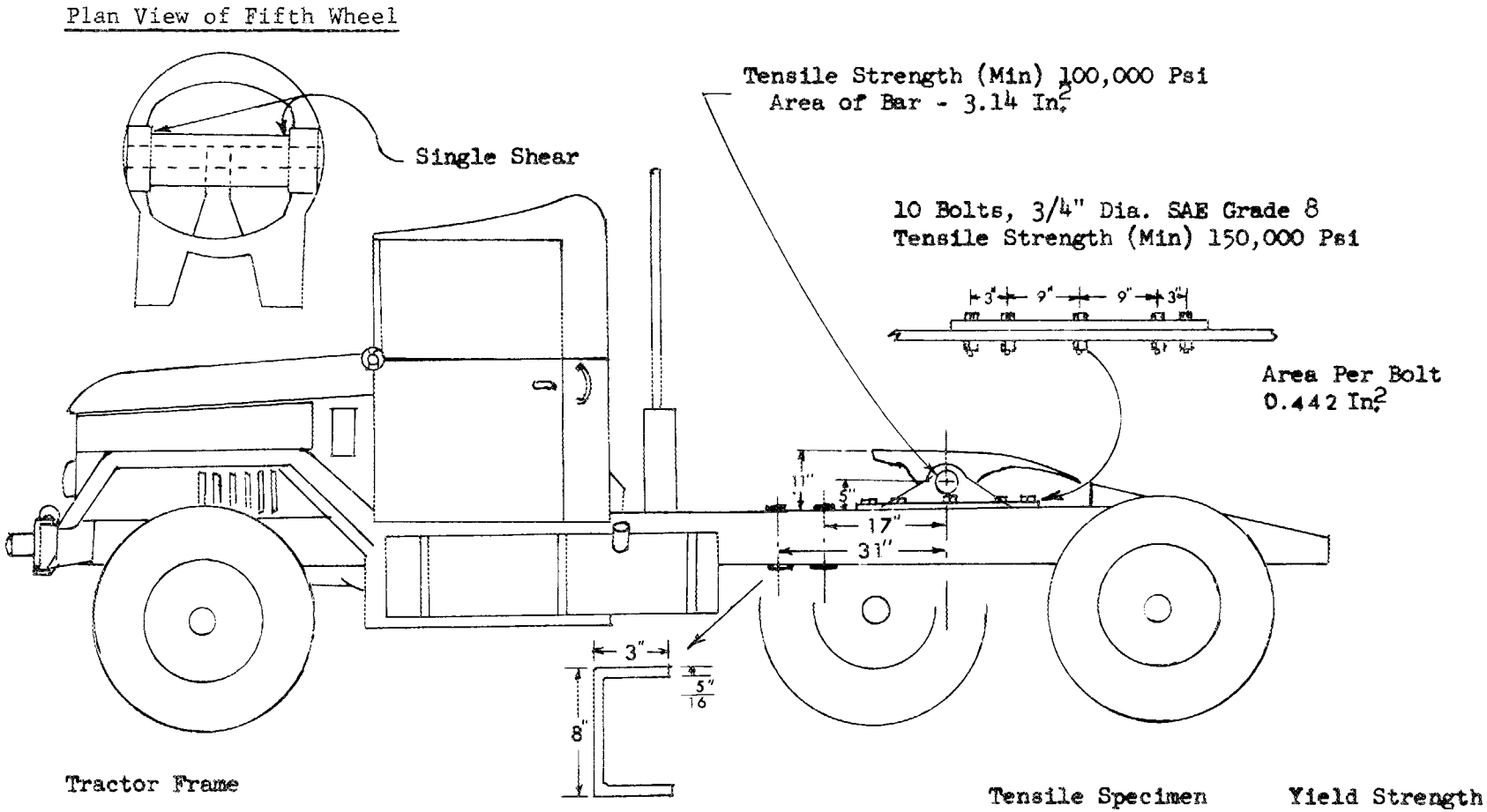

Tractor Frame

Cross Sect Area	4.1 $In.^2$
Moment of Inertia	29.2 $In.^4$
E - Right	30.8×10^6 Psi
E - Left	30.0×10^6 Psi

Tensile Specimen	Yield Strength
Right Side Frame	34,140 Psi
Left Side Frame	35,550 Psi

Fig. 7.2. Dimensions and Physical Properties of the 2.5-Ton M275 Military Tractor Used in the Fourth Impact Test.

Table 7.2. Weight Distribution on Loaded Cask Transport Vehicle Used in the Fourth Impact Test

Wheel Location	Weight on Tractor Wheel Right (lb)	Weight on Tractor Wheel Left (lb)	Weight on Trailer Wheel Right (lb)	Weight on Trailer Wheel Left (lb)
Front	3270	2780		
Intermediate	5380	6015		
Rear	5935	6030	10,710	10,550

7.2 Instrumentation

Substitution of the 2.5-ton 6-by-6 M275 military tractor for the cab-over-motor tractor used in the third test required that the military tractor be completely instrumented for the fourth test. The instrumentation plan for the military tractor was the same as that for the cab-over-motor tractor illustrated in Figs. 6.6 and 6.7 except for the load cells attached to the frame immediately ahead of the fifth wheel. Since the 6-by-6 rear suspension was a bogie arrangement, the double axial force channels ahead and behind the forward spring hanger could not be used as a measure of energy contributed by the unsprung mass of the rear axles. The final arrangement of the accelerometers, load cells, and strain gages for the fourth test is illustrated in Figs. 7.3 and 7.4. The data channels freed by eliminating one axial force measurement on the tractor frame were assigned to the front load cells. Three channels were used to record the measurements of the right load cell, the left load cell, and the sum of both load cells in the fourth impact test.

Telemetry cables from the tractor were suspended from the rear of the tractor under the trailer to a point near the rear of the trailer. This was done in an effort to allow maximum slack in the cables and to prevent damage to them should the tractor and semitrailer become separated as a result of the impact.

One important fact learned from the previous high-speed impact test, the second test, was that dust and dirt from various sources formed a light diffused cloud during the impact that obscured the view of the

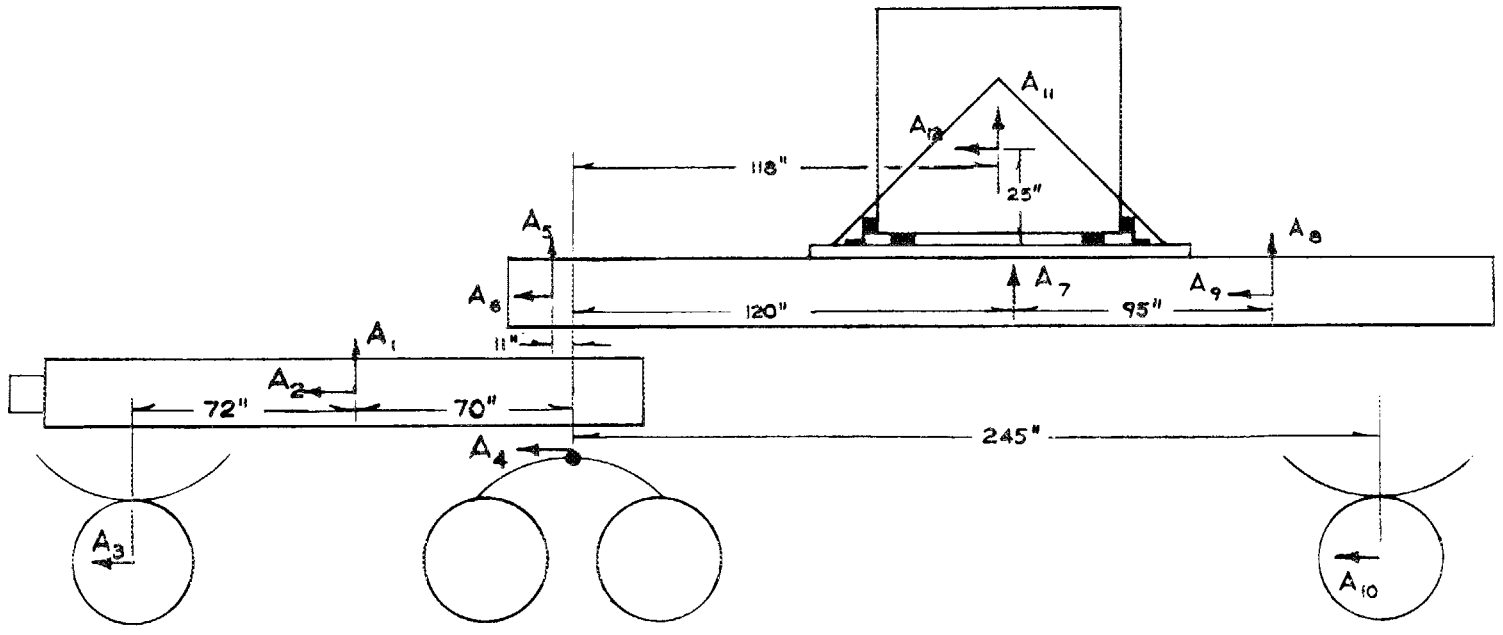

Fig. 7.3. Location of Accelerometers on Cask and Transport Vehicle for the Fourth Impact Test.

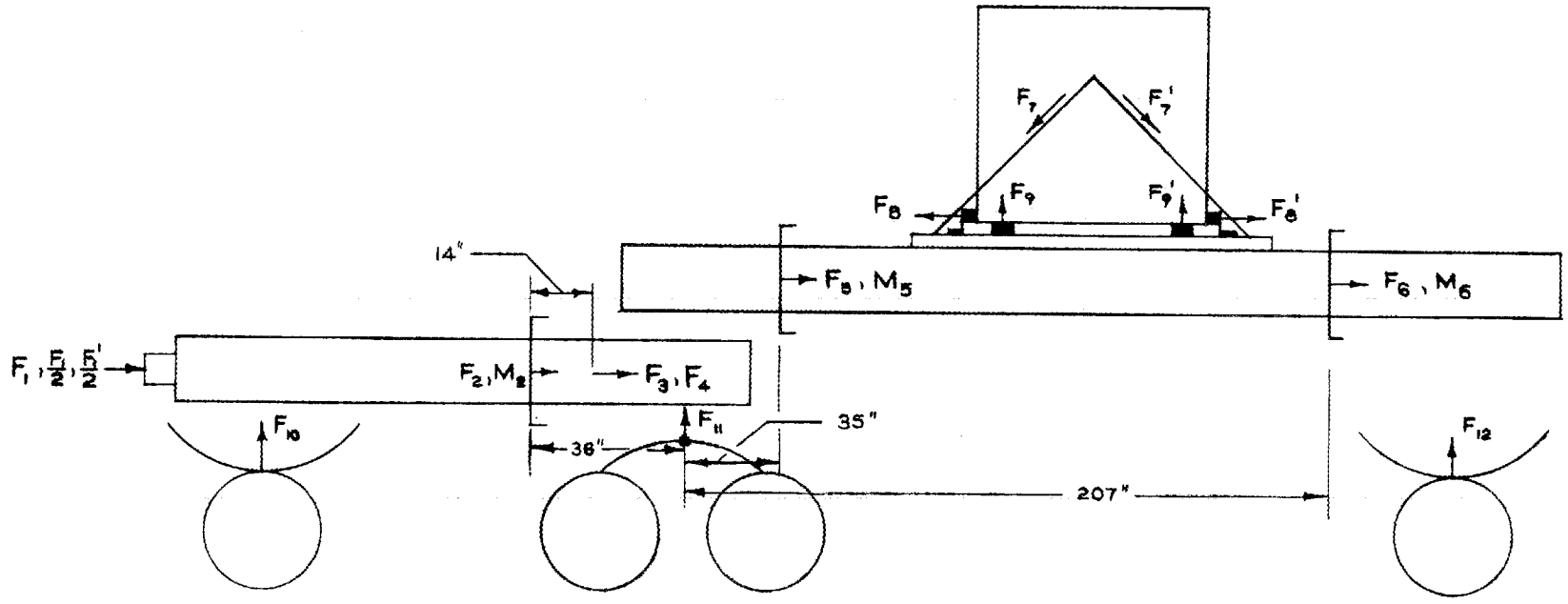

Legend:

F - Axial Force or Strain

M - Bending Strain

Fig. 7.4. Location of Load Cells and Strain Gages on the Cask and Transport Vehicle for the Fourth Test.

cameras. This problem was minimized for the fourth test. The vehicle was cleaned prior to the test, and all rusty surfaces on the vehicle and barrier were painted or oiled to provide a binder for flocculating colloidal particles that would prevent their suspension in the atmosphere as a result of the impact. In addition, the surface of the road within a 25-ft radius around the barrier was wet down with water prior to the test. The test vehicle and cask were marked, as illustrated in Fig. 7.5, to help indicate the displacement of various points during the filming of the impact.

7.3 Determination of Impact Speed for Fourth Test

The impact velocity of the cask transport vehicle against the barrier for the fourth and final test was agreed upon by the Technical Working Group of the Joint AEC-DA Advisory Committee as being 28 $\pm$ 3 mph. The earlier recommendation was about 30 mph, and this recommendation was based on an empirical analysis of the three previous tests. An attempt was made to correlate the results of these tests to determine whether an impact force at a given speed can be predicted.

For this analysis, the rigidity of the M275 military tractor frame was determined by considering the frame to be a simple beam subject to a centrally applied axial force. The buckling force was calculated by using Euler's column formula, and it was found that buckling occurs with as little force as 179,000 lb, depending upon the end support conditions of the beam or tractor frame. Assuming a yield strength for the material of the tractor frame of 35,000 psi, the buckling force was found to be 287,000 lb. The results of this analysis were plotted on the graph shown in Fig. 7.6. By assuming that the curve on the graph describes the phenomenon, the tractor frames buckle at an impact velocity below 10 mph.

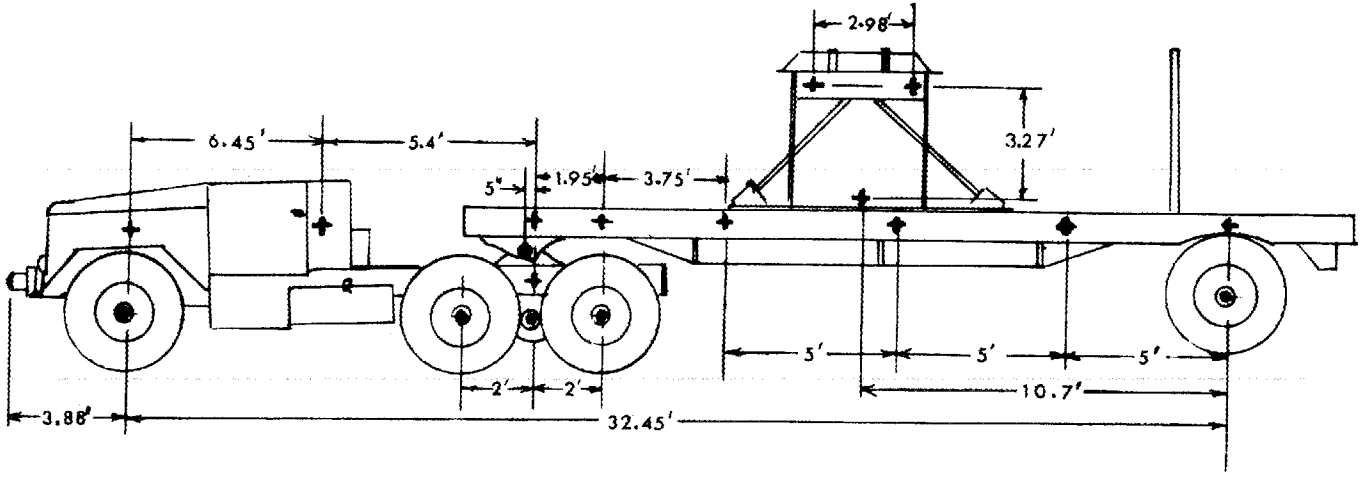

Fig. 7.5. Arrangement of Markers on Test Vehicle and Cask for Photographic Measurement of the Fourth Impact Test.

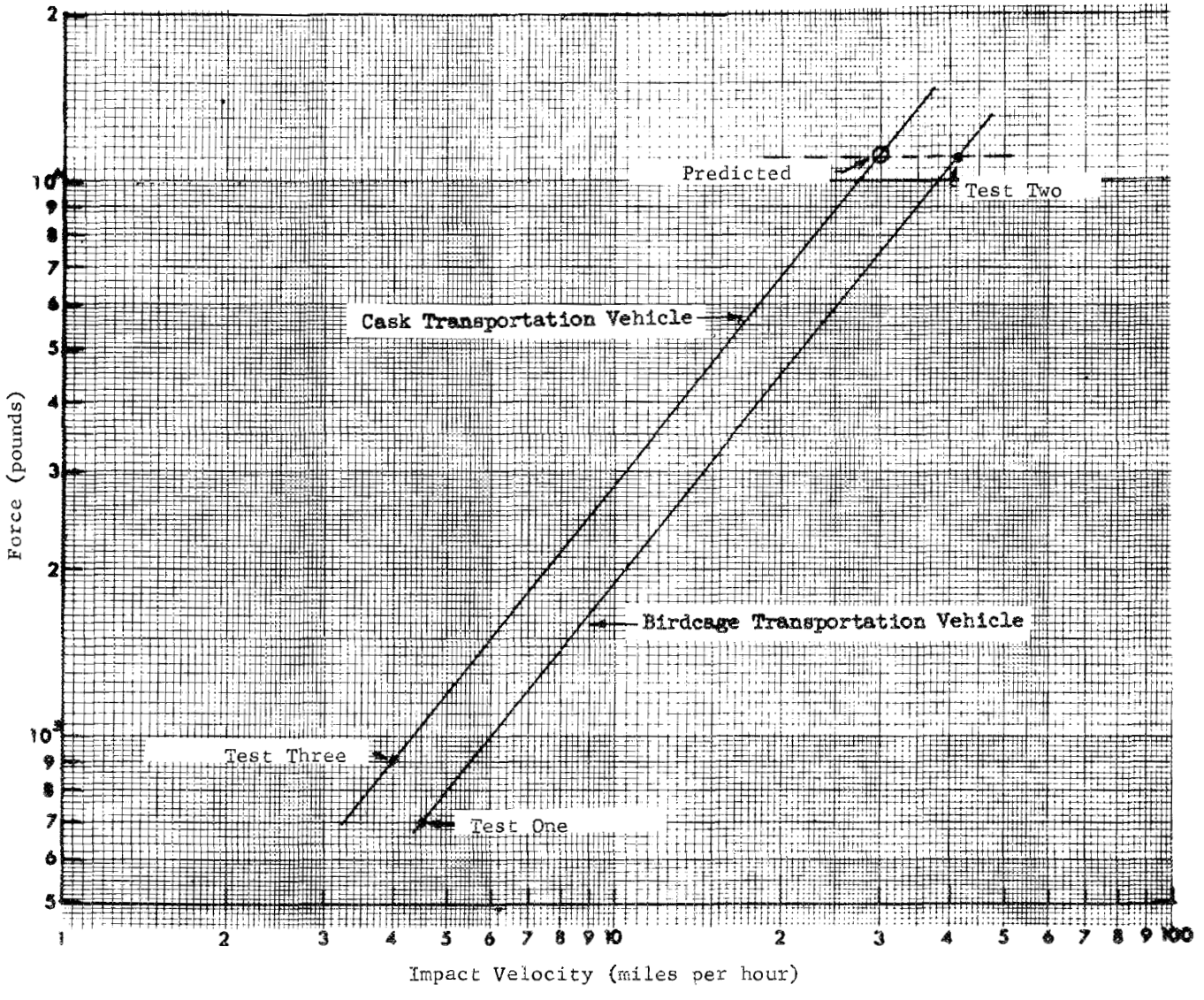

Fig. 7.6. Plot Resulting From Empirical Analysis to Determine Whether the Force at a Given Impact Velocity Can Be Predicted.

7.4 Results of Fourth Test

The cask transport vehicle impacted against the barrier squarely but off center to the extent that the left front wheel missed the barrier. The velocity of the vehicle just prior to impact was clocked at 28.5 mph. The general behavior of the cask transport system is shown in a sequence of still pictures in Fig. 7.7. These photographs were taken from the motion-picture coverage of the impact.

As may be seen in Fig. 7.7, the front load cells hit the barrier squarely but were almost immediately absorbed within the front of the tractor. There was no separation between the tractor and trailer during this impact. However, during the time interval between 30 and 60 msec, the frame of the tractor began buckling immediately ahead of the fifth-wheel attachment in a manner similar to the deformation of the cab-over-motor tractor in the third test. At 100 msec, the tractor frame was bearing on the forward axle of the bogie, as evidenced by the configuration of the tire on that axle. At 130 msec, the frame appeared to be in contact with the surface of the road and began to force the front of the tractor to slide vertically up the face of the barrier. At 170 msec, the tractor fuel tank was being deformed by contact with the road and it ruptured, spilling the colored water over the test site. Crushing of the tractor continued until sometime after 340 msec, when the trailer essentially came into contact with the barrier through the fully compressed material of the tractor.

Although not shown in the sequence of photographs in Fig. 7.7, an overhead motion-picture sequence showed that the entire tractor-trailer combination shifted to the left, pivoting about the fifth-wheel area, allowing the right front corner of the trailer to make rigid contact with the barrier. This is illustrated in Fig. 7.8. The lateral shift was probably a response caused by the left front wheel missing the barrier.

This impact of the right front corner of the trailer against the barrier caused the left rear wheel of the trailer to rise about 4 ft above the surface of the road beginning at 440 msec, as may be seen in

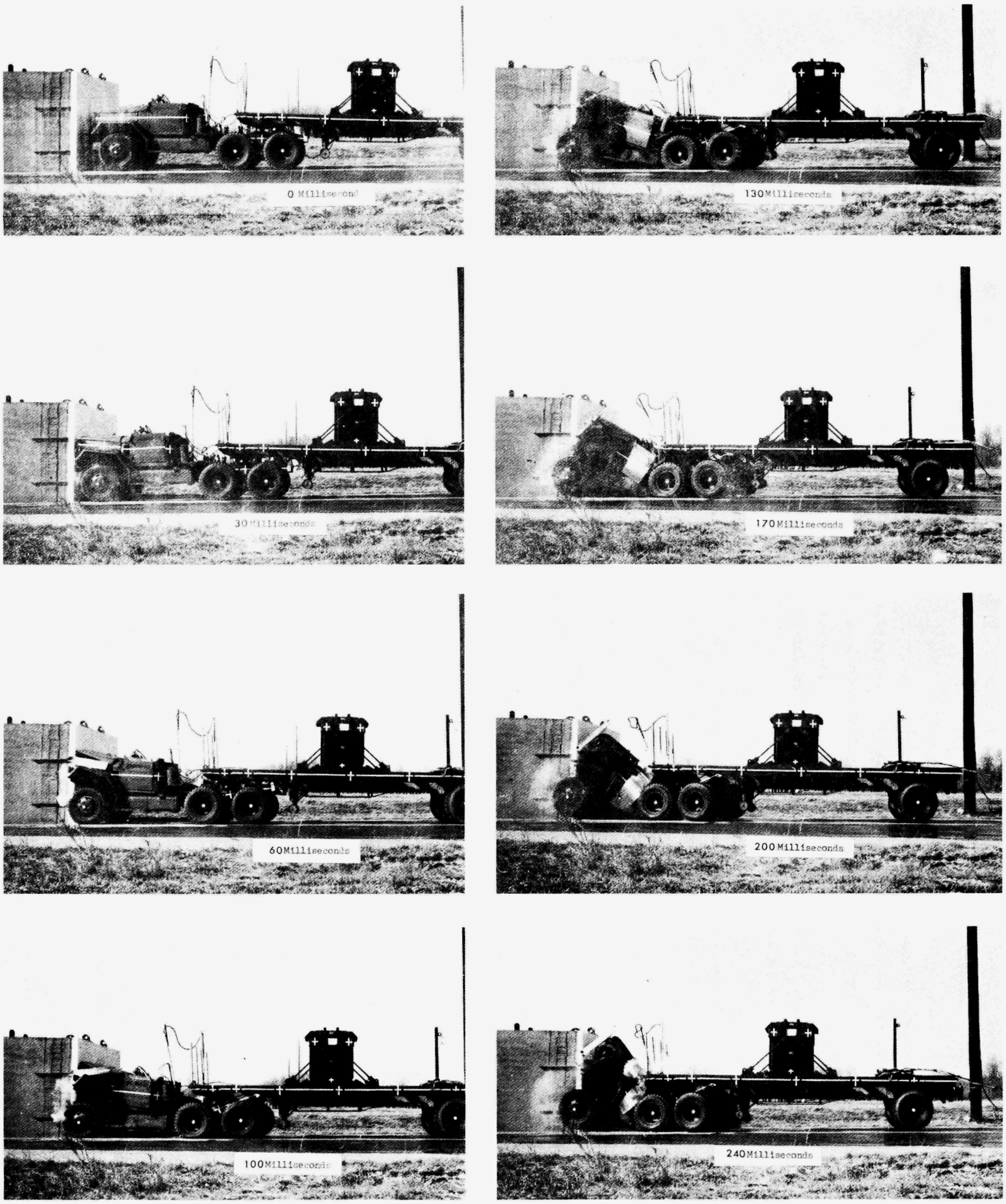

Fig. 7.7. Still Pictures Showing Impact of Cask Transport Vehicle Against the Barrier at a Velocity of 28.5 mph in the Fourth Test.

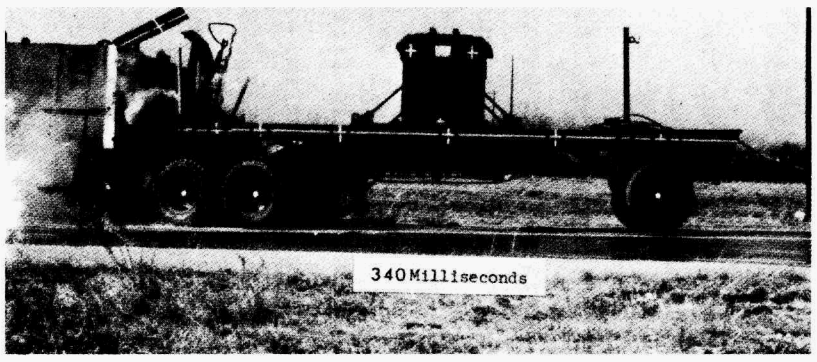

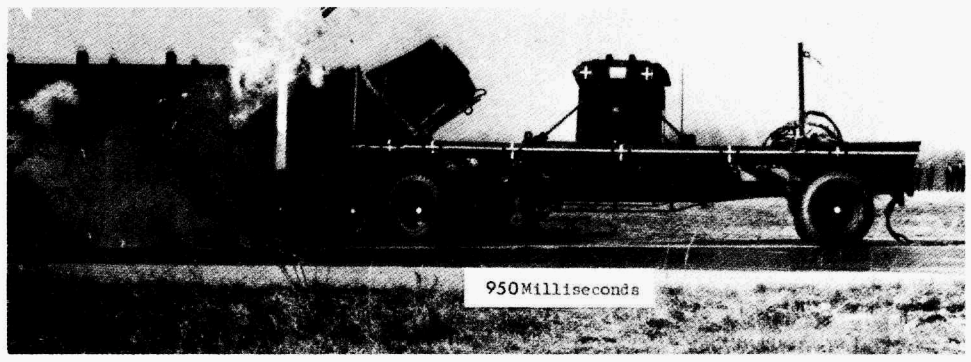

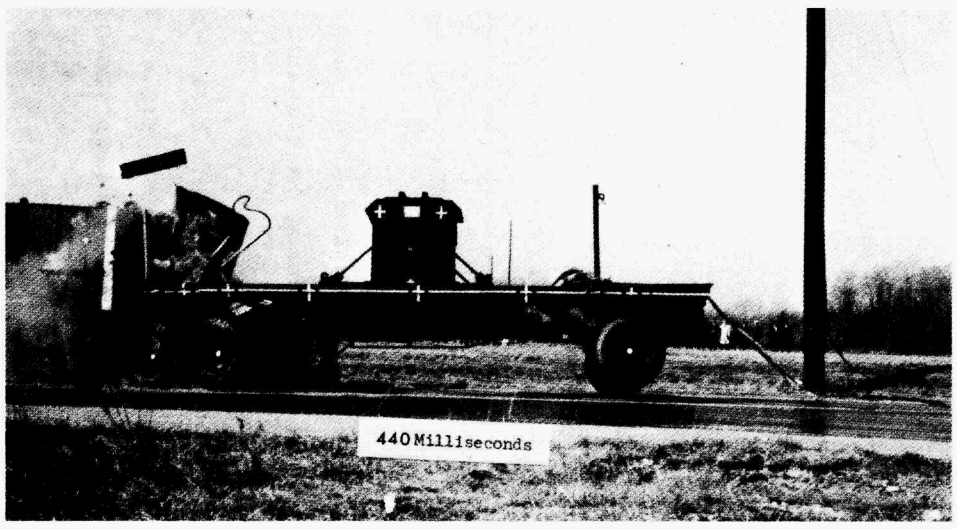

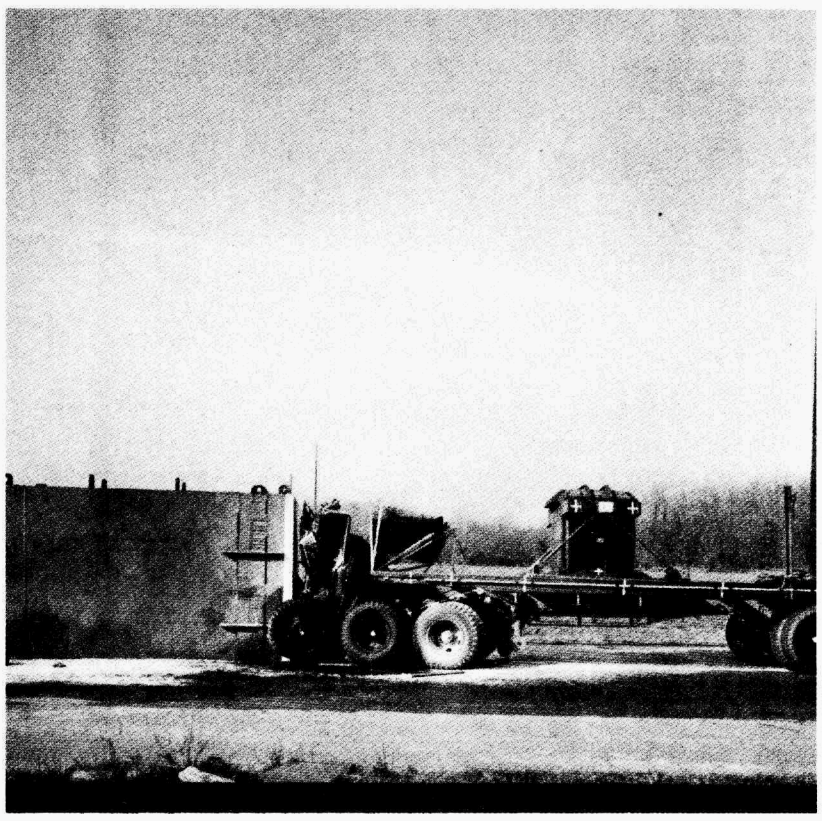

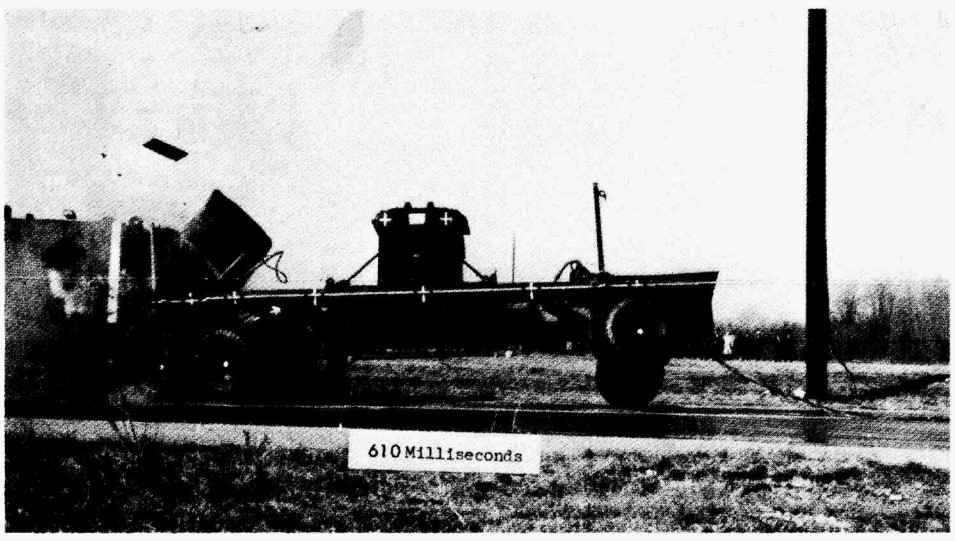

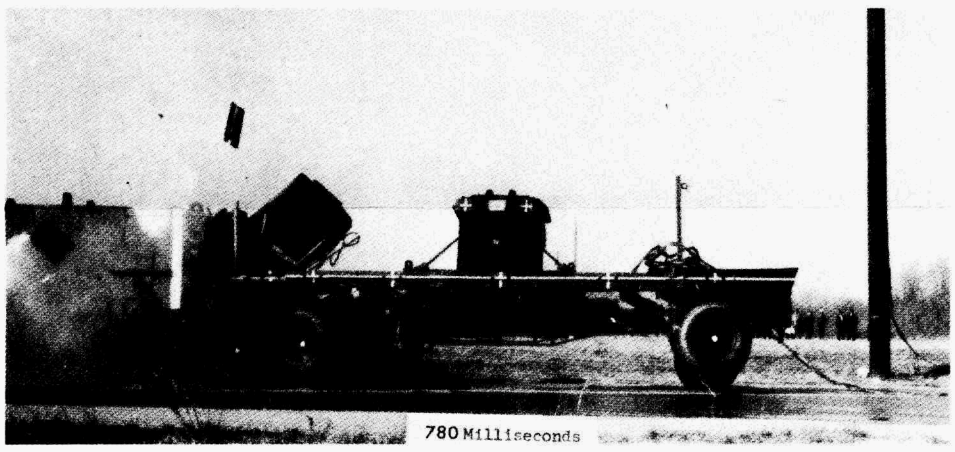

Fig. 7.7. (continued)

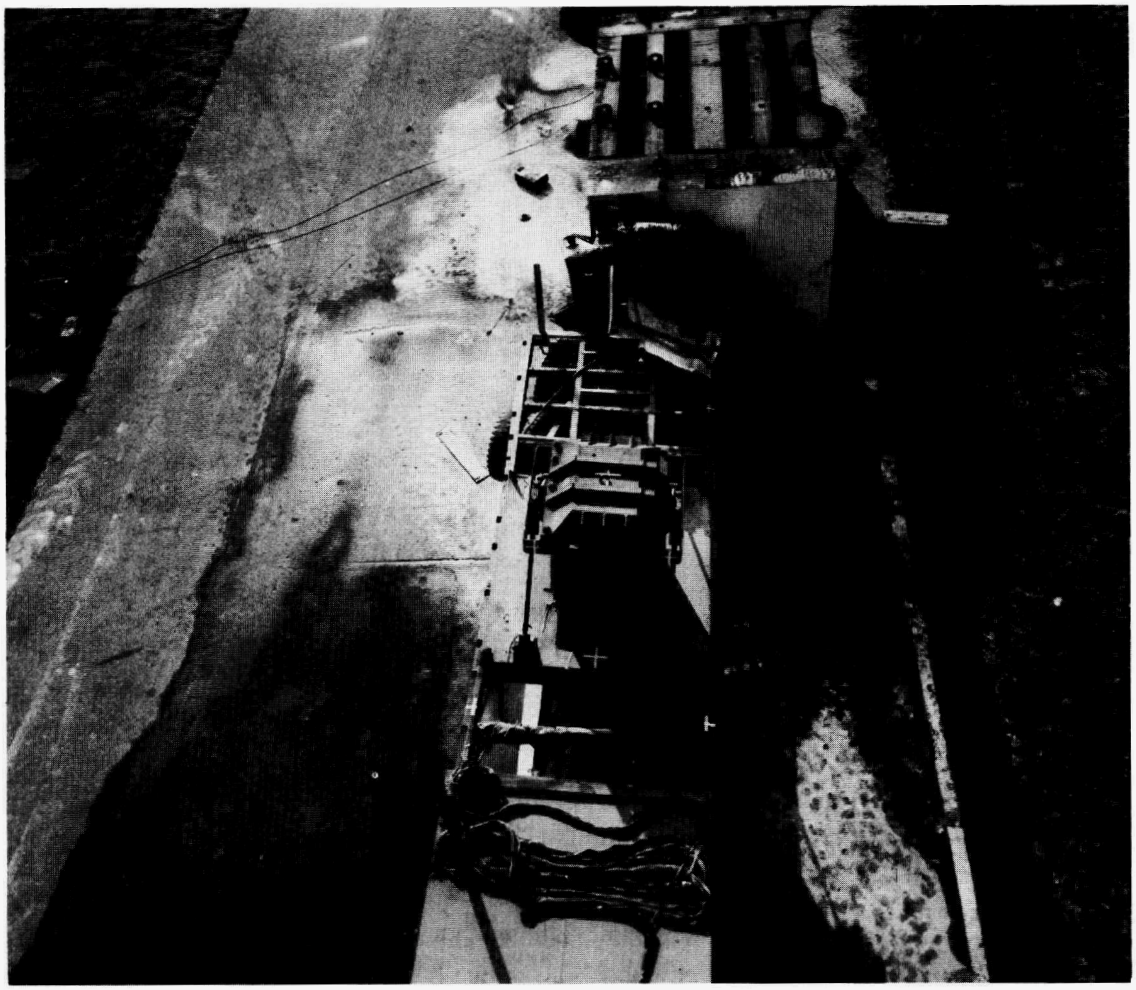

Fig. 7.8. Lateral Shift of Tractor-Trailer Combination About the Fifth-Wheel Area During the 28.5-mph Impact.

Fig. 7.7. By 950 msec, the left rear wheel of the trailer had settled back down on the road. The frame of the trailer showed permanent deformation at the point of contact with the barrier, and both the inner and outer right side frames were deformed about 1 ft ahead of the cask spreader plate.

Fire broke out at 0.7 second after impact. The fuel for this fire came from the gasoline remaining in the auxiliary supply can that initially contained 2 gallons of gasoline. This auxiliary can broke loose from its location on the tractor and spewed vapors over the tractor, as may be seen in the 440-msec frame in Fig. 7.7. The fire was extinguished quickly with foam by the fire fighters who were on standby.

7.4.1 Instrument Measurements

With respect to quantitative measurements, only a limited amount of data were obtained and this was in the area of the cask. Practically all of the other instrument measurements were meaningless because of the early and complete failure of the tractor. The front load cells on the tractor recorded data for only about 4 msec before being absorbed within the tractor, and the force and moment channels were disregarded because of apparent transducer damage. Because the frame of the tractor bore down upon the axle, the suspension measurements were negated in terms of applicability to the mathematical model. The force data obtained for the cask tie-down are illustrated in Fig. 7.9.

7.4.2 Photographic Measurements

The position of a fixed point over the fifth wheel on the side of the semitrailer as a function of time was determined from the high-speed (film speed of 80 frames per second) motion pictures. The camera was located 200 ft to the side of the barrier. An analysis was made of the 51 frames covering the time interval from the initial collision contact with the barrier to the rebound. A random error of 0.017 ft was expected from the film reader. The displacement of the point or compression-versus-time data were least-squares fitted to a power series of the sixth degree in time by using Gram orthogonal polynomials. These results were then differentiated analytically to yield the acceleration and velocity curves. The fit, rms error, and final equations are as follows where t = time in seconds and t = 0 corresponds to an instant 312 msec after the impact.

The fit = sixth degree.

The rms error in Y = 0.019 ft.

The displacement in ft

$$Y = 9.94 + 20.26(t - 0.312) - 45.28(t - 0.312)^2 - 53.28(t - 0.312)^3 - 18.8(t - 0.312)^4 + 361.6(t - 0.321)^5 + 467.6(t - 0.312)^6 .$$

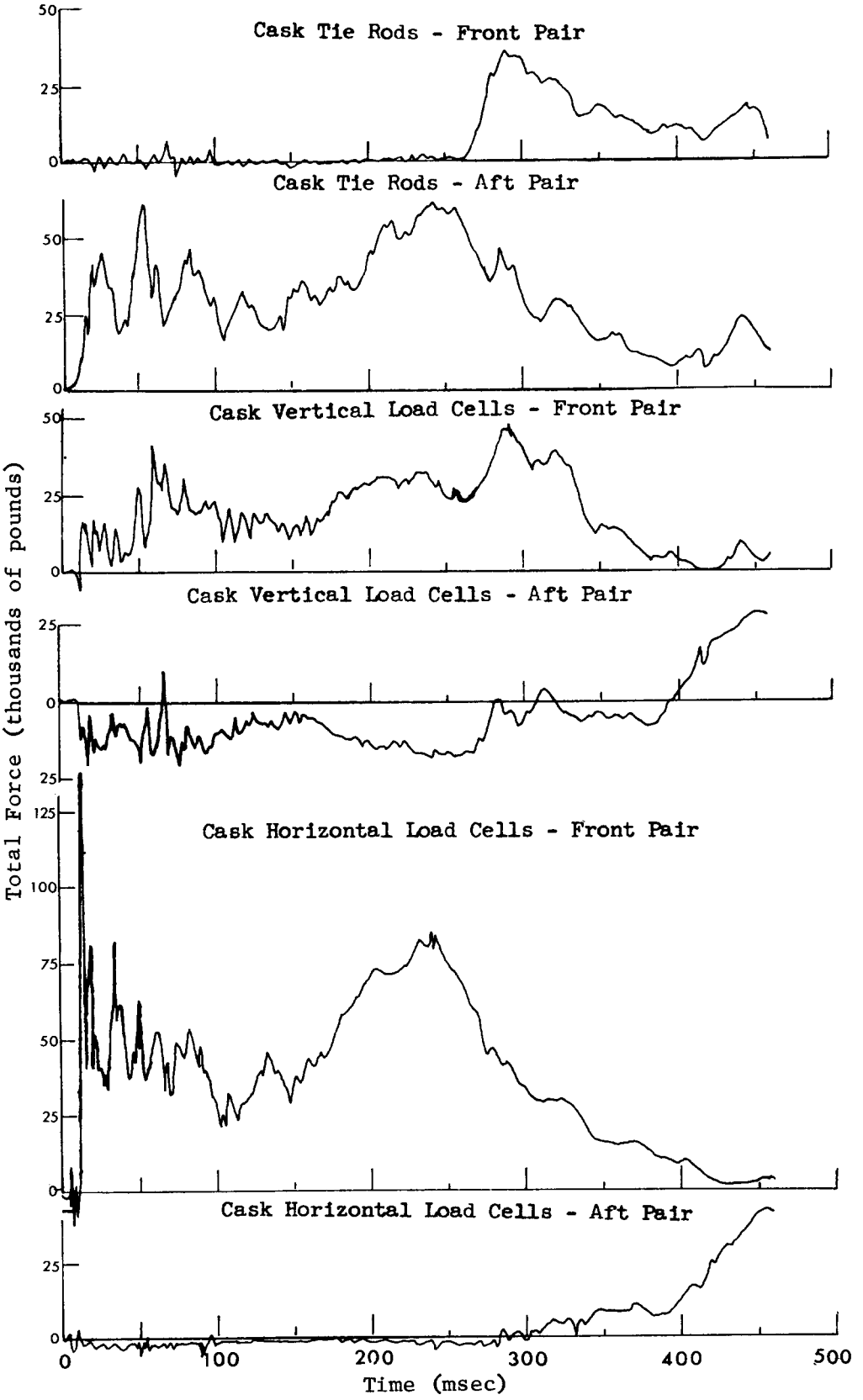

Fig. 7.9. Force Measurements on Cask and Cask Tie Rods as a Function of Time for the 28.5-mph Impact.

The velocity in ft/sec

$$Y' = 20.26 - 90.56(t - 0.312) - 161.52(t - 0.312)^2 - 75.2(t - 0.312)^3 + 1808.0(t - 0.312)^4 + 2805.6(t - 0.312)^5 .$$

The acceleration in ft/sec^2

$$Y'' = 90.56 - 323.04(t - 0.312) - 225.6(t - 0.312)^2 + 7233.0(t - 0.312)^3 + 14028.0(t - 0.312)^4 .$$

As illustrated in Figs. 7.10 and 7.11, the results of this analysis indicate that the displacement of the semitrailer during the first 500 msec of the impact may be described within the accuracy of the data by a smooth function of time. This implies that the dynamics were controlled by a single source of resistance such as the bending of the tractor frame. The shallow minimum in the acceleration at 176 msec is certainly consistent with such a conclusion. Thus, the tractor frame failed shortly after impact and the transmitted force decreased from the initial rigid elastic buildup. At a time 176 msec after impact, the force began to increase as the accordian effect of crushing of the tractor body took place.

The acceleration values for the semitrailer that were calculated from motion-picture coverage of the test are illustrated in Fig. 7.11. This plot of the sixth-degree fit describes the behavior of the semitrailer as a low-frequency phenomenon. Basic values of acceleration cannot be correlated with the piezoelectric accelerometer measurements because the accelerometers do not respond to frequencies under about 5 Hz. However, the magnitude of forces measured in the cask tie-down tend to appear reasonable in terms of the calculated acceleration of the semitrailer.

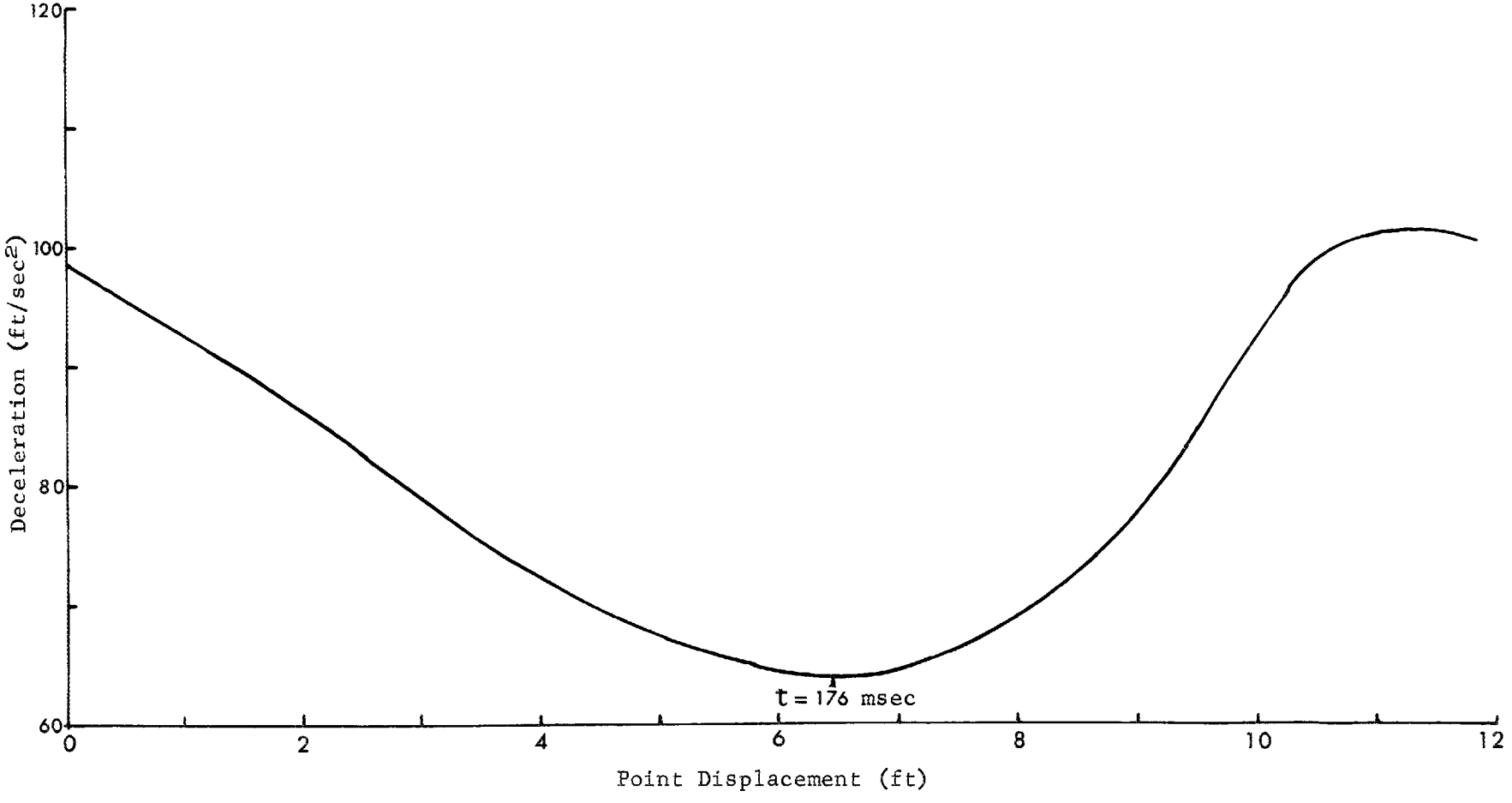

Fig. 7.10. Sixth-Degree Fit for Deceleration Versus Displacement of Point on Semitrailer Over Fifth Wheel for the 28.5-mph Impact.

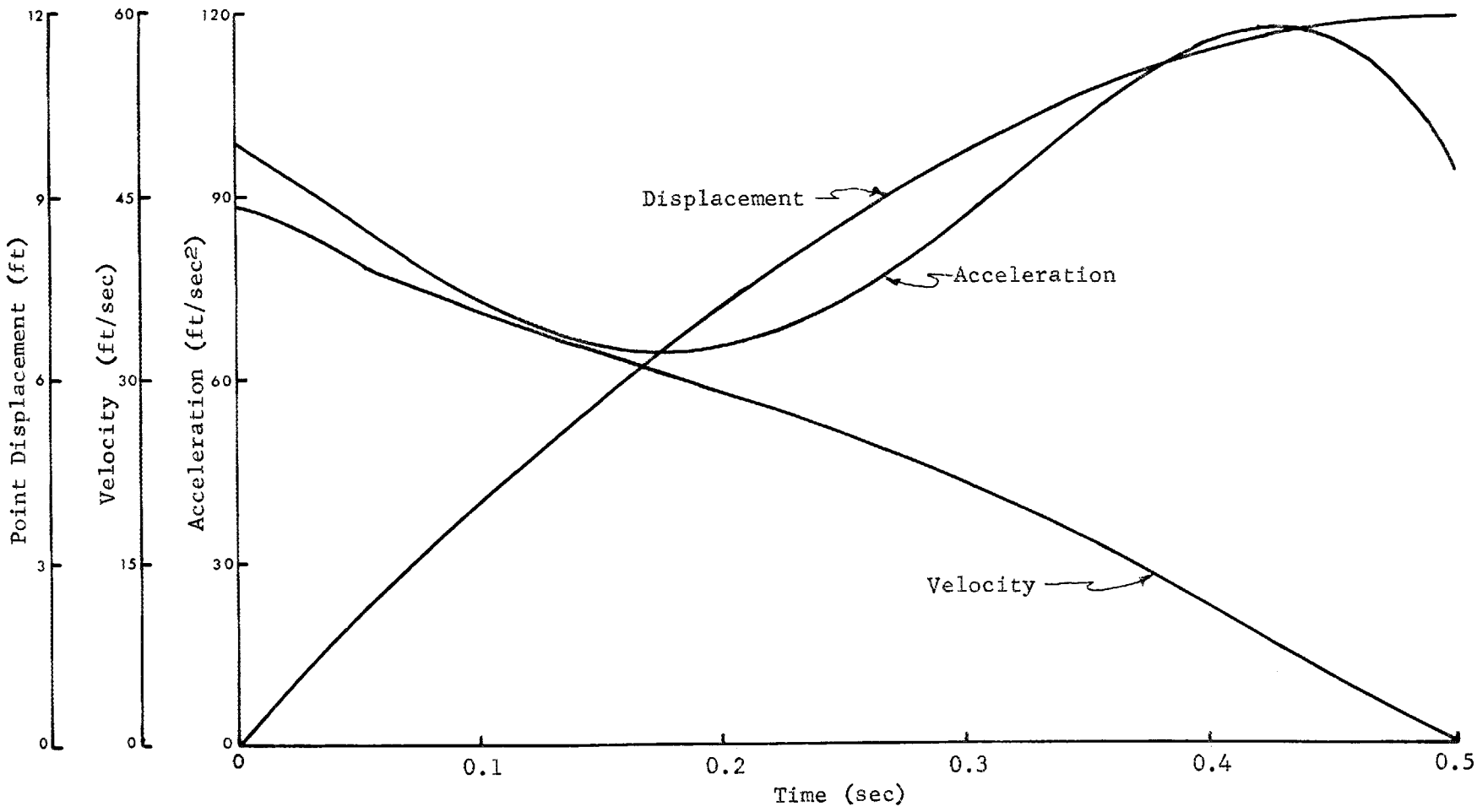

Fig. 7.11. Sixth-Degree Fit for Point Displacement, Velocity, and Acceleration as a Function of Time for the 28.5-mph Impact.

The significant dynamic collision conditions derived from this analysis of the high-speed photographs are summarized below. These conditions were measured from the marked point on the side of the semi-trailer over the fifth wheel.

The total vehicle compression = 11.9 ft.

The compression time = 490 msec.

The calculated initial velocity = 30.0 mph.

The initial acceleration = -3.06 "g".

The minimum acceleration = -1.99 "g".

The maximum acceleration = -3.64 "g".

8. MATHEMATICAL ANALYSIS OF TESTS

The analysis work done in conjunction with the pilot study, which was the initial phase of the Joint AEC-DA Study on the Transportation of Nuclear or Fissile Materials, was performed by personnel of The Franklin Institute Research Laboratories. The pilot study included the series of full-scale head-on collision tests described in the previous chapters of this report that were conducted at the Aberdeen Proving Ground and the analysis of those tests that was carried out under contract with the Development and Proof Services of the Aberdeen Proving Ground. During the course of the study, feedback between the experimental and analytical efforts was maintained as far as was feasible.

The pilot study represents a beginning and first effort of its kind. Because of this, the environmental and loading conditions for the full-scale tests were somewhat idealized, and some simplifying assumptions were introduced in the analysis. Moreover, both the experimental and analytical work had to undergo a process of development, and several aspects of the work required modification during the course of the study. However, the nature of the analytical work, especially the computer programming, made it impractical to provide a detailed documentation of the various stages of this development.

8.1 Definition of Problem

To define the analytical problem, the objectives and scope of the pilot study and some of the factors leading to them must be considered. Since the pilot study represented the first phase of the Joint Program, its principal objective was the development of experimental methodology and analytical techniques suitable for studying the dynamic behavior of the transport vehicle system under a variety of accident conditions. Only one accident condition could be examined in the pilot study, and this was chosen to be a longitudinal collision on the basis of available accident studies.

A further restriction on the type of collision was deemed necessary for experimental purposes, and a head-on collision against a fixed barrier was selected as the test environment. From the analysis viewpoint, no great advantage was to be gained by studying a head-on collision rather than a rear-end collision. In principle, similar techniques would be applicable for the solution of both of these types of longitudinal collision. However, the simplification in analysis of the head-on collision appeared desirable when the structural interaction between colliding objects is considered.

In the analysis of response under the conditions of a longitudinal collision, one source of complexity arises from the need to consider the structural interaction between the transport-vehicle-container-tie-down system and the object of collision (vehicle, barrier, etc.) whose configuration is not unique. Such an interaction can be accounted for in one way, at least, if the forces experienced by the vehicle during the collision are known a priori. Normally, such forces are indeterminate and cannot be evaluated without performing an analysis such as the one under consideration. For the collision tests planned in the pilot study, it appeared feasible to measure the external forces applied to the vehicle that could be assumed as known a priori. However, it must be emphasized that such an assumption was made only to reduce the effort required in this analysis. The interaction effects should be incorporated in succeeding phases of the work done under the Joint Program.

It can therefore be stated that the specific problem of the analysis considered in this report was to develop procedures for evaluating the dynamic response of a given transport-vehicle-container-tie-down system under application of known forces (observed in the collision tests). The response is determined by defining the variation of displacement, velocity, acceleration, and force with respect to time in the various elements of the physical system.

8.2 Approach to Solution Formulation

In developing an approach to the solution of the analysis problem, two general courses of action are available. First, one could use the test observations to empirically devise procedures that would predict the response of a specific element or set of elements in the system within a specified margin or error. For example, one could consider the response of the container and its tie-down only and prescribe methods by which container acceleration and tie-down force could be evaluated directly without examining the behavior of the other elements in the system. Such an approach could provide response values for selected elements in the system, but of necessity, it would be restricted in application to a limited range of physical parameters in the system.

As a second course of action, one could approach the problem in a somewhat more fundamental manner by studying the dynamic behavior of the physical system as such. In doing so, one would take into account the role of interaction between various elements in the system in affecting the response values for elements of particular interest. This type of approach would also yield procedures that are applicable over a broad range of system parameters rather than being restricted to a specific set of elements in the system. However, this approach would require a systematic development of one's understanding of the behavior of the physical system and of the analytical procedures necessary to describe this behavior. Consequently, it may not be feasible to finalize the analytical procedures within the limited scope of a pilot study. In spite of these disadvantages, the second and more general approach was taken for the present analysis. Only in this way can repetition of experimental and analytical investigations typical of empirical approaches employed in the past to solve similar problems be avoided.

The analysis in the present study involves four principal steps. These are the

1. development of a mathematical model of the system,
2. analysis of this mathematical model,
3. numerical evaluation of response, and

4. comparison of numerical response with pertinent test results and, if necessary, feedback to the first step to improve the mathematical model.

In context with the scope of the pilot study, the mathematical model should initially provide a reasonable but somewhat simple representation of the physical setup. With such a beginning, the process of feedback between the experiment and analysis can be optimized, especially in view of our present limited understanding of the behavior of the vehicle under collision conditions.

For an analysis of the mathematical model, which would represent a strongly nonlinear physical system, numerical methods offer the most promise. The equations of motion for such a system are solved effectively by numerical integration methods. The numerical integration would be performed on a digital computer.

The efficiency of the mathematical model and of the procedure for its analysis can only be tested by comparison with numerical response and appropriate experimental observations. The overall plan of the pilot study provided an excellent opportunity to effect such a test of the proposed analysis methods.

8.3 Mathematical Model

A mathematical model is an idealized representation of a physical system, and it incorporates the behavioral characteristics of the system. It reduces a complex system to a less complex but representative form which can be used to study analytically the behavior of the parent system. The extent of idealization depends largely upon the level of accuracy desired from the analytical solution. On the other hand, the manner of idealization depends upon the environmental and loading conditions and upon the type of system response desired under such conditions. For example, to develop the mathematical model of a transport-vehicle-container-tie-down system under collision environments, one would need to know the type of collision (longitudinal, oblique, etc.) and the type of response (structural response of system elements, accelerations in

the cab region, deformation of trailer frame, etc.) required. In this respect, mathematical models of the same physical setup can differ widely in form and complexity.

For the problem defined in this report, two general guidelines were followed in developing the mathematical model. First, with regard to the level of accuracy desired from analytical solution, it was recognized that the present effort represented a beginning in both experimental and analytical effort. It was therefore deemed appropriate to start with a somewhat simple model and improve it if necessary as appropriate experimental observations became available. The present understanding of the physical processes of vehicle collision is limited, and it precludes incorporation of all pertinent factors in the model. Second, the behavior of the tractor-semitrailer combination and the container as a system of elements was recognized and emphasized in the establishment of an appropriate mathematical model. The various elements of the physical system were examined collectively rather than one or a group of them at a time.

Certain observations concerning the structure of the vehicle can be made. The tractor and semitrailer are built of two distinct types of elements: components and connections. The components account for most of the weight of the vehicle, while the connections, being less stiff, account for the flexibility in the vehicle. The components include elements such as axles with wheels, tractor and trailer frames (which are flexible to an extent), motor and transmission blocks, and the fifth wheel. The connections include suspension springs, motor mounts, tie-downs, etc.

The dynamic behavior of a tractor-semitrailer combination loaded with a container and undergoing a head-on collision against a barrier can be qualitatively described in six steps as follows.

1. Prior to collision, every element of the system is moving at a uniform speed in the longitudinal direction.

2. The tractor frame, which strikes the barrier first, slows down at the instant of collision, while the other components are still moving at the initial velocity.

3. The motion of the components of the vehicle that are attached to the frame of the trailer is inhibited by the presence of the connecting elements between them. These connecting elements are deformed and stressed as a consequence.

4. This tendency progresses to other components and a vibratory motion develops within the physical system.

5. In addition to the connecting elements being deformed, the components such as the tractor frame undergo permanent deformation under direct impact. Other components, such as axles, motor block, etc., are strained under the action of dynamic loads transmitted to them through various connections.

6. In the course of the dynamic response of the system, failure may take place in one or more connections. As a result, one or more components connected by these failed connections may separate from the system at a finite velocity. Such an occurrence could cause secondary collisions. For example, kingpin failure would permit the trailer carrying the container to separate from the tractor and possibly collide with the barrier.

These observations supplemented with a close examination of the structural layout and design of the vehicle provide a reasonable basis for developing an appropriate mathematical model. The four important characteristics of the system can be identified as follows.

1. The motion of the elements of the system during a collision would be primarily confined to the vertical plane through the axis of the vehicle in view of the symmetry of its configuration and of the collision.

2. The system can be represented by components and connecting elements, and the mass of the system will be concentrated in the components. The error introduced by assuming the connections to be without mass should be negligible.

3. In general, the components can be treated as rigid bodies when compared with the flexible connecting elements. Since two components, the tractor and trailer frames, are relatively flexible, each of them could be satisfactorily idealized by two or more rigid mass elements with joints between them to account for the flexibility of the frame.

4. The dynamic force-displacement characteristics of the connecting elements would be nonlinear in general, and they would include such effects as hysteresis and coupling of motions in the longitudinal, x, and vertical, y, directions.

Consistent with these observations, a mathematical model of the physical system was developed, a solution technique based on Runge-Kutta numerical integration using a digital computer was proposed, and a computer program was developed. These are described in detail in The Franklin Institute Research Laboratories Report F-B2397 authored by K. D. Doshi and entitled "Analysis for the Longitudinal Vehicle Collision Test of Joint AEC-DA Pilot Study". This report is readily available and was included in the original Joint AEC-DA Study. Therefore, no further discussion of the computer program is presented here.

8.4 Limitations of Mathematical Model

The approach taken for analysis of the vehicle response does not include consideration of the structural interaction between the objects involved in collision. For the pilot study, these objects consisted of the moving test vehicle and the stationary barrier. The effect of their interaction is indirectly accounted for in this study by the assumption of knowledge about the forces applied to the vehicle during collision. Since such forces are generally not known a priori, their assumption limits the applicability of the analysis to situations where they are obtainable from experimental observation.

Development of the mathematical model remains the most important aspect of the analysis. Once defined, it will determine the type, extent, and accuracy of the response of the vehicle system that one can expect at most from subsequent analysis of the model. In this respect, the model developed can define response which is characterized by (1) motions in the x, y, and θ directions only and (2) failure patterns that involve either bending modes in tractor and trailer frames or rupture of connections in the system. Response involving instability of frame members or

jackknifing of the trailer body is not feasible with the present model. To include the frame instability, one would need to consider an alternate representation of the frame members.

No significant limitations result from the methods considered for evaluating the dynamic response of the system. In principle, the numerical solution of the equations of motion can be made as accurate as desired by choosing an appropriate size for the time step, Δt. However, in practice, this may not always be economically feasible within the range of the size and speed capabilities of available computers.

9. APPRAISAL OF RESULTS, CONCLUSIONS, AND RECOMMENDATIONS

An appraisal of the results of this pilot study of simulated highway longitudinal head-on collisions and the general conclusions drawn from the results are presented in this chapter. Recommendations are also presented for future studies that may be made and to assist researchers and investigators engaged in similar work.

9.1 Appraisal of Results

Four collision tests were performed with three different combinations of truck tractors and semitrailers, and these tests are described in Chapters 4, 5, 6, and 7 of this report. The test site, procedures, and general instrumentation plan are described in Chapter 3. The mathematical analysis work done in conjunction with these tests is discussed in Chapter 8. An appraisal of the results of this pilot investigation is presented in this section.

9.1.1 First Test

There was no physical damage inflicted on either the tractor or the trailer as a result of the first exploratory impact test conducted at a velocity of 4.5 mph to familiarize personnel with the test techniques and facilities. The total force measured by the load cells reached a peak value of about 62,000 lb, and time histories of forces and accelerations were recorded during this impact.

9.1.2 Second Test

With regard to the requirements for providing an accident environment and photographic record, the second impact test conducted at a velocity of 41 mph with a loosely stowed cargo that included six types of

birdcage containers was highly successful. However, with regard to the next test to be conducted with the cask transport vehicle, several definite problem areas were indicated by the results of the second test. The early failure of the fifth-wheel attachment did not permit the maximum transmission of force through the tractor. Loss of total force measurements by the load cells on the front of the tractor was brought about by inherent weakness in the foremost portion of the tractor frame that permitted the load cells to be absorbed within the material of the tractor upon impact.

This method of measuring total force was reviewed to determine alternate or improved techniques. However, the success of any method of using non-deforming load cells on the tractor would be contingent upon the integrity of the frame of the tractor. An alternate method considered was the use of a weighing barrier that would measure the total force, including that caused by loose or flying objects. While this capability of the barrier had merit, it was not available and required development. It was not specifically designed into the mathematical model at that time, and recording of the measurement would be separate from and not time correlated with other measurements on the vehicle.

9.1.3 Third Test

In the third collision test at a velocity of 4 mph conducted with the cab-over-motor tractor and the flatbed semitrailer with the 15-ton cask as cargo, the cab-over-motor tractor was weaker than anticipated even after localized strengthening. It must be recognized that when reinforcement is applied to a localized weak point, the point of failure is transferred to the next weakest link in the system. Thus, localized strengthening becomes a never-ending process. The more rigid the system, the more force that will be transmitted.

With respect to rigidity, the cask as installed on the flatbed semitrailer was essentially a rigid or integral part of the trailer. As such, the total kinetic energy in the cask was transmitted through the fifth wheel to the tractor. The cask was a different form of cargo than

the loosely stowed birdcage containers where some of the energy could be absorbed through displacement.

With respect to quantitative measurements, the validity of the values recorded by the dynamometers shortly after the initial impact may be suspect because tension forces were indicated by cells mechanically arranged to measure only compressive forces. On data channel B-1, this phenomenon appears to be a zero shift, while there is no specific rationalization for the data recorded on channel B-2. The effects of permanent deformation are reflected in the force and moment measurements on the tractor frame. Measurements of forces in the cask tie-down appear reasonable in terms of value and in behavior correlation with time.

Because the cab-over-motor tractor was damaged beyond economical repair in the third test and because of its inherent weakness in this low-speed impact, another type of tractor was instrumented for the fourth test, which was to be a relatively high-speed impact that was actually clocked at a velocity of 28.5 mph.

9.1.4 Fourth Test

With respect to quantitative measurements, only a limited amount of data was obtained from the fourth test and this was in the cask and cask tie-down area. Practically all other measurements were meaningless because of the early and complete failure of the tractor. The load cells recorded data for only about 4 msec before being absorbed within the material of the tractor, and force and moment channels were disregarded because of apparent transducer damage. Because the tractor frame bore down on the axle, the suspension measurements were negated in terms of applicability to the mathematical model.

Displacement values for the trailer calculated from photographic measurements were least-squares fitted to a sixth-degree polynomial and the resulting equation described the behavior of the trailer as a low-frequency phenomenon. The basic values of acceleration obtained by differentiation cannot be correlated with piezoelectric accelerometer measurements because the accelerometers do not respond to frequencies below about 5 Hz. However, the magnitude of forces measured in the cask

tie-down tend to be reasonable in terms of the acceleration calculated for the trailer.

9.1.5 Comparison of Test Results

In both of the relatively high-speed head-on collisions with the barrier, the tractors were completely destroyed. Thus, the tractors may be described as one-time energy absorbers. The weakest point in the tractor-semitrailer combination is the tractor itself. This point is further isolated in the front-end area of the tractor and in the area of the frame around the fifth wheel attachment. The strength of the connection between the fifth wheel and the frame dictated the magnitude of acceleration measured on the semitrailer in each of the high-speed impacts conducted in the study.

When separation occurred between the fifth wheel and the frame of the tractor, a lesser amount of energy was absorbed by the tractor. This caused an acceleration peak of some 20 "g" in a total time frame of 250 msec at the semitrailer. When there was no separation between the fifth wheel and the tractor, more energy was absorbed in deforming the tractor. Thus, the acceleration peak at the semitrailer was limited to some 4 "g" in a total time frame of about 500 msec. The difference in the initial velocity of the two vehicles at the instant of impact is neglected in this comparison, but it does indicate a pattern.

The limited structural analysis of the various tractors and trailers used in this investigation indicates one significant point. The ratio of the calculated cross-sectional area between the trailer frames and the tractor frames is about 2.5 to 1. The ratio of the calculated frame strength between the cask transport trailer and the M275 military tractor was about 3 to 1. This difference in strength between the frames of the tractor and the trailer can be rationalized on the basis of bending, the trailer frame being the longer and more critically loaded beam.

The inherent weakness of the tractor frame with the resulting behavior of the tractor is perhaps the most significant finding in this investigation. Because of this weakness, many of the implied objectives

of the test program could not be met. The total force of the dynamic mass could not be measured at the front of the tractor, the transmission of force through the tractor frame was not isolated and plotted, and finite inputs for the mathematical model were not determined.

9.1.6 Mathematical Analysis

The comparison of results from the mathematical analysis and the actual experimental test for the 4-mph impact shows little correlation between the computed and observed values. The lack of input data for the 28.5-mph impact precluded comparison of analytical results with the observed results. Absorption of the load cells on the front of the tractor over a time frame of 4 msec was responsible for this lack of data.

Although a mathematical model, equations for motion, and a computer program for their numerical solution were developed; there is not yet a basis for judging the basic efficiency of the model. As pointed out in The Franklin Institute report, the entire model is based on the assumption that forces experienced in the vehicle during collision, particularly the total input forces, are known before analysis. However, in the high-speed impacts, this total force could not be measured because of the inherent weakness of the transport systems. In the 4-mph impact test where an input was determined a priori, friction between the various elements in the system, which was neglected in developing the model, plus the inability to establish elastic-stiffness values with reasonable accuracy for important connections in the model were cited as the reason for "considerable" discrepancy between the analytical and experimental values.

In retrospect, it appears that for this mathematical model, the tractor portion of the transport system is considered as a structure capable of transmitting large forces to and through the trailer into the cask and tie-down arrangement. Knowing the path of transmission and the magnitude of these forces, the model could be used to evaluate the various energy absorption features which could be built into the vehicle or

the tie-down. As previously stated, the highway transportation systems examined in this pilot study were not capable of transmitting these large forces. The tractors were weak and in effect one-time energy absorbers, and the mathematical model representation of the tractors was invalid. Actually, the tractor may be considered as a nonlinear spring, and acceleration forces at the front of the trailer become the first quantitative values of interest. Acceleration values determined from photographic coverage of the tests show the forces to be relatively low (less than 20 "g") and the pulse widths of acceleration to be relatively long (250 msec or longer). Since the two high-speed impact tests tend to define opposite ends of the vehicle behavior spectrum, it would appear that responsible guidelines or limits are available for synthesizing a family of theoretical tractor behavior patterns to be used as inputs for a more simplified mathematical model.

9.2 General Conclusions

From consideration of the appraisal of the results of the pilot study, the following conclusions were made.

(a) The test site, barrier, remote-control capability, and the operating procedures and techniques developed for and used in this investigation were entirely satisfactory.

(b) The inability to obtain complete quantitative measurements resulted from early failure of the tractor frames, which did not behave according to pretest theory.

(c) Photographic measurements provided the most meaningful description of the dynamic behavior of the transport systems during the impact tests.

(d) Diverse behavior patterns were demonstrated during this pilot study involving head-on collisions with a barrier. In the test with the loosely stowed cargo of birdcage containers, only a minimum of energy was absorbed by the tractor because of fifth wheel separation. Near maximum energy was absorbed by the more complete crushing of the tractor in the high-speed test conducted with the 15-ton cask as the cargo.

(e) Meaningful, although limited, structural and transportability data were obtained for use in developing the method of approach in the comprehensive basic study.

9.3 Recommendations

It is recommended that

(a) the instrumentation plan be revised as follows if future tests are conducted and

1. The impact force should be measured on the barrier if correlation with a mathematical model is required.
2. The tractor should be recognized as being subject to large deformations and receive little or no instrumentation.
3. Unbonded strain-gage accelerometers having direct-current response should be used at the trailer and cargo load.
4. The behavior of the tractor should be measured by high-speed photography.
5. Quantitative electronic measurements should be made primarily on the trailer and cargo.
6. Consideration should be given to individual tension and compression forces in each of the trailer frame members.
7. Data transmission should be handled with radio frequency telemetric means rather than hard wiring.

(b) the inherent weakness of the truck tractor and trailer combination and physical limitations in measuring the transmission of force through the tractor be considered in any future development of a mathematical model.